SHEAR TRANSFER IN FIBER REINFORCED CONCRETE

by

Mariano O. Valle

B.C.E., The Catholic University of America, Washington, D.C.
(1989)

SUBMITTED TO THE DEPARTMENT OF CIVIL ENGINEERING
IN PARTIAL FULFILLMENT
OF THE REQUIREMENTS FOR THE
DEGREE OF

MASTER OF SCIENCE
IN CIVIL ENGINEERING

at the

MASSACHUSETTS INSTITUTE OF TECHNOLOGY

February 1991

Signature of Author_____
Department of Civil Engineering
February 1991

Certified by_____
Oral Buyukozturk
Thesis Supervisor

Accepted by_____
Ole S. Madsen
Chairman, Departmental Graduate Committee

SHEAR TRANSFER IN FIBER REINFORCED CONCRETE

by

Mariano O. Valle

Submitted to the Department of Civil Engineering
on February 1991 in partial fulfillment of the requirements for the
Degree of Master of Science in Civil Engineering

ABSTRACT

The objective of this thesis is to investigate the strength and ductility of fiber reinforced concrete under direct shear forces. Both experimental and modeling studies have been performed.

In the experimental study, push-off fiber reinforced concrete specimens made of high strength and normal strength concrete were tested. Two types of fibers were used: polypropylene and steel fibers. Another experimental variable was introduced by including conventional stirrups in some specimens. Load and shear deformation characteristics as well as failure modes of the specimens were studied and a comparative evaluation of the results made.

An existing model with further development for the present study was used for the analytical prediction of the shear stress-shear strain relations for these specimens. The model assumes a uniform stress distribution along the shear plane and is based on: 1) equilibrium, 2) compatibility, 3) stress-strain relations for concrete. The model also includes the compression softening phenomenon for concrete under biaxial stress state (compression - tension).

In general, fibers proved to be more effective in high strength concrete than in normal strength concrete, increasing both ultimate load and overall ductility. This is attributed to the improved bond characteristics of concrete-fiber interfaces associated with high strength concrete. For the case with steel fibers, significant increases in ultimate load and ductility were observed for both normal and high strength concrete. In the case of polypropylene fibers, a relatively lower increase in ultimate load were obtained when compared to the increase due to steel fibers; while major improvements in the overall ductility were obtained, especially for high strength concrete reinforced with polypropylene fibers. In the tests involving normal strength concrete reinforced with fibers and conventional stirrups, no increases in maximum load were observed compared to plain normal strength concrete with stirrups only; while major improvements in overall ductility were obtained. For high

strength concrete reinforced with steel fibers and stirrups, significant increases in maximum load and ductility were observed when compared to high strength concrete reinforced with stirrups alone. For the case of high strength concrete reinforced with polypropylene fibers and stirrups, increases in ductility were obtained, with no strength increase over high strength concrete reinforced with steel stirrups only.

Overall, good agreement between model and test results was found. This model represents a good tool for further studies on the parameters involved in the shear transfer behavior of beams and other structural elements.

Thesis Supervisor: Dr. Oral Buyukozturk
Title: Professor of Civil Engineering

ACKNOWLEDGEMENTS

I wish to thank all the persons responsible for the completion of this thesis, especially:

Professor Oral Buyukozturk, who gave me a fascinating topic to work on, and was never too busy to meet with me. Thanks to him, my stay at MIT was a rich learning experience.

W. R. Grace Co., in Waltham, MA., who donated the polypropylene fibers, silica fume and superplasticizer used in this investigation.

Dr. Chris Leung, who was never too busy to answer my questions or help me when ever the Fluke would break down.

My friends, Ayad Oumera, Kwang Lee, and Mourad Bakhoum, who were always there to listen to my problems and help me. (And of course to have lunch)

My parents, who, for as long as I can remember, have always encouraged and supported me. Thanks to them I am here now.

Luz M. Gonzalez, the love of my life, who has given me all the love and understanding I could have possibly asked for.

TABLE OF CONTENTS

LIST OF FIGURES

LIST OF TABLES

CHAPTER 1

INTRODUCTION

Concrete is one of the most widely used structural materials in the world. Among the advantages this material presents are: that its readily available, its cost is relatively low, it can easily be moldable into almost any shape, and is reasonably durable. However, when compared to steel, concrete shows significantly lower compressive strength, Young's modulus and ductility. Also, the tensile strength of concrete is several orders of magnitude lower, resulting in a brittle material behavior[1].

Recently, the relative low compressive strength of concrete has been improved by the development of high strength concrete. While conventional or normal strength concrete(NC) has a compressive strength ranging from 3,000 to 6,000 psi, high strength concrete(HC) with compressive strength of up to approximately 20,000 psi has been achieved. In practice, however, the compressive strength of HC ranges from 9,000 to 15,000 psi. Further, this improvement in strength has also led to an increase in the Young's modulus of the material accompanied by marginal increases in tensile strength. The down fall of this has been that HC presents an even more brittle behavior than NC. Nevertheless, HC has several advantages over NC, among them: reduced member size due to higher strengths and

modulus, which in turn reduces costs, improved deformation behavior, due to higher modulus, and faster erection process, since HC develops a higher strength earlier than NC allowing for a faster construction pace.

When shear stresses are involved, in addition to the low toughness (brittle) characteristic of concrete a relatively low shear strength behavior may also be observed in concrete. Shear failure can be sudden and catastrophic[2]. This is especially true for critical sections where, due to construction constraints, little or no reinforcing steel may be placed. For a broader application of high strength concrete to innovative concrete structures there is a need for the development of a fundamental understanding of the shear behavior and ductility of this material. The addition of short, high strength and ductile randomly oriented fibers may represent a potential solution for improving the toughness and shear strength of concrete.

1.1 BACKGROUND ON THE SHEAR TRANSFER OF REINFORCED CONCRETE

The shear transfer mechanism in reinforced concrete has been the object of several experimental as well as analytical studies[3,4]. This type of behavior is of great importance when sections under predominantly shear stresses, like corbels, deep beams, bearing shoes, etc., are involved. In general, two distinct shear transfer behaviors can be identified according to the initial state of the shear

plane which may be initially cracked or uncracked (Fig. 1.1a). For the case where shear is being transferred across a cracked plane, the behavior will be dominated by 1) aggregate interlock, 2) dowel action of the steel reinforcement crossing the shear plane, and 3) constraints in the direction normal to the shear plane. Final failure occurs along the pre-existing crack, due to sliding. This type of behavior is best described by the well known shear friction theory; which is the basis for the present design practice for reinforced concrete under shear stresses[5].

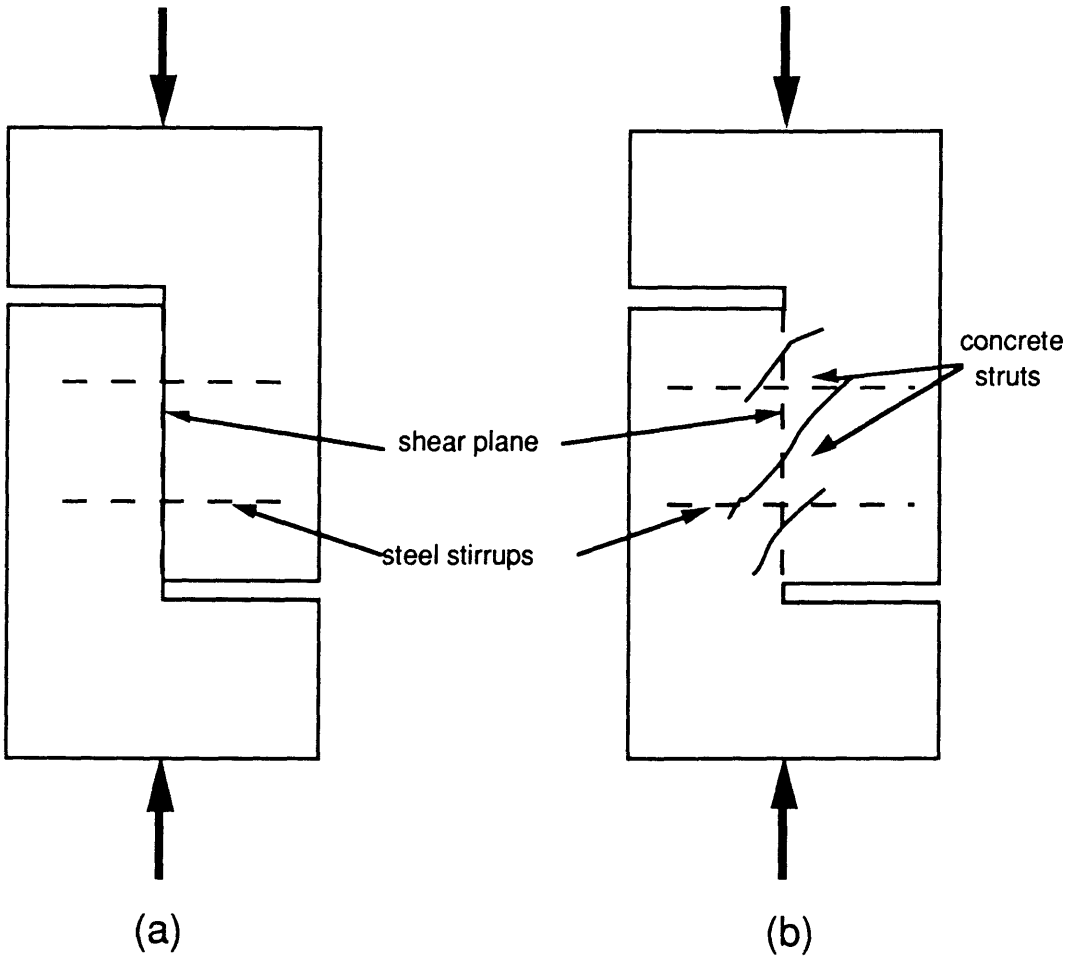

Fig. 1.1 Shear transfer push-off test specimen: (a) initially cracked shear plane; and (b) initially uncracked shear plane

For the initially uncracked plane reinforced with stirrups, the shear mechanism behavior is quite different. As the shear plane is loaded several cracks form in a direction inclined to the shear plane, creating well defined compression struts in the concrete(Fig 1.1b). For this stage, shear is being transferred through a truss-like action produced by the combination of the compressive force in the concrete struts and the tensile force that the steel reinforcement crossing the shear plane develops. Final failure usually occurs due to crushing of the concrete. For this type of behavior, the shear friction theory does not correlate well with test results. Several investigators have proposed different theories based on this truss-like action to describe this type of shear transfer[6,7].

In general, it has been found that initially uncracked shear planes can develop higher ultimate shear loads than initially cracked planes; while initially cracked planes show larger deformations than the initially uncracked ones. While both type of shear behavior, across an initially uncracked and cracked planes, are important; more understanding of the basic concepts governing the behavior of the initially uncracked concrete is needed.

1.2 OBJECTIVE AND SCOPE OF RESEARCH

1.2.1 Objectives

The shear transfer in concrete represents a very promising application area of fiber reinforced concrete(FRC). The addition of fibers has been shown to increase the tensile strength and toughness

of concrete, the two very important aspects related to the shear transfer behavior. This is specially true for the case of high strength concrete, due to the very brittle behavior it presents.

The objective of this work is, through experimental and analytical programs, to provide a fundamental understanding of the shear behavior of fiber reinforced high strength and normal strength concrete, and to develop qualitative data.

1.2.2 Scope

In view of the limited knowledge available on the shear behavior of fiber reinforced concrete, an experimental and analytical program has been conducted. In the experimental program, a total of 25 push-off specimens were tested. In these experiments, three variables were studied:

1. concrete type: high strength concrete vs. normal strength concrete
2. fiber type: steel vs. polypropylene fibers
3. the presence of steel reinforcement crossing the shear plane

From the tests performed, the load-displacement characteristics and failure modes for the shear specimens were obtained. In addition to high strength concrete, the program includes normal strength concrete in order to be able to compare the effects of the fibers on the shear behavior of these two materials. The two types of fibers, steel and polypropylene, were selected due to the different properties each possesses producing different characteristics of the concrete. By combining the two types of concrete, high strength and normal strength, with the two fibers used and including concrete

with no fiber reinforcement, six types of concrete were used in the testing program: normal strength concrete (NC), steel fiber reinforced normal strength concrete (SNC), polypropylene fiber reinforced normal strength concrete (PNC), high strength concrete (HC), steel fiber reinforced high strength concrete (SHC), and polypropylene fiber reinforced high strength concrete (PHC). Finally, the steel reinforcement crossing the shear plane was included as a variable in order to be investigate the interaction of fiber and steel stirrups as shear reinforcement.

In the analytical program, a softened truss shear transfer model based on "The Theory of Shear Transfer for Reinforced Concrete" proposed by Hsu et al.[7], is presented. The theory is based on the truss model and incorporates a softened stress-strain relation for the concrete. For the purpose of this work, this model has been modified in order to account for the addition of fiber to the concrete mixture, and to predict with more accuracy the pre-cracking behavior.

1.3 ORGANIZATION OF THE THESIS

This thesis is divided into five parts. Chapter 2 reviews the applications of fibers in concrete and the shear behavior of FRC materials. Chapter 3, briefly reviews some of the shear transfer models available, and describes in detail the softened truss shear transfer model used in the analysis. Also, the material laws (stress-strain relations) used for the different materials involved, and the

application of the model to the shear transfer problem being studied are presented.

Chapter 4 deals with the experimental work performed, describing the test specimens and materials used, the manufacturing procedure, the test set-up, and the testing procedure. Chapter 5 reports and discusses the results obtained in the experimental program, and compares these results to the predictions obtained from the model described in Chapter 3. Chapter 6 summarizes the conclusions obtained in Chapter 5, and suggests possible directions for future research.

CHAPTER 2

REVIEW OF THE SHEAR TRANSFER BEHAVIOR OF FRC

2.1 USE OF FIBERS IN CONCRETE

The problems of low tensile strength and relatively low toughness that concrete shows, may be overcome by the addition of short, randomly oriented, high strength and ductile fibers. As with other ancient building materials, like sun-dried mud bricks (adobe), the addition of fibers to a brittle matrix is not new. In the case of the adobe, such improvements as better cracking resistance, and better resistance to fragmentation, were obtained by adding straw fibers to the mud[8].

In the case of portland cement, patents dating as early as 1847 exist, where the addition of continues fibers in the form of a wire mesh to concrete was suggested[8]. This idea in turn developed into what is now known as ferrocement and fiber reinforced concrete. Since then, it has been the dream, and challenge of civil engineers to develop a cementitious material which is ductile with relative high tensile strength, and that it can be easily produced. The research effort in this area has intensified in the last 30 years, leading to publications with design applications as the ACI Committee 544 report "Design Considerations for Steel Fiber Reinforced Concrete"[9].

Up to now, the applications of fiber reinforced concrete(FRC) has been limited to laboratory experiments, with some full scale uses like airport runways, roadways[8,10], and special applications in bank vaults, missile silos, pile caps, and in heavy duty industrial flooring in workshops.

In general, the advantages of adding fibers to concrete can be summarized as: 1) significant increase in toughness or energy absorption capacity, increase of ultimate tensile load, and 2) provide a good crack-control mechanism. These characteristics are usually present at low percent volume of fibers, at 2% or less. Nevertheless, these advantages are accompanied by two main problems: reduced workability of the fresh concrete mixture, and added cost due to the addition of fibers.

In general, the fiber properties, will determine the characteristics of the composite. The main purpose of adding the fibers to a concrete matrix is to slow down or arrest crack propagation by bridging possible cracks. This can be achieved by using:1) high modulus fibers which absorb considerable amounts of energy due to the work required to pullout the fiber from the matrix; or 2) low modulus fibers that absorb energy by yielding and plastic deformation. Addition of fibers with a higher modulus than the matrix and with tensile strength higher than the fiber-matrix bond strength, will result in higher cracking strength and ultimate load for the composite. On the other hand, the addition of fibers with low modulus of elasticity, high ductility and a tensile strength lower than the fiber-matrix bond will produce a very ductile composite, with no significant increase in the cracking or ultimate loads.

Many types of fibers have been used in the manufacture of FRC as: steel fibers, glass fibers, carbon fibers, natural vegetable fibers, synthetic fibers (polypropylene, nylon, polyethylen, acrylic, spectra), and aramid. A short description of the mostly used fibers follows:

Steel fibers. Steel fibers have been the most widely used type of fibers in the manufacturing of FRC. This type of fiber presents characteristics as: high tensile strength, high elastic modulus, sensitivity to corrosion[11], and relatively low cost. Composites with steel fibers are characterized by higher cracking and ultimate load strengths.

Polypropylene fibers. The use polypropylene fibers in FRC is relatively new, therefore its use has been limited when compared to steel fibers[12,13]. This synthetic fiber has a relatively low modulus, and the fibers tend to debond easily from the matrix, resulting in low pullout strengths. Some of the advantages these fibers presents are: resistance to most chemical attacks[14], and very low cost. Composites reinforced with polypropylene fibers are characterized by relatively high ductility, while cracking and ultimate strengths usually remain unaffected.

Glass fibers. Glass fibers have good tensile strength and modulus of elasticity. While this fiber shows good mechanical properties, it has durability problems when exposed to an alkali environment like concrete[15]. One of the main objectives on recent research of this type

of fiber has been the possibility of replacing asbestos fibers with glass fibers.

Carbon fibers. Carbon fibers are obtained from organics such as polyacrylonitrik and agricultural waste. These type of fibers are characterized by high stiffness and tensile strength, with good resistance to alkali attack[16,17]. The main problem with these type of fibers is their high cost of manufacture.

Aramid fibers. Aramid fibers are an organic fibers, with a high modulus of elasticity. These fibers have a questionable durability in concrete[18,19]; therefore, further research to assess the durability of aramid in concrete is needed.

2.2 APPLICATION OF FRC TO SHEAR TRANSFER

As before mentioned, FRC has the advantages of being a more ductile material and having higher ultimate tensile strength than conventional concrete, two characteristics that are very desirable in the shear transfer mechanism, specially in the case of high strength concrete. Previous research efforts on the shear behavior of FRC are limited compared to those on tension or flexure[20]. Furthermore, in the existing reports on the shear behavior of FRC, steel fibers have been mostly used. While other fibers used in cement composites include, glass fibers, carbon fibers, natural vegetable fibers, synthetic fibers (polypropylene, nylon, polyethylen, acrylic, spectra), and

Aramid; very little is known on the shear behavior of FRC with these fibers[21].

2.2.1 Review of Previous Work

In the following review of the literature on the shear behavior of FRC, the tests performed have been categorized in two main groups: direct shear tests, and tests on beams or corbels. The direct shear tests are required in order to understand the basic shear transfer behavior of FRC; while the tests on beams and corbels, are necessary to understand the behavior of FRC structures.

Kohno et al.[22] have performed direct simple and double shearing strength tests to investigate the effects of factors such as the aggregate size, fiber content, and the aspect ratio of steel fibers on the shearing strength of steel fiber reinforced concrete(SFRC). In this study, it was found that the optimum fiber aspect ratio was approximately 60, while the optimal fiber content was found to be between 1.0 to 1.5% by volume. Also, in this report, the authors recommended a 10-15 mm maximum aggregate size for SFRC.

Hara[23] used push-off specimens to study the capacity of SFRC under combined shear and compressive loading. In order to achieve different levels of compressive loading, the shear plane angle in the push-off specimens was varied from 0 to 20 degrees. The author reported significant shear strength increases at a fiber contents of 1.0 and 1.5% by volume. Hara also investigated the improvements of SFRC when used in conjunction with standard steel reinforcement, finding significant ultimate strength and ductility gains. Individual

fiber pullout test reported by Hara showed significantly higher strength for crimped fibers over plain fibers.

Van de Loock[24] performed shear test on precracked fiber reinforced concrete push-off specimens with external bars normal to the cracked plane, which provided a passive confining stress. In his study, he reported that fiber influence decreased as the normal stress was increased.

Swamy et al.[25] used push-off specimens with both initially uncracked and cracked shear planes, to investigate the effect of steel fiber content, stirrup amount, and concrete type (normal vs light weight) on the shear transfer behavior. The shear strength was found to increase on both initially cracked and uncracked specimens by the addition of fibers. Fibers did not affect the initial shear stiffness, while they contributed significantly to post-maximum load deflection and strain softening. In general, the authors found steel stirrups to be more effective than fibers alone in shear transfer of normal strength reinforced concrete; but when comparing light weight concrete to normal weight concrete, fibers showed to be more beneficial to the light weight concrete shear transfer behavior. For the case of initially cracked specimens, Coulomb's friction criterion was found to relate well to experimental results.

Barr[26], studied the effect of the specimen geometry and fiber content on the direct shear strength of FRC, including three types of fibers: steel, polypropylene and glass fibers. From the experimental results, he found that the geometry of the test specimen did not affect significantly the shear strength of FRC. For the case of SFRC, the shear strength remained unchanged for different fiber contents,

while for polypropylene fibers the shear strength decreased for increasing fiber content. The shear strength of glass fiber reinforced concrete was found to increase with increasing fiber content.

Tan et. al.[27], studied the effect of steel fibers and steel stirrups in the shear transfer of push-off specimens with initially uncracked shear plane. In the experiments performed, it was found that steel fibers enhance the strength and deformation characteristics of normal strength concrete; and that the shear resistance increases substantially with increases in the amount of steel stirrups crossing the shear plane.

Shear tests involving corbels have been reported by Fattuhi[28] and Hara and Kitada[29]. A number of researchers have also reported combined shear and flexural tests on beams to investigate the mechanical improvements provided by the use of SFRC. For example, works by Shanmugan and Swaddiwudhipong[30], Swamy and Bahia[31,32], Narayan and Darwish[33], and Sharma[34]. Ward et al.[35] have also performed shear and flexural tests on beams made of fiber reinforced mortar, including steel, aramid, acrylic, and high-modulus polyethylene fibers. From these tests, Ward et al. have found that, in general, the shear strength of beams can be described by two functions depending on the shear span to depth ratio (a/d) of the beam. For a/d ratios equal or less than 2.5, the shear strength was found to be a function of: the splitting tensile strength, the flexural strength, the longitudinal reinforcement, and a/d. On the other hand, for a/d ratios greater or equal to 2.5, the shear strength was found to be depend on: the flexural strength, the longitudinal reinforcement, and a/d.

From the review of these reported tests it can be stated that the addition of fibers generally improves the shear strength and ductility of the concrete. Some researchers have reported that SFRC could complement or completely replace stirrups[36,37,38,39]. However, thus far, very few tests have been reported on the shear behavior of FRC, with limited parameters and thus the results may be regarded as interim. This lack of previous research is even greater for the shear transfer behavior of fiber reinforced high strength concrete, where no previous work was found for this type of material; probably due to the relative short history of this material. More experimental research efforts are needed in this respect.

CHAPTER 3

SHEAR TRANSFER MODELING

3.1 REVIEW OF SHEAR TRANSFER MODELS

Several mechanisms or models for the transfer of shear forces can be identified depending on the structural element being studied. In general, all the mechanisms are derived from one or a combination of the two theories mentioned in Section 1.1: 1) shear friction theory, and 2) truss action theory. A brief review of the shear transfer mechanism for some selected structural elements follow.

In the case of beams, the shear transfer behavior before cracking can be represented by assuming the member to be homogeneous, isotropic and elastic[3,40]. After cracking, the shear transfer mechanism changes. For beams with a shear span to depth ratio (a/d) equal or greater than 5 the shear mechanism is shown in Fig. 3.1. The shear resistance in this new mechanism can be described by the sum of: 1) the shear transferred by the still uncracked portion of the concrete section, V_c, 2) the interface shear transfer across the crack by aggregate interlock and friction, V_a, 3) the dowel action by the longitudinal reinforcement, V_d, and 4) the

force transferred in direct tension by the web reinforcement, if present, V_s.

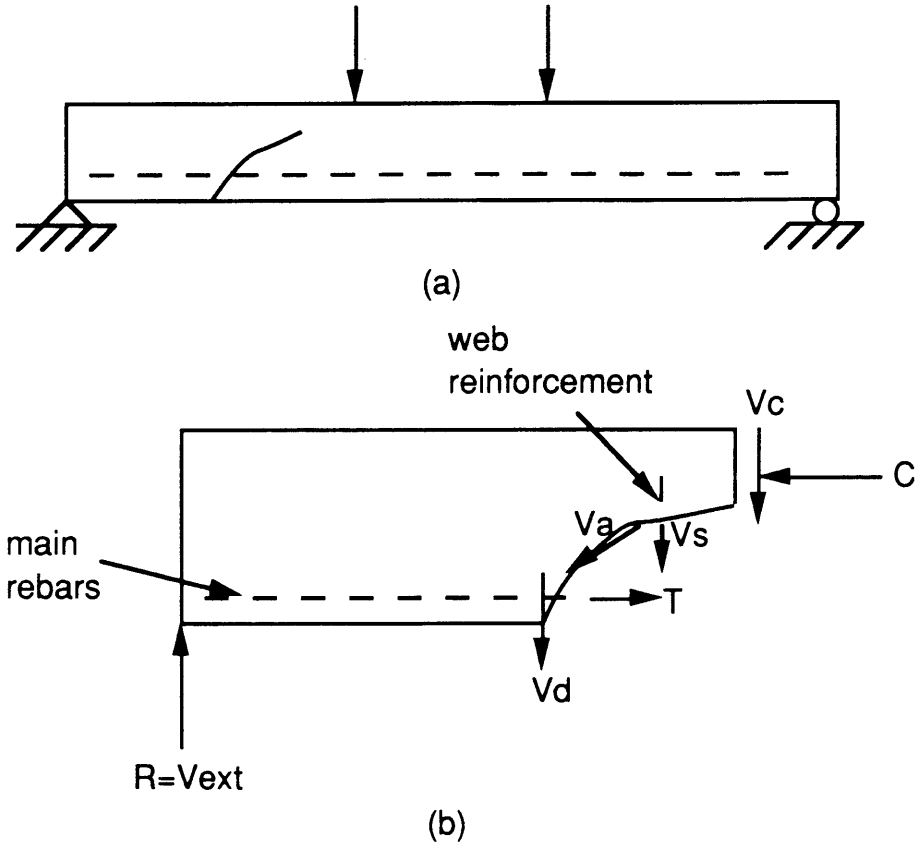

Fig. 3.1 Shear transfer in diagonally cracked beam: (a) cracked beam, (b) free body of the beam to the left of the diagonal crack.

For deep beams, that is beams having a ratio of span to depth of 5 or less, the shear transfer mechanism after cracking can be represented as a tied-arch[40], as shown in Fig. 3.2. Here, the shear forces are being transferred by direct transfer of thrust between the point of load application and the supports. The horizontal components of this thrust are balanced by the compression carried by the concrete on the top of the beam, and by the tensile force

carried by the main longitudinal reinforcement on the bottom. For this mechanism to be effective a/d should be 2 or less; and good anchorage of the main reinforcement should be provided[3].

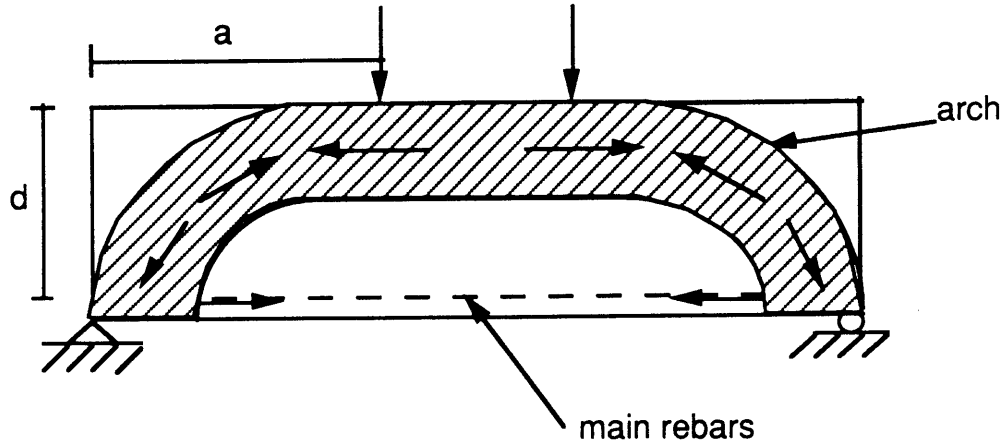

Fig. 3.2 Tied-arch mechanism for shear transfer in deep beams.

In the case of brackets or corbels, a truss-like action develops[40], as shown in Fig. 3.3. The compressive force, C, is carried in the diagonal compression struts isolated by the cracks, while the main reinforcement develops the tensile force, T, creating a truss-like action.

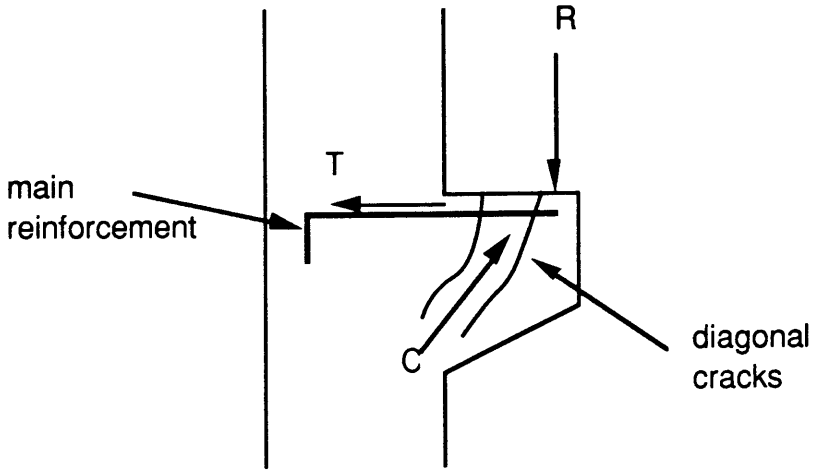

Fig. 3.3 Truss mechanism for shear transfer in corbels.

In general, analytical models describe the precracking shear behavior of reinforced concrete by assuming the material to be homogeneous, isotropic and elastic[3,4,40]. Other shear transfer models by Fardis and Buyukozturk[41], Bazant and Gambarova[42], and Walraven[43] have described the shear transfer behavior across a single pre-existing crack. These models have been based on: the interface shear transfer behavior across a single crack, the shear stiffness due to reinforcing bars crossing the crack, and shear-slip relations. In the case of the interface shear transfer behavior of a single crack, this crack has been idealized as having a sawtooth shape with an initial crack width, w_o, and a coefficient of friction ϕ_u for the crack surfaces. The shear stiffness due to the reinforcing bars crossing the crack has been described in terms of two components: the normal stiffness, K_n, dependant on the bar area, the bar modulus of elasticity, and the average crack spacing; and the dowel stiffness, K_d, function of the bar size, embedment length, support conditions of the bar given by the surrounding concrete, concrete strength, deterioration of the bond between the bar and the concrete, splitting of concrete, etc. Shear-slip relations have been modeled to be primarily to be a function of: the crack width, wo, the dowel stiffness, K_d, and the stiffness normal to the crack, K_n. In order to apply this model, an overall crack pattern, i.e. orthogonal cracking pattern, has to be assumed. This is necessary since it is almost impossible to accurately predict the location of cracks in a given element.

The shear transfer behavior of reinforced concrete is difficult to model due to the usually complicated stress distribution induced by shear loading in structural elements, and the uncertainty of the

shear behavior of plain concrete. In practice, this lack of understanding of the shear transfer behavior of reinforced concrete has resulted in design philosophies based on empirical or semi-empirical approach[5]. For this reason, there is a need for a theoretical shear transfer model that can describe the shear behavior of reinforced concrete as well as plain concrete. This model should be able to predict both shear stresses and the deformations associated with these shear stresses.

3.2 SOFTENED TRUSS SHEAR TRANSFER MODEL

The model presented in this thesis is based on the "Theory of Shear Transfer Strength of Reinforced Concrete" proposed by Hsu et al.[7]. The main difference between this theory and other porposed models mentioned before, is that this theory deals with the overall shear behavior and is not based on the behavior of a single pre-existing crack. Here, the proposed theory has been modified in order to incorporate the effect of fibers in the concrete mix. Also, a successful attempt to improve the model predictions for the pre-cracking stage in the load-deflection curve has been included. The objective of the model, is to predict the shear stress vs. shear strain relationship for the shear transfer problem being studied.

3.2.1 Overview

The model is based on the truss model theory, considering the softening of concrete in compression due to the presence of a biaxial stress state. A brief description of the model follows. Considering an orthogonally reinforced concrete element, the stress state of this element can be represented by in-plane shear, τ_{lt}, and normal stresses, σ_l and σ_t, as shown in Fig. 3.4a. By assuming that the steel reinforcement only develops normal stresses, σ_{ls} and σ_{ts}; the stress state of the reinforced concrete element can be resolved into the contribution of the concrete element and the reinforcing steel (Fig. 3.4b&c). Furthermore, the stresses in the concrete can be resolved into the d-r axes, which coincide with the principal stress and strain axes for the concrete element (Fig. 3.4d&e). The reinforced concrete element is assumed to behave as a truss system at all loading stages, where the concrete is subjected to biaxial stress state, compression in the d-direction and tension in the r-direction, and the steel reinforcement only carries normal stresses. The steel reinforcement develops tensile stresses in the longitudinal direction, σ_{ls}, and compressive stresses in the transverse direction, σ_{ts}. This truss action must satisfy: a) equilibrium, b) compatibility, and c) materials laws. In the material laws, each direction, r and d-direction, is treated separately, taking into account the biaxiality effects in both the tensile and compressive behavior of concrete. Also, no confinement effects from the steel bars on the concrete behavior are considered.

For the pre-cracking behavior, the reinforced concrete element is assumed to behave as linear elastic material, that satisfies the 3 requirements of: equilibrium, compatibility and material laws. Also, for this phase, the biaxiality effect is addressed by softening the concrete's pre-cracking tensile behavior[44]. Since the concrete is assumed to be under a biaxial state of stress (compression-tension), as shown in Fig. 3.4e, the compressive stress induces strain in the direction of the tensile stress, lowering the apparent stiffness of the concrete in the tensile direction. For this, an empirical constant was

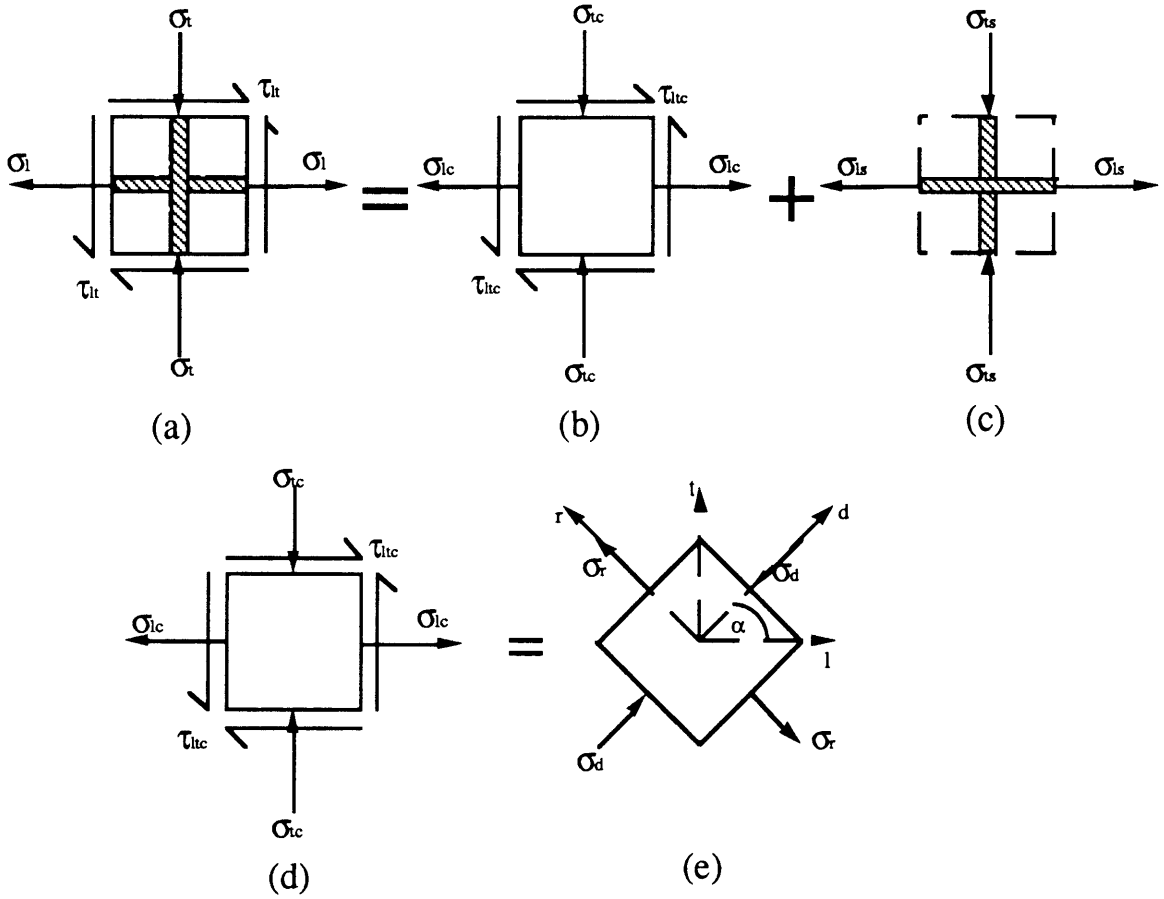

Fig. 3.4 Shear transfer model: (a) Reinforced concrete element, (b) stresses in the concrete element, (c) stresses in the steel, (d) stresses in the concrete in l-t axes, (e) stresses in the concrete principal axes d-r.

found for normal and high strength concrete equal to 0.35 and 0.40 respectively. These constants were obtained from the shear tests performed on plain normal strength and high strength concrete, which will be explained in Chapter 4. These empirical constants were used to lower the pre-cracking stiffness of concrete in tension for all the tests analyzed, by multiplying them with the respective uniaxial stiffness of concrete (E_t). The softening of concrete in compression due to biaxiality effects is addressed at both pre-peak and post-peak stages by λ, which in turn is a function of the tensile strain, ε_r, and the compression strain, ε_d. The model assumes a uniform shear stress and shear strain distribution over the shear plane at all stages of loading. In a shear test performed, described later in Chapter 4, the shear strain distribution at all loading stages was studied. From this test it was found that the assumption of uniform distribution was valid for the post cracking behavior, but did not apply to the precracking stage. For this reason, the precracking behavior was calibrated as described in Chapter 5.

3.2.2 Equilibrium

By super-imposing the contributions of the concrete and steel stresses in the element shown in Fig. 3.4, the following equilibrium equations can be obtained by using Mohr's stress circle:

$$\sigma_1 = \sigma_d \cos^2(\alpha) + \sigma_r \sin^2(\alpha) + \rho_1 f_1 \qquad \text{Eq. 3.1}$$

$$\sigma_l = \sigma_d \sin^2(\alpha) + \sigma_r \sin^2(\alpha) + \rho_t f_t \qquad \text{Eq. 3.2}$$

$$\tau_{lt} = (\sigma_d - \sigma_r)\sin(\alpha)\cos(\alpha) \qquad \text{Eq. 3.3}$$

where σ_i=normal stress; τ_i=shear stress; f_i=steel stress; ρ_i=steel bar reinforcement ratios, defined as the area of steel, A_S, divided by the total area of the section; α=angle of inclination of the d-r axes with respect to the l-t axes, and i= l,t,d and r for their respective axes. All stresses are positive in tension.

3.2.3 Compatibility

The strain compatibility equations for the reinforced concrete element in Fig 3.4, can be expressed using the Mohr's strain circle as:

$$\varepsilon_l = \varepsilon_d \cos^2(\alpha) + \varepsilon_r \sin^2(\alpha) \qquad \text{Eq. 3.4}$$

$$\varepsilon_t = \varepsilon_d \sin^2(\alpha) + \varepsilon_r \cos^2(\alpha) \qquad \text{Eq. 3.5}$$

$$\gamma_{lt} = 2(\varepsilon_d - \varepsilon_r)\sin(\alpha)\cos(\alpha) \qquad \text{Eq. 3.6}$$

where, ε_i=normal strains, γ_i=shear strain.

3.2.4 Material Laws

(a) Steel Reinforcement

For the transverse and longitudinal steel bars, the steel is assumed to behave as an elastic-perfectly plastic material, as shown in Fig. 3.5.

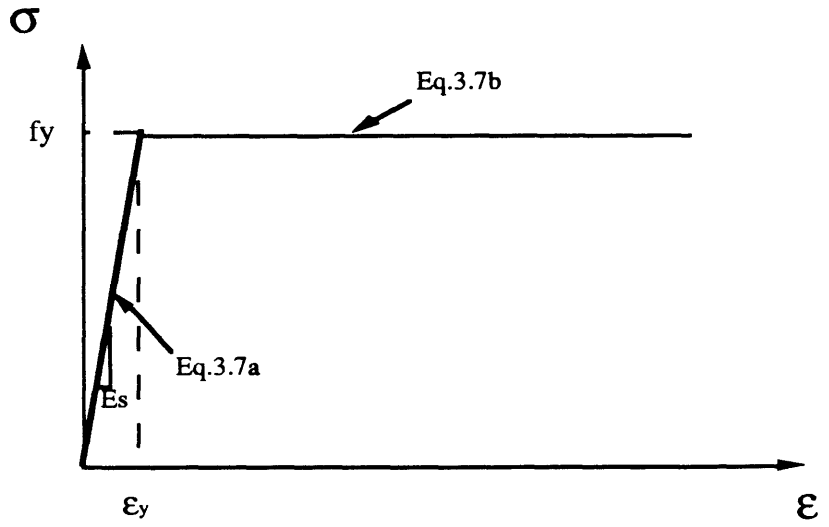

Fig. 3.5 Idealized stress-strain curve for steel

Thus, the behavior of the steel reinforcement can be described by the following equations:

$$\text{for } \varepsilon_{l,t} < \varepsilon_y \quad f_{l,t} = E_s \varepsilon_{l,t} \qquad \text{Eq. 3.7a}$$

$$\text{for } \varepsilon_{l,t} \geq \varepsilon_y \quad f_{l,t} = f_y \qquad \text{Eq. 3.7b}$$

where, E_S=modulus of elasticity of steel, and f_y and ε_y are the yield stress and strain for steel respectively.

(b) Concrete

Since the testing program involved six different types of materials, namely: normal strength concrete (NC), steel fiber reinforced normal strength concrete (SNC), polypropylene fiber reinforced normal strength concrete (PNC), high strength concrete (HC), steel fiber reinforced high strength concrete (SHC), and polypropylene fiber reinforced high strength concrete (PHC); in the

model different stress-strain behaviors for both tension and compression were adopted as needed. The model used the uniaxial stress-strain curves for the compressive and tensile behavior of concrete, taking into account the biaxiality effects. The following is a description of the relations used for each type of concrete.

1. Compressive Behavior of Concrete

For the compressive behavior of the different concretes used, it was assumed that they all behave basically in the same manner as shown in Fig. 3.6, but with different parameters. These parameters, namely the peak and ultimate strains, identify the type of concrete involved, where it is normal or high strength, and whether if steel or polypropylene fibers are included [1,45,46]. The assumed values for these strains for each type of concrete are contained in Table 3.1.

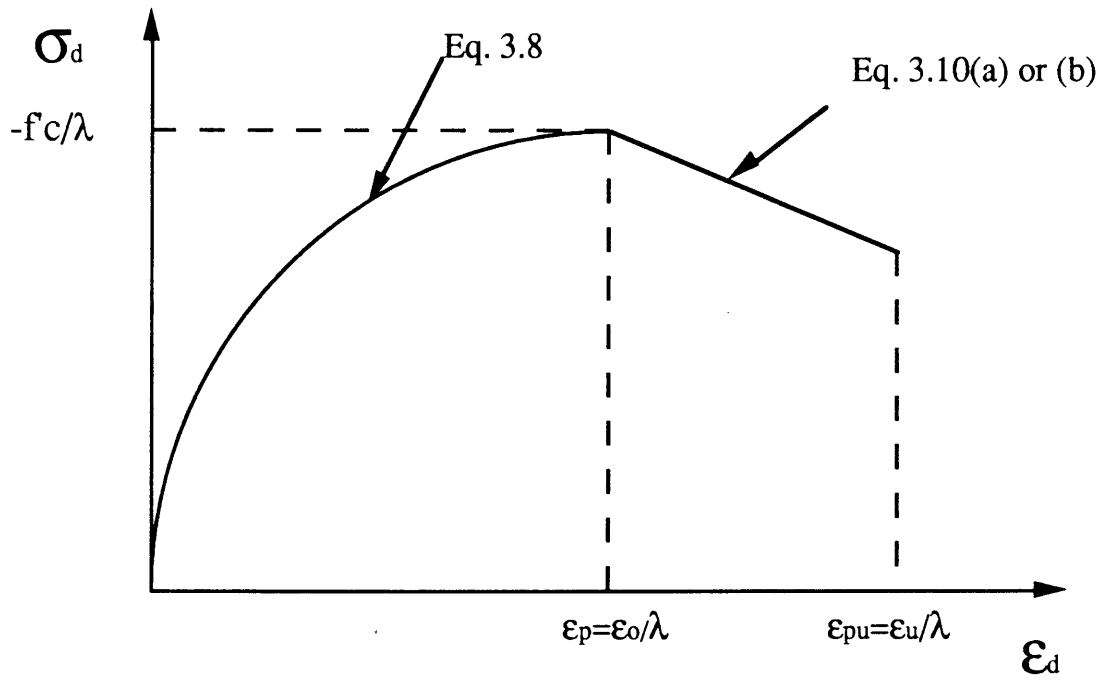

Fig. 3.6 Idealized stress-strain curve for concrete in compression.

Table 3.1 Peak and ultimate strains used for the different types of concrete.

CONCRETE TYPE	PEAK STRAIN(ε_o)	ULTIMATE STRAIN(ε_u)
NSC	-0.002	-0.0035
SFRNSC	-0.0035	-0.005
PFRNSC	-0.002	-0.0035
HSC	-0.0025	-0.003
SFRHSC	-0.003	-0.0045
PFRHSC	-0.0025	-0.0035

For the ascending branch of the compressive stress-strain curve, the same relation was used for all types of concrete[46]:

$$\text{for } |\varepsilon_d| \leq |\varepsilon_p| \quad \sigma_d = f'_c \left[2\left(\frac{\varepsilon_d}{\varepsilon_o}\right) - \lambda\left(\frac{\varepsilon_d}{\varepsilon_o}\right)^2 \right] \qquad \text{Eq. 3.8}$$

$$\lambda = \sqrt{0.7 - \frac{\varepsilon_r}{\varepsilon_d}} \qquad \text{Eq. 3.9}$$

where, ε_d=compressive strain of concrete, ε_o=peak strain for uniaxial compression, $\varepsilon_p=\varepsilon_o/\lambda$, f'_c=cylinder compressive strength, ε_r=tensile strain of concrete, and λ is the coefficient that incorporates the softening of concrete.

Similarly, for the descending branch of the compressive stress-strain curve, the same relation is assumed for all mixes involving NC or NC plus fibers[46]:

$$\text{for } |\varepsilon_d|>|\varepsilon_p| \quad \sigma_d = \frac{f'_c}{\lambda}\left[1-\left(\frac{\frac{\varepsilon_d}{\varepsilon_o}-\frac{1}{\lambda}}{2-\frac{1}{\lambda}}\right)^2\right] \qquad \text{Eq. 3.10a}$$

For the mixes involving HC or HC plus fibers, SHC and PHC, the following relation was assumed[3]:

$$\text{for } |\varepsilon_d|>|\varepsilon_p| \quad \sigma_d = \frac{f'_c}{\lambda} - 0.15f'_c\frac{(\varepsilon_d-\varepsilon_p)}{(\varepsilon_u-\varepsilon_o)} \qquad \text{Eq. 3.10b}$$

Here again, different values for ε_o and ε_u were used according to the type of concrete being analyzed (see Table 1).

2. Tensile Behavior of Concrete

For all types of concrete used, the same behavior was assumed for the pre-peak stage in the stress-strain tensile curve. On the other hand, for the post-peak behavior, significant differences were adopted corresponding to whether or not the mix contained fibers (see Fig. 3. 7). These differences arise due to the effect of fibers, that increase the toughness of the material. In the model, a maximum stress criterion is used to determine first cracking.

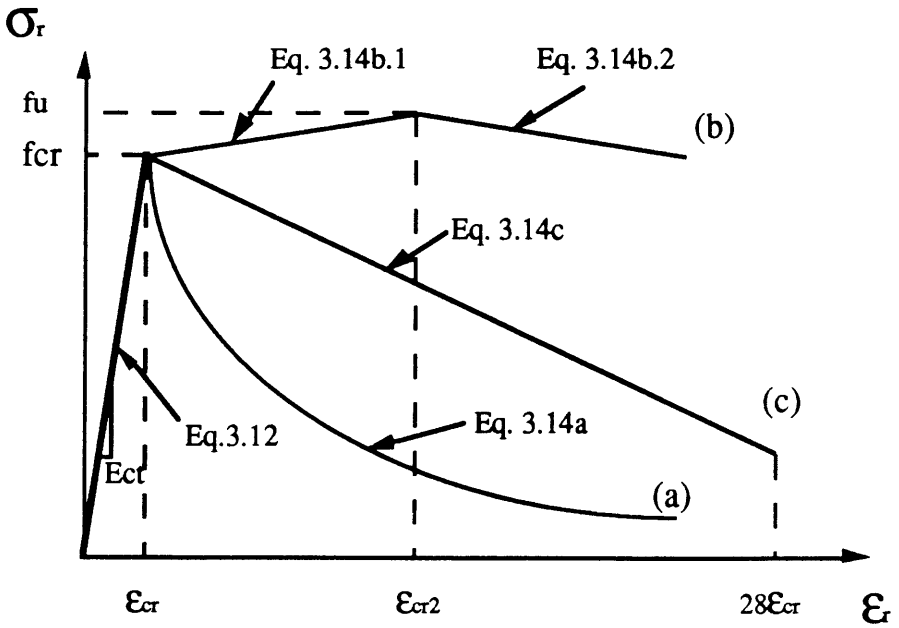

Fig. 3.7 Idealized stress-strain curves in tension for: (a) plain concrete (NC and HC), (b) steel fiber reinforced concrete (SNC and SHC), and (c) polypropylene fiber reinforced concrete (PNC and PHC).

The initial stiffness of the concrete in tension (E_t) was obtained by using a modified law of mixtures, that take into account the addition of randomly oriented fibers to the concrete mix[47]. Further, as mentioned before, this initial stiffness was lowered by means of an empirical constant, C, in order to account for biaxiality effects. The equation used was:

$$E_{ct} = C(E_{mt}V_{mt} + E_f V_f \eta_l \eta_o) \qquad \text{Eq. 3.11}$$

where, E_{ct}=modulus of the composite in tension (psi), C= empirical constant equal to 0.35 and 0.40 for NC and HC respectively, E_m= modulus of the concrete, equal to $E_m = 40{,}000\sqrt{f'_c} + 1{,}000{,}000_{psi}$[48], V_m=volume percent of the concrete in the mix, E_f=modulus of the fibers, V_f=volume percent of fibers in the mix, η_o=orientation factor

(=0.14)[47], and η_l=length efficiency factor[47]. Both η_o and η_l are needed in the formulation because of the random distribution of the fibers in the concrete matrix. For the case where no fibers are used, Eq. 11 becomes:

$$E_{ct} = C(E_{mt}) \qquad \text{Eq. 3.11a}$$

Using the above described equations, the pre-cracking behavior of concrete in tension for NC, PNC, HC, and PHC, can then be defined as:

$$\text{for } \varepsilon_r \le \varepsilon_{cr} \quad \sigma_r = E_{ct}\varepsilon_r \qquad \text{Eq. 3.12}$$

where, ε_{cr}=cracking strain=f_{cr}/E_{ct}, and f_{cr}, cracking stress, is equal to $7.5\sqrt{f'_c}$ for NC and PNC and $6\sqrt{f'_c}$ for HC and PHC.

For the case of SNC and SHC a different equation was used to calculate the cracking strain, in order to account for the increase in cracking strength due to the addition of steel fibers. The cracking strain, ε_{cr}, for these mixes was calculated using the formula proposed by Nathan, Paramasivam, and Lee[47]:

$$\varepsilon_{cr} = \eta_l \eta_o V_f (\varepsilon_{fp} - \varepsilon_{mp}) + \varepsilon_{mp} \qquad \text{Eq. 3.13}$$

where, ε_{cr}=cracking strain of the composite, η'_o=orientation factor at cracking (=0.405)[47], ε_{fp} and ε_{mp} are the strains at the proportionality limit for the fiber and matrix respectively.

The post-peak tensile behavior, as mentioned before, is dependant on the type of fiber present in the mix, or if the mix is plain (no fibers). For the case of NC or HC, the same relation for the post-peak behavior was used (Fig. 3.7a)[46]:

$$\text{for } \varepsilon_t > \varepsilon_{cr} \quad \sigma_t = \frac{f_{cr}}{1+\sqrt{\frac{\varepsilon_t - \varepsilon_{cr}}{0.005}}} \qquad \text{Eq. 3.14a}$$

In the case of concrete reinforced with steel fibers (SNC and SHC), the post-peak behavior was assumed to be bilinear (Fig. 3.7b); described by the following equations:

$$\text{for } \varepsilon_{cr} < \varepsilon_t < \varepsilon_{cr2} \quad \sigma_t = f_{cr} + E_f V_f \eta_1 \eta_o (\varepsilon_t - \varepsilon_{cr}) \qquad \text{Eq. 3.14b.1}$$

$$\text{for } \varepsilon_t > \varepsilon_{cr2} \quad \sigma_t = f_u - E_f V_f \eta_1 \eta_o (\varepsilon_t - \varepsilon_{cr2}) \qquad \text{Eq. 3.14b.2}$$

where, ε_{cr2}= strain at the second peak tensile load= $\varepsilon_{cr}+\sigma_{sfu}/E_{sf}$, $f_u=f_{cr}+\eta_1\eta_o'V_{sf}E_{sf}$, and σ_{sfu} , E_{sf} are the ultimate steel fiber strength and modulus, respectively.

In the case of concrete involving polypropylene fibers (PNC and PHC), since no simple model describing the post-peak behavior was found; it was assumed to be linearly decreasing up to a strain equal to 28 times the strain at cracking, where the stress was 0.3 times f_{cr} (Fig. 3.7c). The equation used was:

$$\text{for } \varepsilon_t > \varepsilon_{cr} \quad \sigma_t = f_{cr} - \frac{0.7 f_{cr}}{28\varepsilon_{cr}}(\varepsilon_t - \varepsilon_{cr}) \qquad \text{Eq. 3.14c}$$

3.2.5 Application of Model to Shear Transfer Problem and Solution

By combining the equations given by equilibrium, compatibility and material laws (Eqs. 3.1-3.14), a system of 11 non-linear equations, involving 14 unknowns (σ_l, σ_t, τ_{lt}, σ_d, σ_r, f_l, f_t, ε_l, ε_t, γ_{lt}, ε_d, ε_r, α and λ) can be defined. These variables, as they are presented in the model, represent the average values for the element being studied. For the shear transfer problem being investigated (Figs. 3.8a,b), the stresses acting on an element located at the shear plane are shown in Fig. 3.8c.

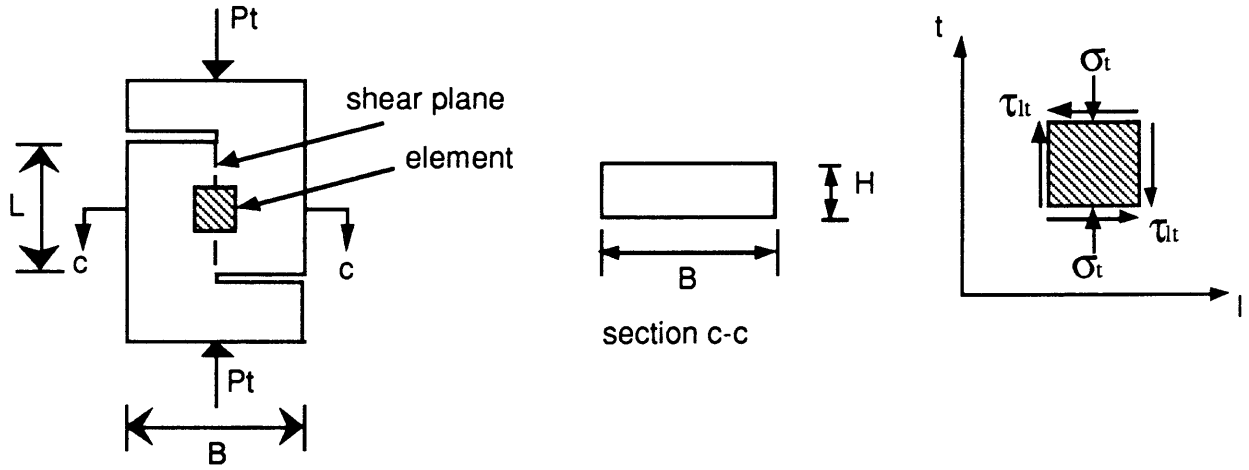

Fig. 3.8 Shear transfer problem: (a) and (b) push-off specimen, (c) stress state of element at shear plane.

τ_{lt} is defined as the average shear stress acting on the shear plane, and is equal to:

$$\tau_{lt} = \frac{P_t}{BL} \qquad \text{Eq. 3.15}$$

where, P_t=externally applied load, B and L are defined in Fig. 3.8a.

Further, Hsu et al.[7] have demonstrated that τ_{lt} can be assumed to be uniform along the shear plane, relating it to σ_t by:

$$\sigma_t = K\tau_{lt} \qquad \text{Eq. 3.16}$$

and, since no load is being applied in the l-direction,

$$\sigma_l = 0 \qquad \text{Eq. 3.17}$$

where, K=L/B, with L and B defined in Fig. 3.8b.

Therefore, by substituting Eqs. 3.15-3.17 into the before described system of equations, a solution for τ_{lt} and γ_{lt} can be found for a given value of ε_d; which in the shear tests performed varied monotonically. The method of solution used for this system of equations was the one proposed by Hsu et al.[7]. A computer program was written for this purpose. A list of the program is contained in Appendix A.

CHAPTER 4

EXPERIMENTAL WORK

4.1 SCOPE

In the experimental program three variables were investigated, namely:

1) concrete type: high strength concrete ($f'c \approx 10{,}000$ psi) and normal strength concrete ($f'c \approx 4{,}000$ psi)

2) type of fiber: steel and polypropylene fibers

3) the presence of steel stirrups as shear reinforcement alone and in combination with either steel or polypropylene fibers

Both high strength and normal strength concrete were included in the program in order to compare the shear behavior as well as the effect of fiber and steel stirrups as shear reinforcement for these two materials. The volume fraction of the fiber was kept constant for all the concrete mixtures at 1% by volume for crimped-end steel fibers (or 3.27% by weight), and 1% by volume for polypropylene fibers (or 0.3% by weight). Crimped-end steel fibers were selected over other type of steel fibers due to the higher strength as well as ductility increases obtained over other type of steel fibers[49]. On the other hand, fibrillated polypropylene fibers were chosen because of high ductile behavior that this type of fibers adds to concrete.

The test program involved six different types of concrete, obtained by combining the two concrete types and one of the fibers, plus including mixes with no fiber reinforcement. The following is a list of the concrete types included in the test program, with the nomenclature used for each type in parenthesis:

1. normal strength concrete (NC)
2. steel fiber reinforced normal strength concrete (SNC)
3. polypropylene fiber reinforced normal strength concrete (PNC)
4. high strength concrete (HC)
5. steel fiber reinforced high strength concrete (SHC)
6. polypropylene fiber reinforced high strength concrete (PHC)

By combining the six types of concrete listed above and the presence of steel stirrups crossing the shear plane, the test program consisted of twelve different types of push-off specimens. That is, six specimen types for each type of concrete with no steel stirrups, and six specimens types for each type of concrete with stirrups. Again, as with the volume fraction of the fibers used, the amount of stirrups was kept constant, with 4 #3 bars crossing the shear plane (A_s=0.44 in^2) resulting in a 1.47% reinforcement ratio (ρ_l), for all the specimen types containing stirrups. The same nomenclature used for the concrete types was used for the specimen types with the variation of adding an "S" at the end of the denomination of specimen types containing steel stirrups (i.e., a specimen made out of normal strength concrete (NC) with steel stirrups was denoted by NCS). Table 4.1 contains the classification by type of shear reinforcement for all the specimen types included in the experimental program.

Table 4.1 Test specimen classification by type of concrete and shear reinforcement

Specimen denomination	Concrete Type	Vol. fraction steel fibers (Vsf %)	Vol. fraction polypropylene fibers (Vpf%)	Steel stirrup reinforcing ratio (ρ_l)
NC	NC	-	-	-
SNC	SNC	1.0%	-	-
PNC	PNC	-	1.0%	-
NCS	NC	-	-	1.47%
SNCS	SNC	1.0%	-	1.47%
PNCS	PNC	-	1.0%	1.47%
HC	HC	-	-	-
SHC	SHC	1.0%	-	-
PHC	PHC	-	1.0%	-
HCS	HC	-	-	1.47%
SHCS	SHC	1.0%	-	1.47%
PHCS	PHC	-	1.0%	1.47%

In the program, two specimens of each specimen types were tested, adding to 24 specimens. Information for cracking and maximum shear stresses as well as load-deflection characteristics of each specimen were recorded. Also, an additional test on a push-off specimen reinforced with steel stirrups was performed in order to investigate: the shear strain distribution along the shear plane of the specimen, and the strain in the steel stirrups as a function of the applied shear stress. The shear tests done on all of the push-off specimens, were complemented with compression and splitting tension tests on cylinder specimens made out of the respective type of concrete.

4.2 TEST SPECIMENS

Two types of specimens were used in this investigation. For the shear tests, push-off specimens, shown in Fig. 4.1, were used. These push-off specimens had overall dimensions of 21x10x3 in.; with a shear plane area of 30 sq. in. These dimensions were obtained from a report by Buyukozturk et al.[50]

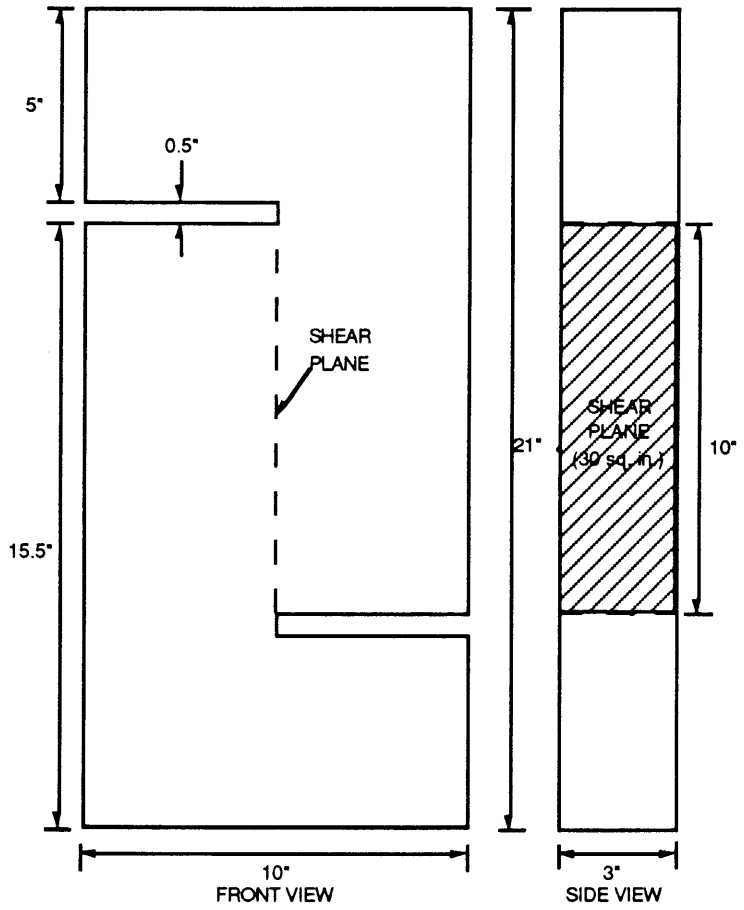

Fig. 4.1 Geometry of push-off specimen

All push-off specimens contained vertical reinforcement, in the form of L-shape #5 steel bars, in order to avoid any local failures anywhere in the specimen with exception of the shear plane (see fig.

4.2). The vertical reinforcement amounted to a reinforcement ratio of 8.27%(ρ_t) in the direction perpendicular to the shear plane. In addition, for the specimen types with steel stirrups crossing the shear plane, two steel hoops made with #3 steel bars were placed. The position of the hoops are shown with horizontal dotted lines in Fig. 4.2.

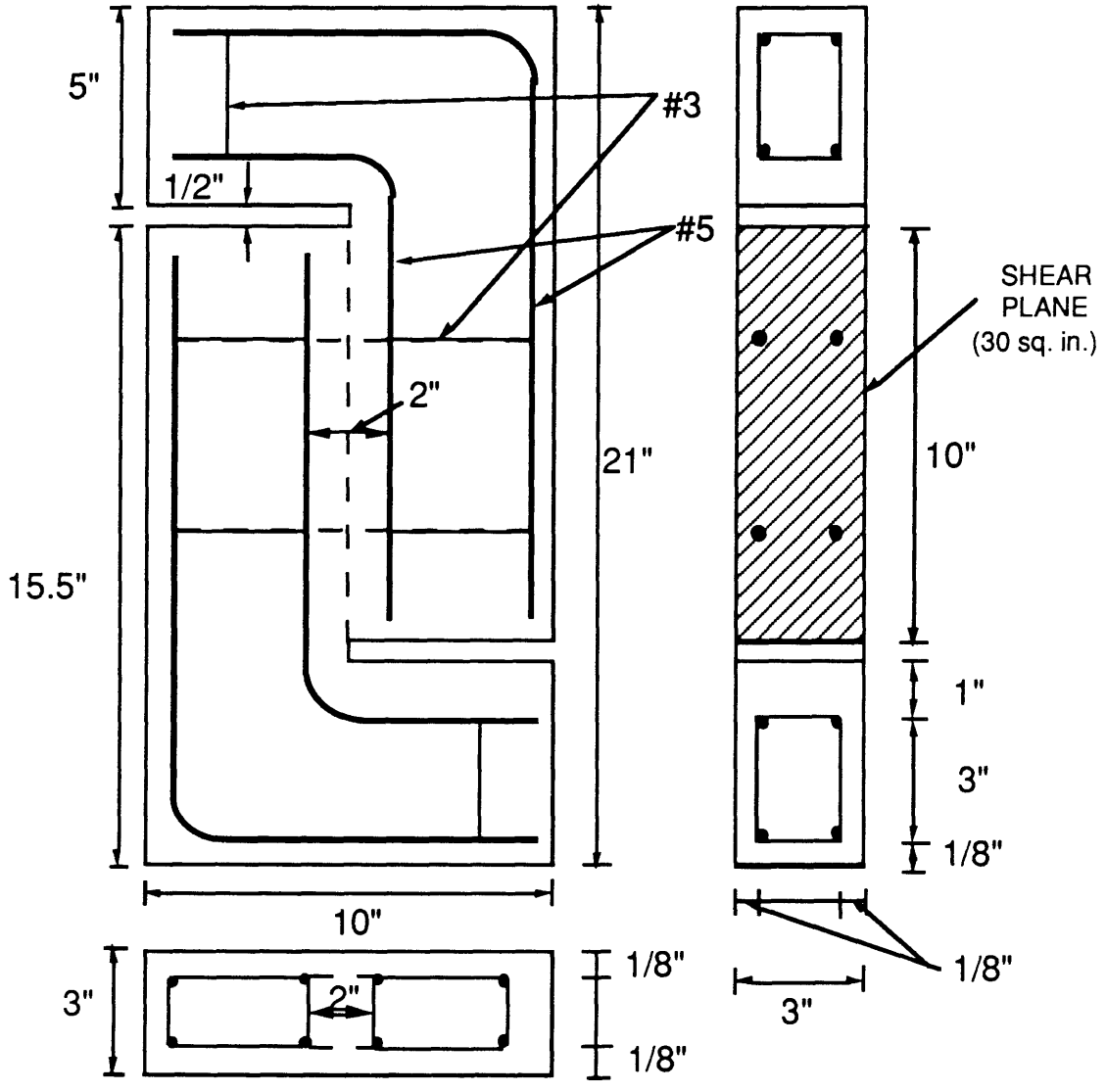

Fig. 4.2 Steel bar reinforcement distribution for push-off specimen.

In the compression and splitting tension tests, cylinders 3" wide by 6" tall were used. These dimensions meet ASTM standards for these type of tests.

4.3 BATCH DESIGN AND MATERIAL SELECTION

In the manufacturing of the test specimens the following materials were used: type I portland cement; pea gravel with maximum size aggregate size of 3/8"; mortar sand; silica fume in slurry form (to obtain high strength concrete); high range superplasticizer WRDA-19 (ASTM C-494 Type A&F); mild steel deformed bars (#3 and #5), with a yield strength of 60 ksi; polypropylene fibrillated fibers, 3/4" long (see Fig. 4.3); and crimped-end steel fibers, Dramix ZL 30/.50 , 30mm long with a 0.50 mm diameter (aspect ratio=60)(see Fig. 4.4), and a minimum yield strength of 150 ksi. The cement, sand and gravel were purchased from Waldo Bro. Co., located in Boston, MA.; the steel rebars were obtained from Barker Steel Co., in Watertown, MA.; and the silica fume, polypropylene and superplasticizer were donated by W. Grace Co., in Waltham, MA.

The mixing proportions used to prepare the normal and high strength concrete mixes are listed in Table 4.2. The high strength mix was designed to obtain a 9,000 to 10,000 psi compressive strength at 28 days, while the normal strength mix was designed to develop a 4,000 psi compressive strength at 7 days. Fibers were added to the fresh mix by volume, taking into account the volume of all the components in the mix. The concrete for each specimen type was

mixed in a separate batch, that is twelve batches were mixed throughout the experimental program.

Table 4.2 Concrete mix proportions by weight.

MIX	cement	sand-cement ratio	aggre.-cement ratio	silica fume-cement ratio	steel fibers (of total weight)	poly. fibers (of total weight)	super plast.-cement ratio	water-cement ratio
HC	1	2.0	2.0	5%	-	-	1%	0.35
PHC	1	2.0	2.0	5%	-	0.3%	1%	0.35
SHC	1	2.0	2.0	5%	3.27%	-	1%	0.35
NC	1	1.7	2.0	-	-	-	0.5%	0.40
PNC	1	1.7	2.0	-	-	0.3%	1%	0.40
SNC	1	1.7	2.0	-	3.27%	-	1%	0.40

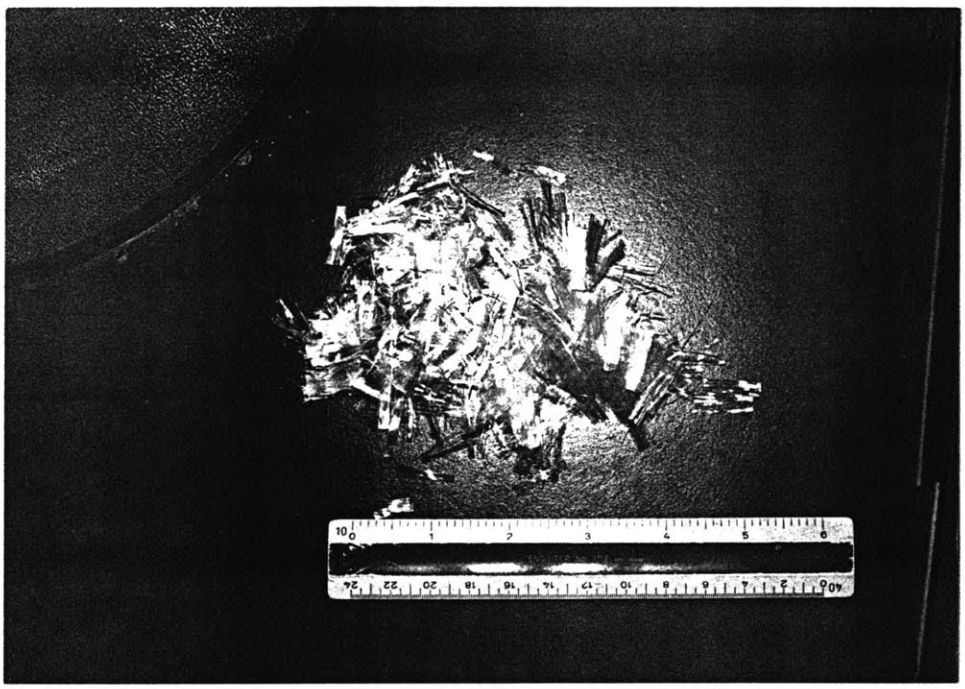

Fig. 4.3 Polypropylene fibers used in the investigation.

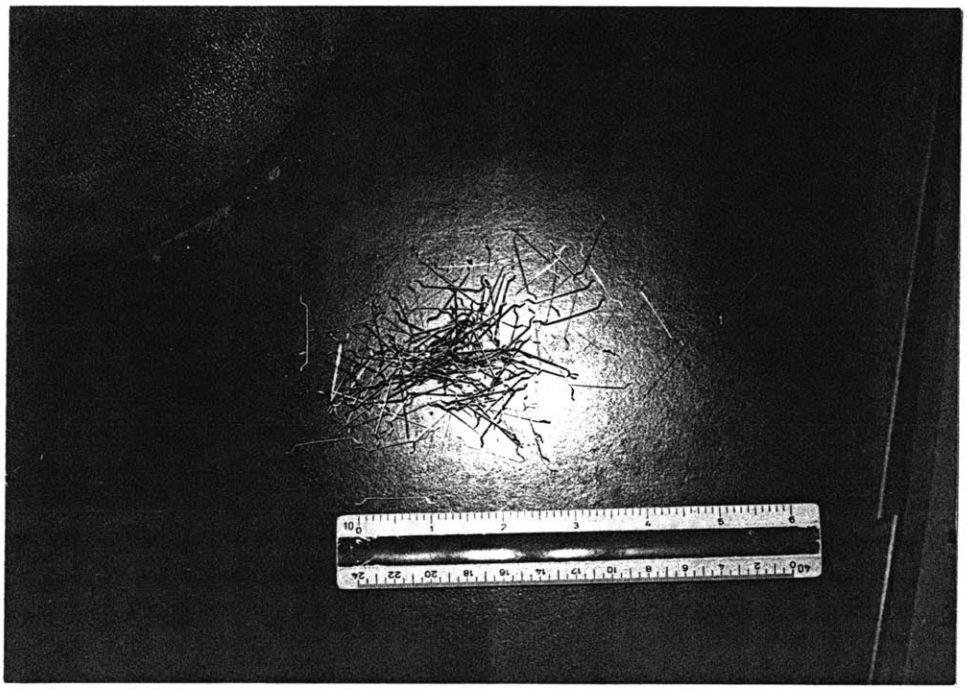

Fig. 4.4 Crimped-end steel fibers used in the investigation.

4.4 MANUFACTURING PROCEDURE OF TEST SPECIMENS

In the manufacturing of the push-off specimens, the first step was to prepare the steel bar reinforcement. The vertical L-shaped #5 bars were tied together using hoops made out of #3 bars. For the specimens with no steel bar reinforcement crossing the shear plane, the longitudinal reinforcement was assembled in two parts using small hoops to tie each portion (see Fig. 4.5). In the case of specimens containing steel stirrups, the bars were assembled as a unit using longer hoops, which made up the steel bars crossing the shear plane (see Fig. 4.6).

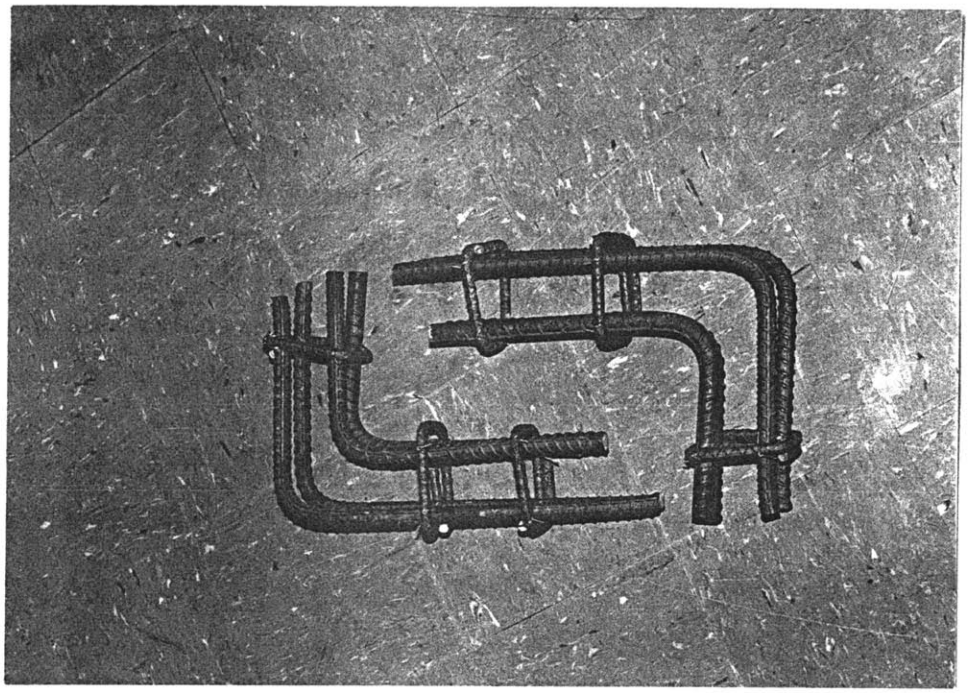

Fig. 4.5 Steel reinforcement for push-off specimens with no steel stirrups crossing the shear plane.

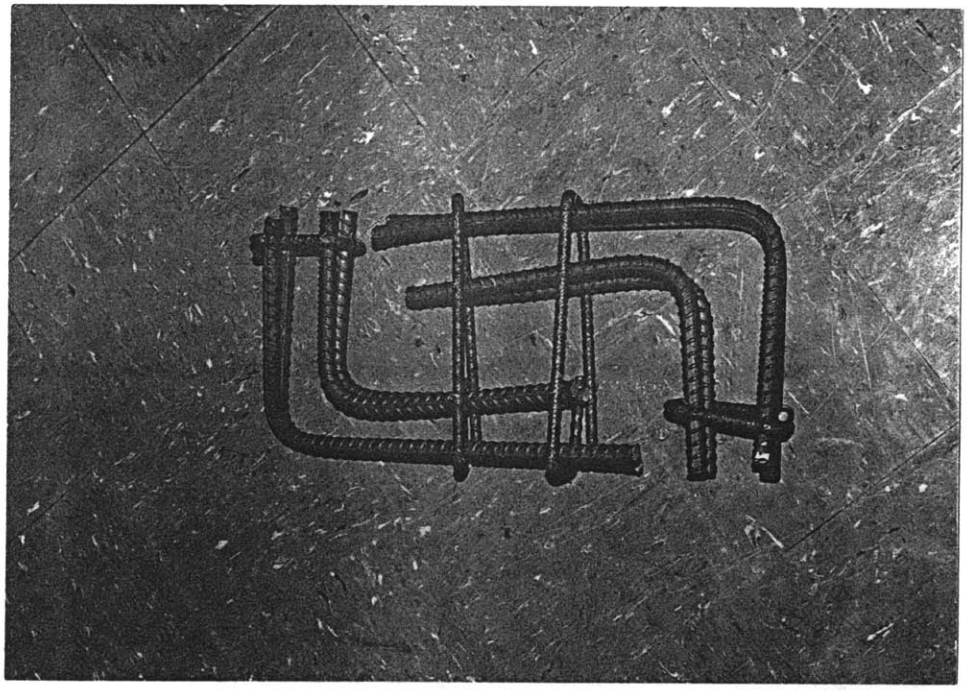

Fig. 4.6 Steel reinforcement for push-off specimens with steel stirrups crossing the shear plane.

Once the steel bar reinforcement was assembled, the next steps were to prepare the molds and mix the concrete. The molds, made of plexiglass, were covered with oil before the concrete was poured in order to facilitate demolding. For mixing, an Omni Mixer, Model OM-30AV, manufactured by Chiyoda & Gar-Bro Corporation, shown on Fig. 4.7, was used. This machine was selected due to its capability to pressurize the mixing chamber, which improves the homogeneity of the concrete mix. Also, ordinary mixer use rotating blades as the mixing mechanism; this tends to cause fiber clumping as fibers accumulate on these blades. On the other hand, the Omni mixer uses as its mixing mechanism a flexible rubber drum attached to a vertical bar. For mixing, this assemblage is wobbled by an externally driven hydraulic motor, which has the capability of continuously varying the mixing speed.

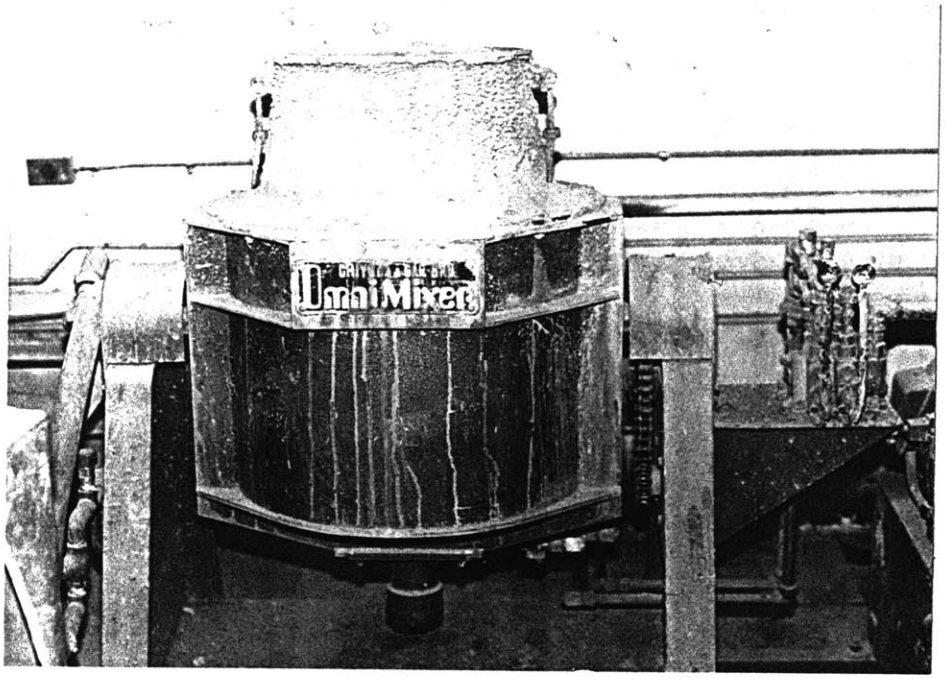

Fig. 4.7 Omni mixer.

The mixing procedure was as follows:

a) mix dry components (cement, sand and gravel) for 2-3 min.

b) add water to the mix. The superplasticizer and silica fume (in the case of high strength concrete), were added to the water before pouring the water into the mixer.

c) the mixing chamber was then closed and pressurized to approximately to 40 cmHg. The fresh concrete was then mixed for 5 min.

d) if the mix called for fibers, these were added by slowly sprinkling them in the mixer to avoid balling. After all the fibers were added, the mixer was closed and pressurized again to 40 cmHg. Then, the concrete with fibers was mixed for 3 min.

The fresh concrete was then poured into the molds, where the steel bars were already placed. After pouring, the molds were externally vibrated for 3 min, to ensure proper placing of the concrete. Also, six control cylinders (3" wide by 6" tall) were poured to measure the compressive and splitting tensile strengths. Fig. 4.8 shows both the push-off and cylinder specimens after they had been vibrated. The molds and cylinders were then covered with plastic for 24 hours. After the 24 hours had passed, the specimens and cylinder were removed from their molds and placed in water until testing (see Fig. 4.9). High strength concrete specimens were tested at 28 days; while normal strength concrete specimens at 7 days.

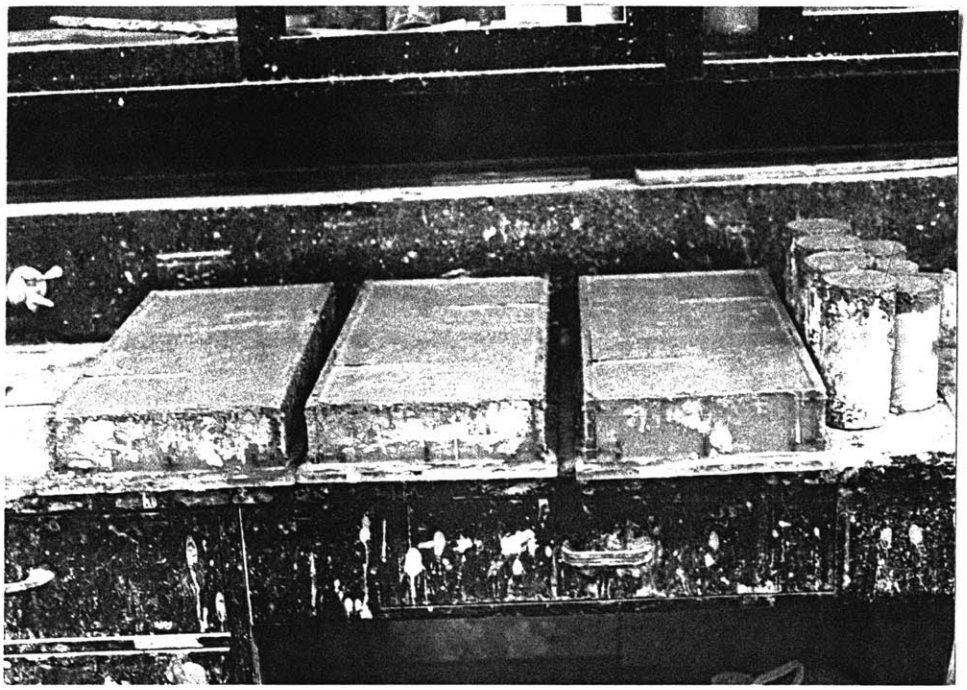

Fig. 4.8 Push-off and cylinder specimens in molds.

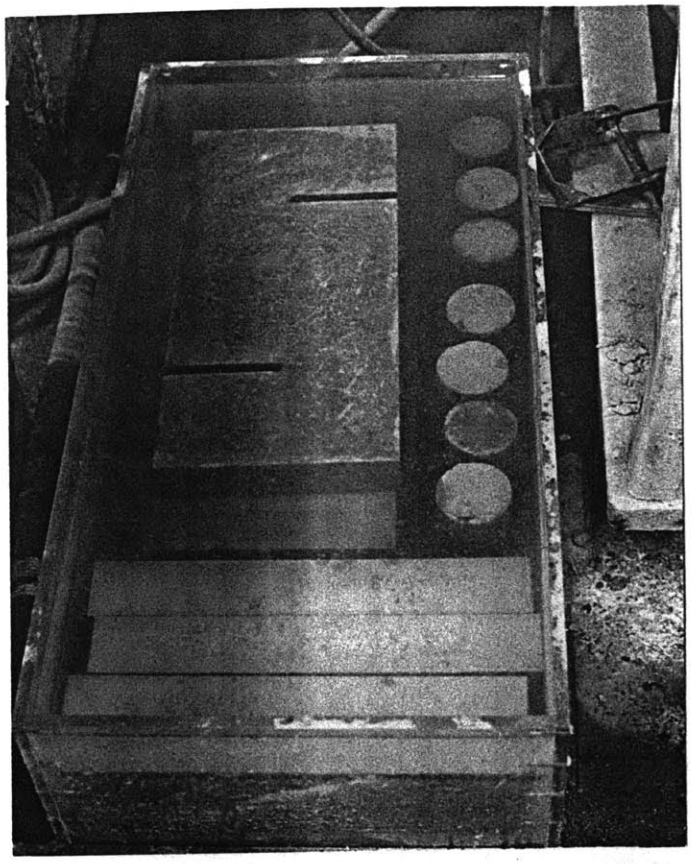

Fig. 4.9 Push-off and cylinder specimen in water.

4.5 TEST SET-UP AND PROCEDURE

4.5.1 Compression and Splitting Tension Tests

For the compression test, the cylinder specimen was placed in the loading frame of a MTS machine, as shown in Fig. 4.10. Prior to testing, the cylinders were capped using hydrostone in order to ensure an even and smooth contact surface between the top of the cylinder and the loading platen. The compression test lasted approximately 5 minutes. The cylinders were loaded in a stroke control configuration, at a displacement rate of 1/250 mm/sec. From these tests, the maximum load was recorded. The compressive strength of the concrete(f'_c) was set equal to the average strength of four cylinder tested.

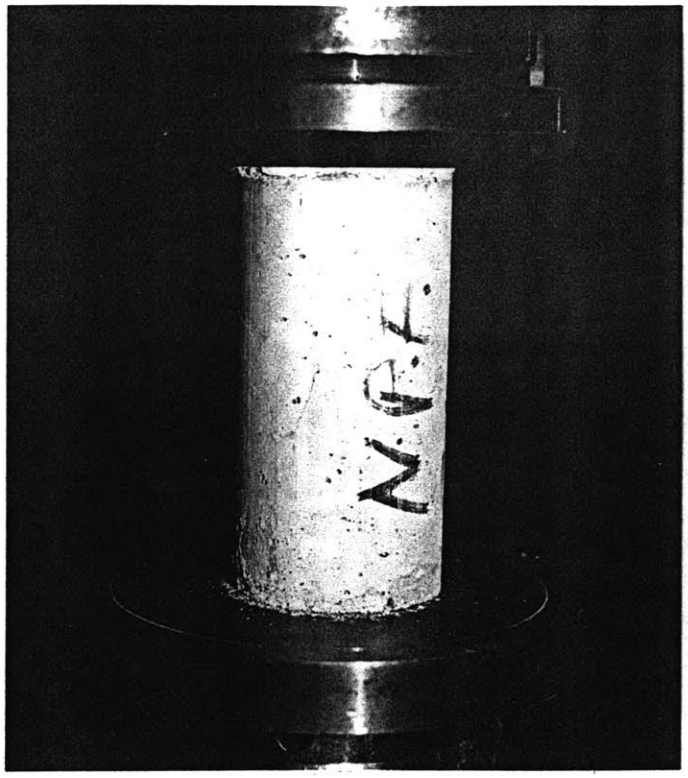

Fig. 4.10 Compression test on cylinder specimen.

To perform the splitting tensile test, the cylinders were placed on their side and loaded as shown on Fig. 4.11. Again, a stroke control configuration was used with the same displacement rate as above. These splitting tension tests were done only to have same measure of the tensile strength of concrete, and the values obtained were not used in the analysis. For the case of fiber reinforced concrete, ACI Committee 544 does not recommend the use of the splitting tension test for the measurement of the tensile strength of FRC, due to the fact that the stress distribution after cracking cannot be accurately defined[51].

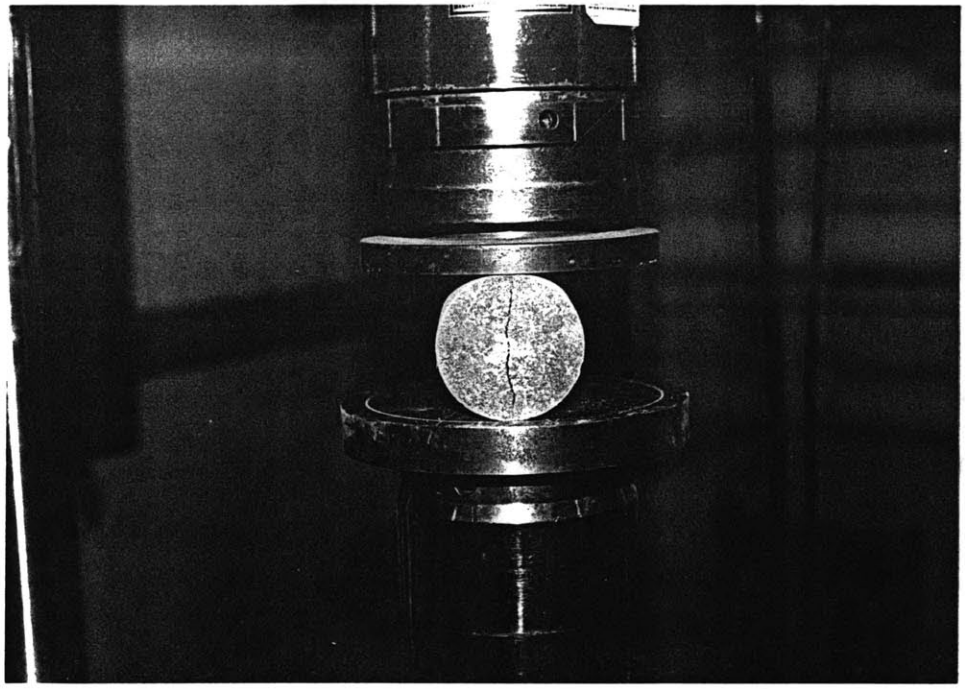

Fig. 4.11 Splitting tensile test on cylinder specimen.

4.5.2 Shear Tests

For the shear tests, the push-off specimens were used. The test setup was identical for the first 24 specimens cast. In order to measure the horizontal and vertical displacements at the shear plane, two linear variable displacement transformers (LVDT) were attached on the front of the specimens. There was no need to place LVDTs in the back of the specimens, since in tests performed by Beattie et al.[46], it was found that for the same size of specimen there was no difference between the displacements measured on the front or the back as long as the applied load had no eccentricity. The position of the LVDTs as well as the loading configuration are shown in Fig. 4.12.

The specimen was placed in the MTS machine loading frame, as shown in Fig. 4.13. A Fluke data acquisition system, Model 2285B Data Logger, was used to record the two displacements signals from the LVDT's as well as the applied load signal from the MTS machine. The Fluke system in turn was operated thru an IBM AT (see Fig. 4.14). A schematic flow chart of the configuration used is shown in Fig. 4.15. The specimens were tested in a strain controlled configuration, with a strain rate of 1/750 mm/sec. The shear tests lasted for approximately 30 minutes; and they were stopped when the specimen was no longer able to carry load with increasing cross-head displacement.

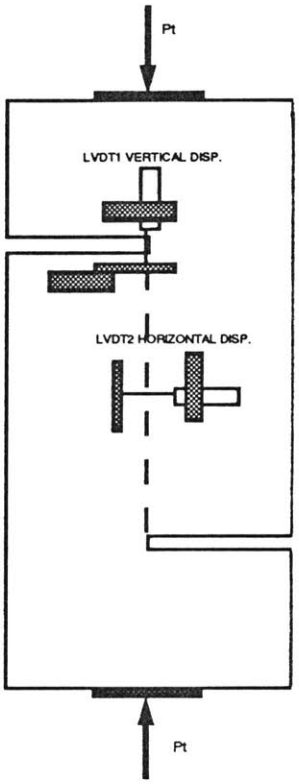

Fig. 4.12 Loading configuration and position of LVDT's for push-off specimen.

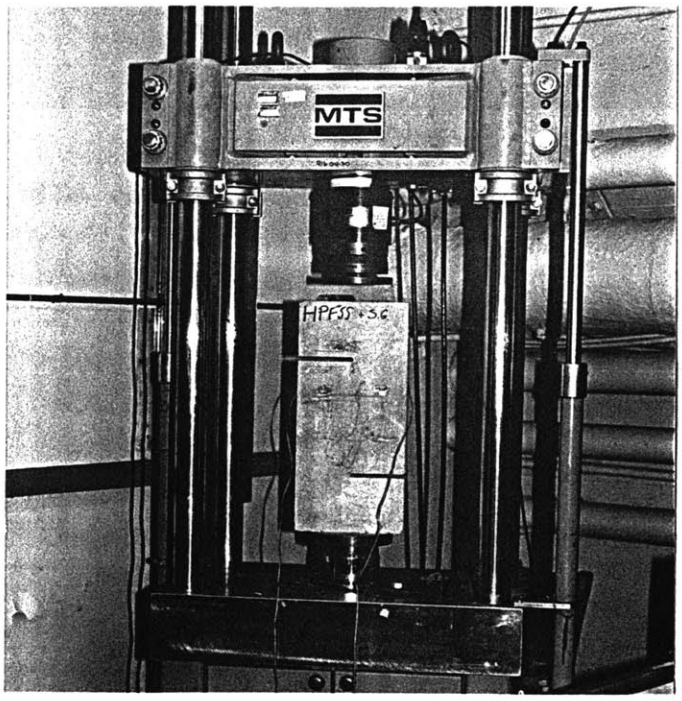

Fig. 4.13 Push-off specimen placed in MTS loading frame.

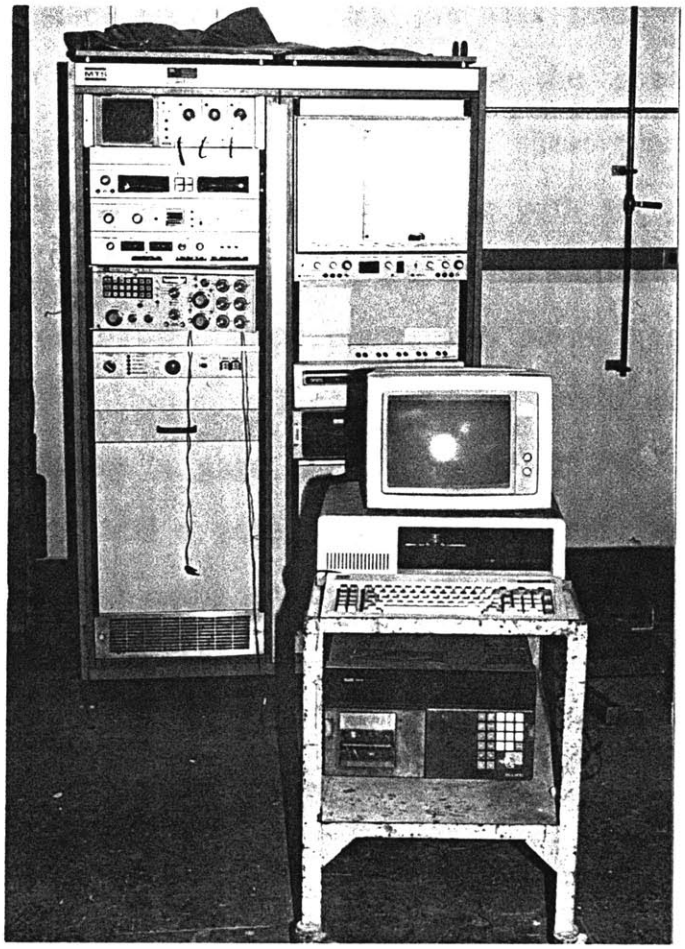

Fig. 4.14 MTS control panel, Fluke system and IBM AT.

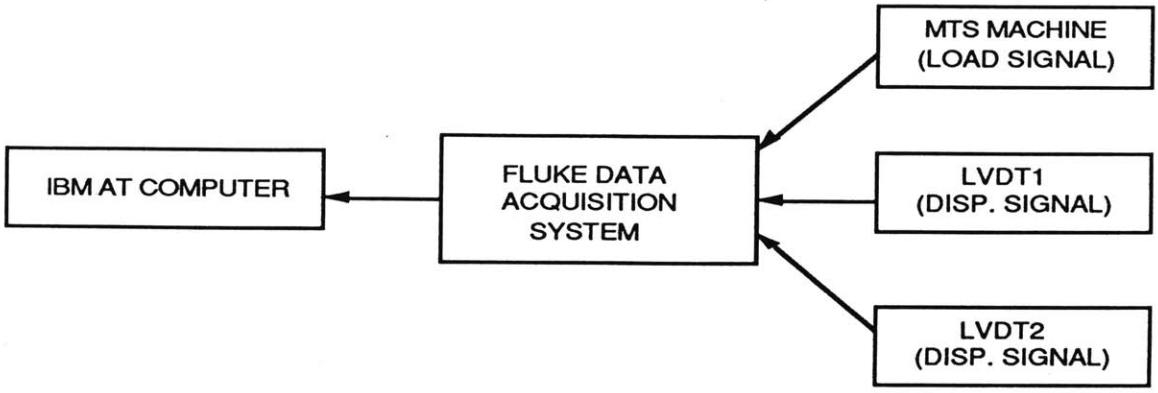

Fig. 4.15 Schematic chart for experimental setup

For the last test performed on a high strength concrete specimen with steel stirrups (HCS), the test setup was altered. In order to investigate the relation between the shear displacement (vertical) at the top and the center of the shear plane; two LVDT's were placed in the specimen, but this time with the same orientation (see Fig. 4.16a). Also, with the purpose of monitoring the strain in the steel stirrups crossing the shear plane, two strain gages were placed on the steel bars as shown in Fig. 4.16b. The strain gages were of the type FAE-25-12, with a gage factor of 2.07 ± 1%, a resistance of 120.0 ± 0.2 ohms, and a gage length of 6.35 mm. The output of the strain gages was read using a Portable Digital Strain Indicator 1200B, from BLH Electronics. The rest of the signals being monitored, the two displacement measurements and the load, were recorded in the same manner as explained before.

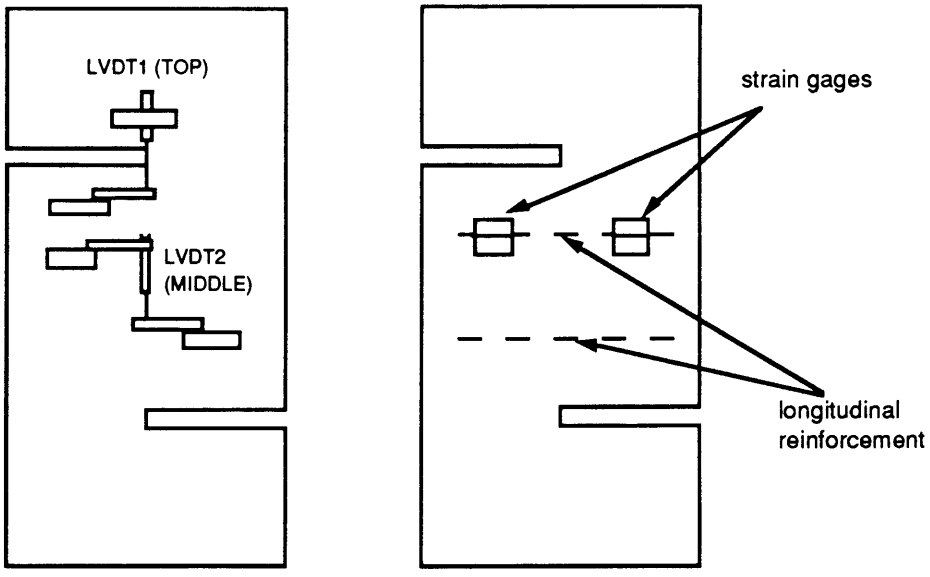

Fig.4.16 Experimental setup for test: (a) position of LVDT's to measure shear deformations along shear plane, (b) position of strain gages to monitor strain in longitudinal steel bars.

CHAPTER 5

RESULTS AND DISCUSSION

5.1 EXPERIMENTAL RESULTS

5.1.1 Production

In general, the addition of fibers to the concrete mixture did not present major problems from a production point of view. Some decrease in workability of the fresh concrete mix were encountered in mixes reinforced with fibers. Comparing the two types of fibers used, the addition of polypropylene fibers resulted in the least workable concrete, especially for the case of PNC. This mixture resulted in a very porous hardened cement matrix, which in turn lowered the initial stiffness of the specimens manufactured with this concrete. This will be discussed later.

The Omni mixer proved to be very effective in the manufacturing process of the concrete mixes; especially for fiber reinforced mixes. Preliminary attempts to use a conventional mixer with rotating blades were unsatisfactory since a large portion of the fibers added clumped as they accumulated in the blades. Also, the use of superplastizacer was indispensable in the production of FRC to ensure proper workability. On the other hand, the addition of

superplasticiser in excess of 2% of the weight of cement acted as a retardant. This effect was observed on a preliminary mix of SNC with a superplasticiser amount of 2% of the weight of cement, where the concrete developed a compressive strength of only about 1,000 psi at 14 days, when it originally had been designed to reach a compressive strength of approximately 4,000 psi at 7 days.

5.1.2 Compression and Splitting Tension Tests

The compressive and splitting tensile strengths obtained in the experimental program are summarized in Tables 5.1 and 5.2, for normal strength and high strength concrete specimens respectively. The compression strengths (f'_c) and splitting tensile strengths (f'_{sp}) measured from the cylinder specimens, were consistent with the expected values. The addition of polypropylene fibers did not significantly affect the compressive or splitting tensile strengths of either normal strength or high strength concrete. Only improvements in ductility were observed from the addition of this type of fiber.

For the case of steel fibers, both increases of strength as well as ductility were obtained for all mixes. In the SNC mixes manufactured, no significant increases in compressive strength were observed over plain NC mixes, while improvements of approximately 86% were measured in the splitting tensile strength. Increases in compressive and splitting tensile strength were observed in SHC mixes. Average increases of 20% for the compressive strength and 116% for the splitting tensile strength were obtained in SHC mixes over plain HC.

These increases in strength due to the addition of steel fibers in normal strength concrete have been studied by Narayan and Kareem-Planjian[52]. From the results obtained, one can conclude that fibers are more effective in high strength concrete, since higher strength increases were obtained for this type of concrete than for the normal strength concrete. This can be attributed to the better fiber-matrix bond characteristics that high strength concrete presents.

5.1.3 Shear Tests

(a) Strength and Deformation Behavior

The results obtained from the first 24 shear tests are summarized in Tables 5.1 and 5.2 for HC and NC mixes, respectively. The shear stress was obtained by dividing the applied load by the area of the shear plane (30 sq.in.). In these tables both the obtained maximum shear stresses, τ_{max}, and their normalized values with respect to $\sqrt{f'_c}$ are given. This normalization is intended to eliminate the material strength variable for each type of concrete. The average percent increase in maximum shear stress (%incr. avg. τ_{max}) with respect to the τ_{max} obtained from the plain concrete specimens, is given in the tables. This value was calculated by comparing the normalized average maximum shear stress from the two specimen of the same type with the normalized average maximum shear stress obtained from the unreinforced specimens, NC and HC, respectively. Also, the shear stress at first cracking, τ_{cr}, is reported. In general the results obtained from the two tests for each specimen type were very consistent; therefore, there was no need to perform an additional third test.

Table 5.1 Test results for normal strength concrete specimens.

SPECIMEN	f'c (psi)	f'st (psi)	τmax (psi)	τmax/ $\sqrt{f'c}$	% incr. avg. τmax	τcr (psi)
NC-1	4,500	350	775.06	11.55	-	775.06
NC-2	4,500	350	744.13	11.09		744.13
SNC-1	4,200	784	1,010.10	15.6	36.00	618.26
SNC-2	4,200	784	985.07	15.2		693.44
PNC-1	4,010	380	788.39	12.45	9.76	788.39
PNC-2	4,010	380	785.22	12.4		785.22
NCS-1	4,950	470	1,308.63	18.6	62.10	823.87
NCS-2	4,950	470	1,273.45	18.1		805.58
SNCS-1	3,800	740	1,200.83	19.48	68.20	669.46
SNCS-2	3,800	740	1,146.58	18.6		621.99
PNCS-1	4,900	460	1,284.50	18.35	62.32	747.6
PNCS-2	4,900	460	1,288.00	18.4		755.3

Table 5.2 Test results for high strength concrete specimens.

SPECIMEN	f'c (psi)	f'st (psi)	τmax (psi)	τmax/ $\sqrt{f'c}$	% incr. avg. τmax	τcr (psi)
HC-1	9,000	481	828.11	8.73	-	827.90
HC-2	9,000	481	897.57	9.16		869.07
SHC-1	11,600	1,078	1516.46	14.08	58.58	1151.35
SHC-2	11,600	1,078	1539.08	14.29		1129.81
PHC-1	9,100	557	992.10	10.4	17.16	884.30
PHC-2	9,100	557	1007.36	10.56		903.38
HCS-1	9,680	500	1738.50	17.67	112.69	1024.21
HCS-2	9,680	500	2005.13	20.38		1054.71
SHCS-1	10,930	1,040	2251.93	21.54	139.68	1259.79
SHCS-2	10,930	1,040	2231.03	21.34		1323.55
PHCS-1	9,020	560	1645.90	17.33	92.45	1009.57
PHCS-2	9,020	560	1624.05	17.1		1001.67

For the specimens involving normal strength concrete with or without fiber reinforcement only, that is NC, SNC, and PNC, the normalized shear stress vs. vertical displacement for one of the two specimens tested is shown in Fig. 5.1. Also, in Fig. 5.2, the normalized shear stress vs. horizontal displacements at the center of the shear plane for the same specimens are shown. The horizontal displacement can be interpreted as a crack width across the shear plane. Also this measurement can be interpreted as Poisson's effect, but since the shear tests were symmetric there was almost no displacement before cracking. For specimens NC, SNC and PNC, the horizontal displacement is approximately zero up to cracking; after which NC specimens failed, and SNC and PNC specimens were able to tolerate increasing horizontal deformation. This horizontal measurement is a good way to determine the cracking shear stress, τ_{cr}, since it is at this point that the displacement deviates from zero. In the case of NC specimens, the shear stress vs. vertical deformation behavior was linear up to failure, which for the NC specimens coincided with first cracking. Since no reinforcement was provided along the shear plane, immediately after the first crack appeared, the specimen failed. In the case of the specimens reinforced with fibers only, SNC and PNC, the behavior up to first cracking was very similar to that of the NC specimens. After cracking, the SNC specimens were able to carry higher loads due to the steel fibers in the concrete mix, resulting in increases of up to 36% of the maximum load over the NC specimens. After reaching the maximum shear stress level, the SNC specimens failed in a very ductile manner showing a softening behavior due to the pull-out of the steel fibers from the matrix. The

PNC specimens did not show an increase in maximum load, as did the SNC specimens. For the PNC specimens, after first cracking occurred, the shear stress decreased with increasing vertical deformation. This leads to the assumption that right after first cracking, polypropylene fibers started to pull-out of the matrix, without contributing to the transfer of higher shear stress levels.

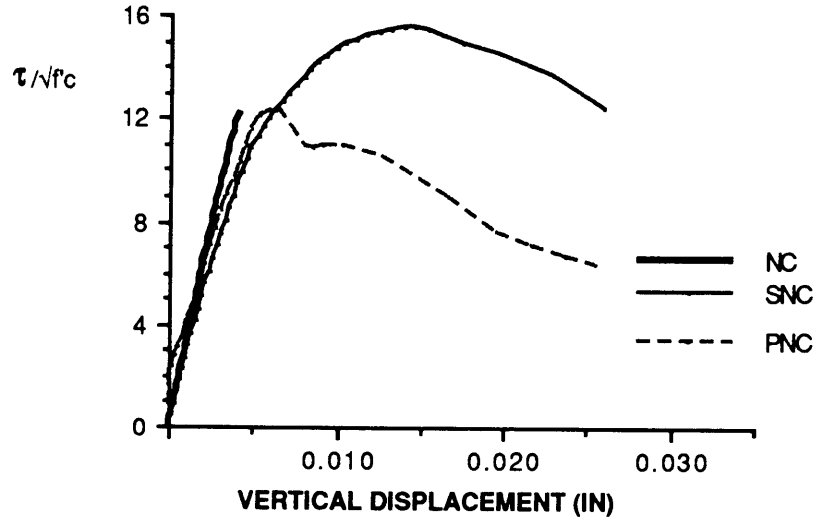

Fig. 5.1 Normalized shear stress vs. vertical displacement for NC, SNC, and PNC specimens.

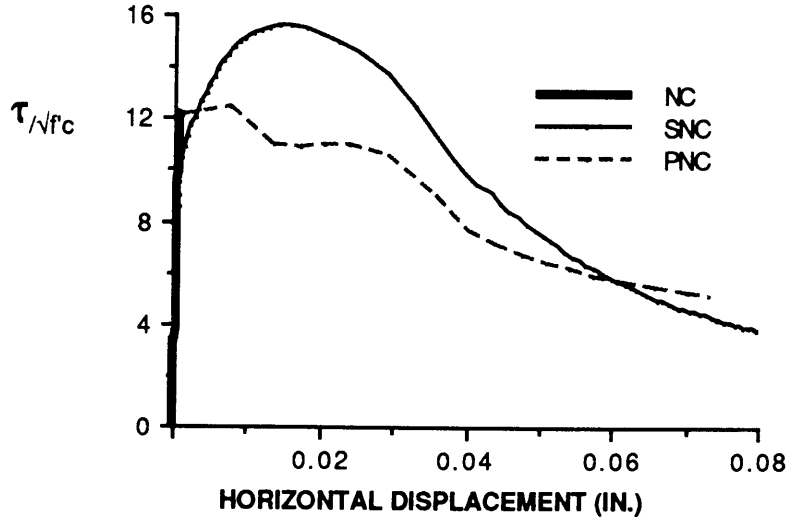

Fig. 5.2 Normalized shear stress vs. horizontal displacement for NC, SNC, and PNC specimens.

In Fig. 5.3 and 5.4, the normalized shear stress vs. vertical displacement and normalized shear stress vs. horizontal displacement for normal strength concrete specimens reinforced with stirrups and stirrups plus fibers, specimens NCS, SNCS and PNCS, are shown, respectively. Here again, the horizontal displacement as a function of the applied shear stress was almost zero up to cracking, with the exception of the PNCS specimens that showed a relatevily low initial stiffness. This low stiffness is attributed to production problems. The shear stress vs. vertical displacement behavior for the NCS specimens was linear up to cracking (τ_{cr}=823.87 psi); after which the steel reinforcement enables the specimen to carry higher loads of up to 62% over the plain NC specimens. Soon after the maximum load was reached, these specimens showed a softening behavior. After failure of the concrete in the NCS specimen, the shear stress vs. vertical deformation showed an "unloading" behavior to zero vertical displacement that will be explained in the Failure Modes section. For the specimens with both steel stirrups and fibers, SNCS and PNCS, the shear stress vs. vertical deformation behavior was similar to the NCS specimens up to cracking. After cracking (see Table 5.1 for values of τ_{cr}), these specimens with fibers and stirrups were not able to develop significantly higher shear stress levels when compared to the NCS specimens, but they did show a more plastic behavior by sustaining the maximum load with increasing vertical deformation. After the concrete failed, these specimens, SNCS and PNCS, showed a similar unloading phenomenon of the NCS specimens. In addition, the PNCS specimens showed an overall less stiff behavior than either the NCS or the SNCS specimens. This is

probably due the compaction problems during manufacture, because of the low workability that this mix presented.

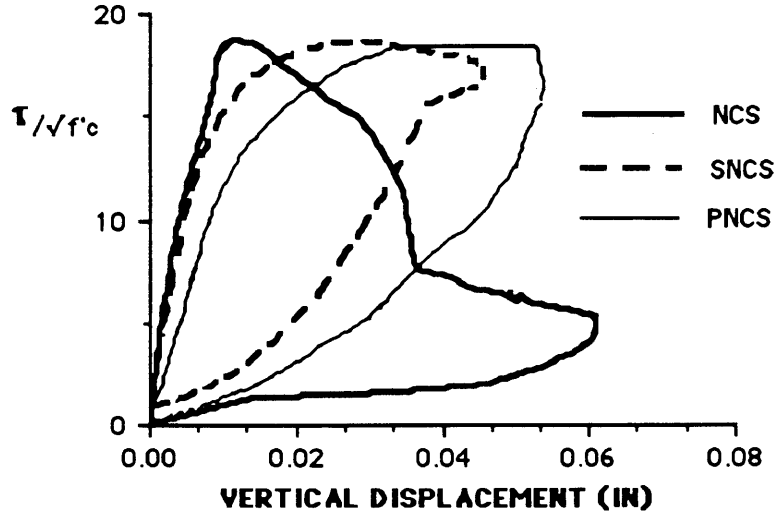

Fig. 5.3 Normalized shear stress vs. vertical displacement for NCS, SNCS, and PNCS specimens.

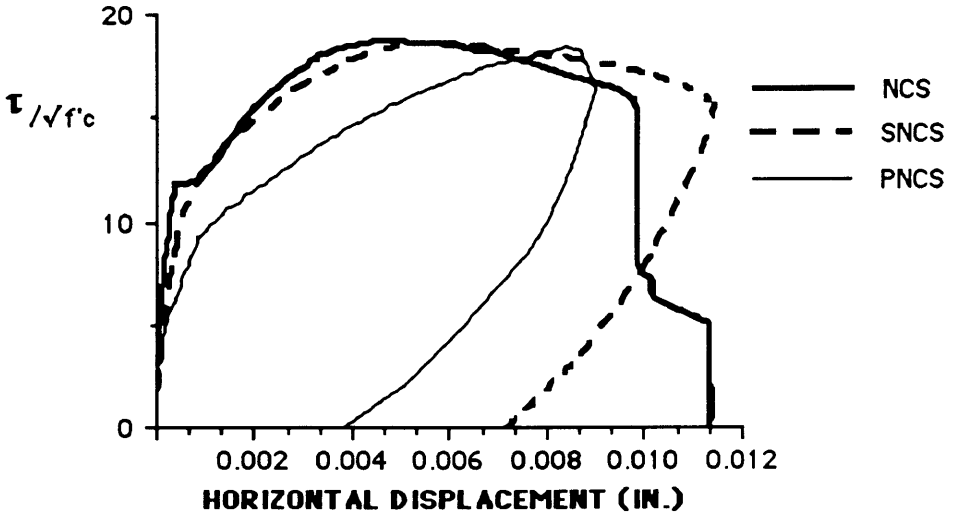

Fig. 5.4 Normalized shear stress vs. horizontal displacement for NCS, SNCS, and PNCS specimens.

The shear stress vs. vertical deformation for one of the two specimens tested involving high strength concrete with or without fiber reinforcement only, that is HC, SHC and PHC specimens, are shown in Fig. 5.5. Also, the shear stress vs. horizontal displacement for these same specimens are shown in Fig. 5.6. The behavior of the HC specimens was almost identical to the NC specimens, being linear up to failure; with the difference that the HC specimens carried a higher load at failure. For the SHC and PHC specimens, the shear stress vs. vertical deformation was also linear up to first cracking, following the HC specimens. In the case of the SHC specimens, after cracking considerably higher shear stresses of up to approximately 60% were developed when compared to HC specimens. After the maximum shear stress was reached in the SHC specimens, there was a softening behavior which was followed by a sudden drop in load. This softening and subsequent drop are attributed to the steel fibers yielding and braking, rather than pulling-out as in the normal strength concrete. In the PHC specimens, after first cracking occurred, the specimens was able to develop higher shear stress level of approximately 17% over the HC specimens. This increase was not observed for the specimens with normal strength concrete and polypropylene fibers. After reaching the maximum shear stress level, the PHC specimens showed a softening behavior attributed to the pulling-out of the polypropylene fibers out of the high strength concrete matrix.

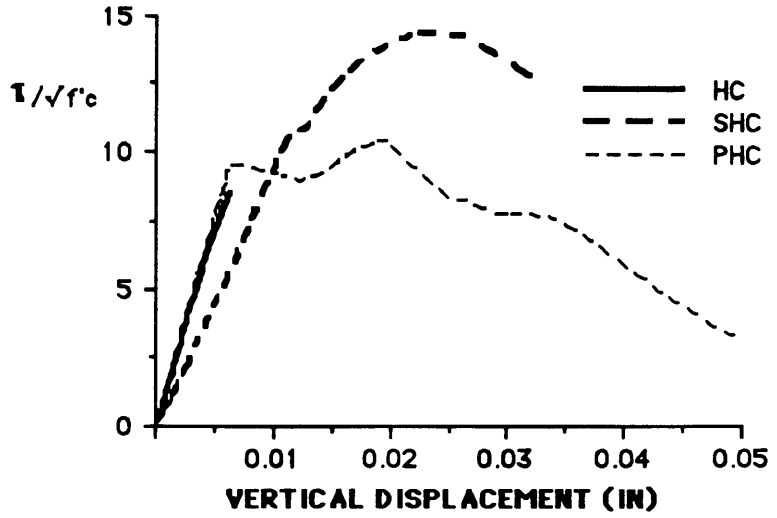

Fig. 5.5 Normalized shear stress vs. vertical displacement for HC, SHC, and PHC specimens.

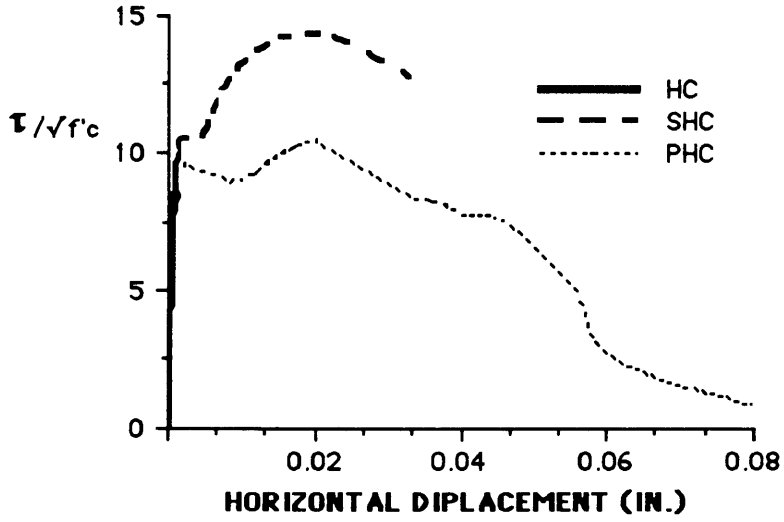

Fig. 5.6 Normalized shear stress vs. horizontal displacement for HC, SHC, and PHC specimens.

Fig. 5.7 shows the normalized shear stress vs. vertical displacement for one of the two specimens involving high strength concrete reinforced with stirrups alone and with stirrups plus fibers,

specimens HCS, SHCS and PHCS. Similarly, Fig. 5.8 shows the normalized shear stress vs. horizontal displacement for the same specimens. Specimens HCS showed a linear behavior up to cracking, after which with the aid of the steel stirrups significantly higher loads were developed; up to 112% higher shear stresses than the plain HC specimens. After the maximum shear stress was reached, HCS specimens showed a softening behavior for a short period; followed by the failure of the concrete and a sharp unloading behavior as the NCS specimens, but this time to a permanent deformation. For the specimens SHCS and PHCS, the behavior was also linear up to first cracking. In the case of SHCS specimens, increases in maximum shear stress of approximately 24% over the HCS specimens were observed. Also, the SHCS specimens developed a plateau after the maximum shear stress was reached, behaving as a perfectly plastic system. After this plateau, the SHCS specimens showed a softening behavior, followed by failure of the concrete and an unloading to a permanent deformation. The behavior of PHCS specimens after first cracking was characterized by a more ductile behavior than HCS specimens, developing the maximum shear stress at higher vertical displacement values. Here again, after the concrete failed, the PHCS specimens showed an unloading behavior of the vertical displacement to a permanent deformation.

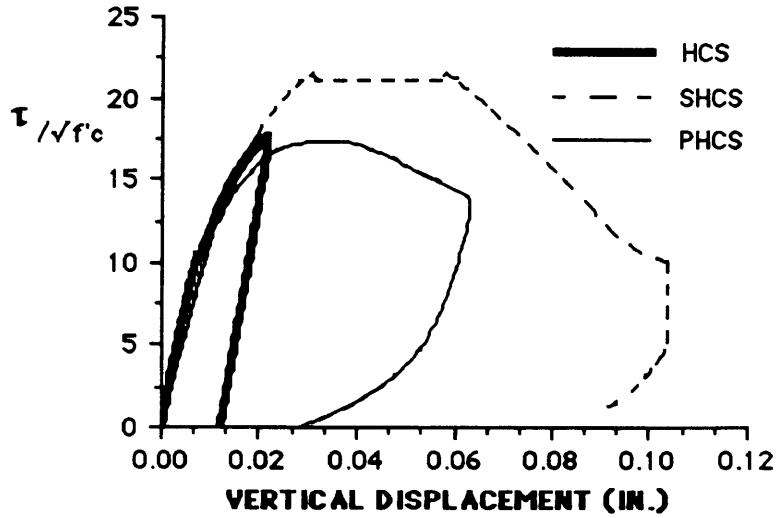

Fig. 5.7 Normalized shear stress vs. vertical displacement for HCS, SHCS, and PHCS specimens.

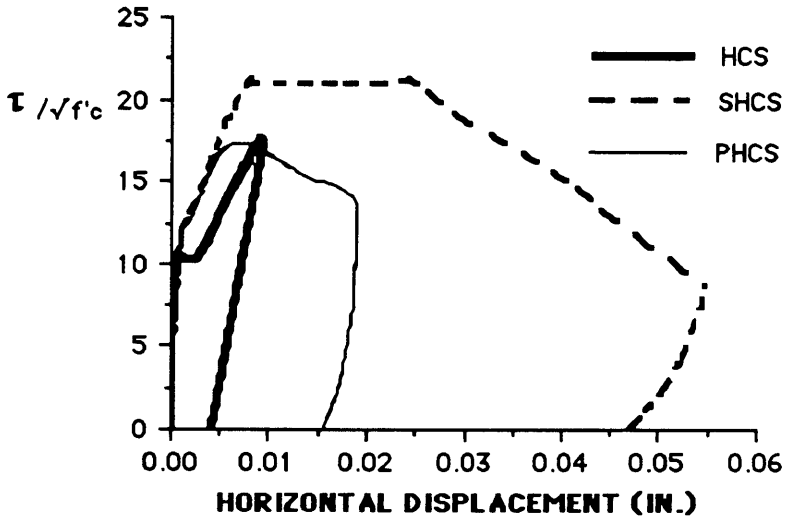

Fig. 5.8 Normalized shear stress vs. horizontal displacement for HCS, SHCS, and PHCS specimens.

In general, both types of fibers, steel and polypropylene, proved to be more effective in HC mixes than in NC mixes, since higher maximum shear stress as well as overall ductility were obtained. This is attributed to the improved bond between the fibers

and the matrix, that HC mixes present. Concrete reinforced with steel fibers only was characterized by higher maximum shear stress levels, while in concrete with polypropylene fibers only an overall improvement in ductility was present. Steel stirrups alone proved to be more effective than fibers alone as shear reinforcement, although for the case of high strength concrete with steel fibers alone higher maximum shear stresses were obtained than in normal strength concrete with steel stirrups only. For SHCS specimens, there was a significant increase of approximately 24% in maximum shear stress when compared with the maximum shear stress obtained in HCS specimens. For the case of the other specimens reinforced with both fibers and steel stirrups, SNCS, PNCS and PHCS, no improvements in the maximum shear stress were observed when compared to specimens reinforced with stirrups alone. Nonetheless, for all instances, the combination of steel stirrups and fibers resulted, in more ductile characteristics than the specimens reinforced with steel stirrups only. This aspect of the behavior will be discussed to more detail in the Toughness section.

(b)Failure modes

Two distinct failure modes were encountered in the shear tests performed depending on the presence or absence of steel stirrups. For specimens with no shear reinforcement or reinforced with fibers only, several inclined cracks formed along the shear plane (Fig. 5.9a). Failure occurred when these cracks joined and formed a single crack band along the shear plane. In the case of specimens reinforced with stirrups alone or with stirrups and fibers, cracks formed inclined to

the shear plane. These cracks extended to form well defined compressive struts in the concrete, which in combination with the tensile force being carried by the steel stirrups, created a truss action (Fig. 5.9b). Ultimate failure occurred when the compression struts crushed in compression.

The failure mode of the concrete specimens with no fiber or steel stirrup reinforcement (NC and HC), was very brittle, with no warning before collapse. These specimens lost their integrity, breaking into several pieces. In Figs. 5.10 and 5.11, photographs of the specimens NC and HC after failure is shown, respectively. The rest of the specimens tested, failed in a more ductile manner, developing diagonal cracks at the shear plane. Specimens reinforced with fibers only developed several small diagonal cracks as shown in Fig. 5.9a. For the specimens SNC, PNC, and PHC, ultimate failure occurred when these series of diagonal cracks joined together forming a single crack along the shear plane and the fibers bridging the cracks pull-out. All these specimens (SNC, PNC and PHC) showed a softening behavior after the maximum shear stress was reached, attributed to fiber pull-out. Even after failure, the fibers were able to preserve the integrity of the specimen. Figs. 5.12, 5.13 and 5.14, show specimens PNC, PHC and SNC after failure, respectively. In the case of SHC specimens, the above was also true, with the difference that soon after the maximum load was reached, a softening behavior followed by a sudden drop in load occurred. This phenomenon is attributed to that some of the steel fibers bridging the crack along the shear plane first yielded in tension, and thereafter, with increasing deformation ruptured. This yielding and braking of the

fibers was possible due to the bond provided by the HC. Even though some of the steel fibers broke, the remaining fibers were able to preserve the integrity of the specimen. Fig. 5.15 shows a photograph of an SHC specimen after failure.

For specimens involving steel stirrups crossing the shear plane (NCS, SNCS, PNCS, HCS, SHCS, and PHCS), the failure mode was also ductile, with the formation of diagonal cracks. As these cracks extended at an angle of 50 to 75 degrees with respect to the horizontal direction, they created well defined compressive struts in the concrete, which in combination with the tensile force being carried by the steel stirrups, created a truss like action (see Fig. 5.9b). Ultimate failure occurred when the concrete struts crushed in compression. Figs. 5.16 to 5.21 show pictures of one of each of the push-off specimens reinforced with steel stirrups after failure, that is specimens NCS, HCS, PNCS, PHCS, SNCS and SHCS respectively.

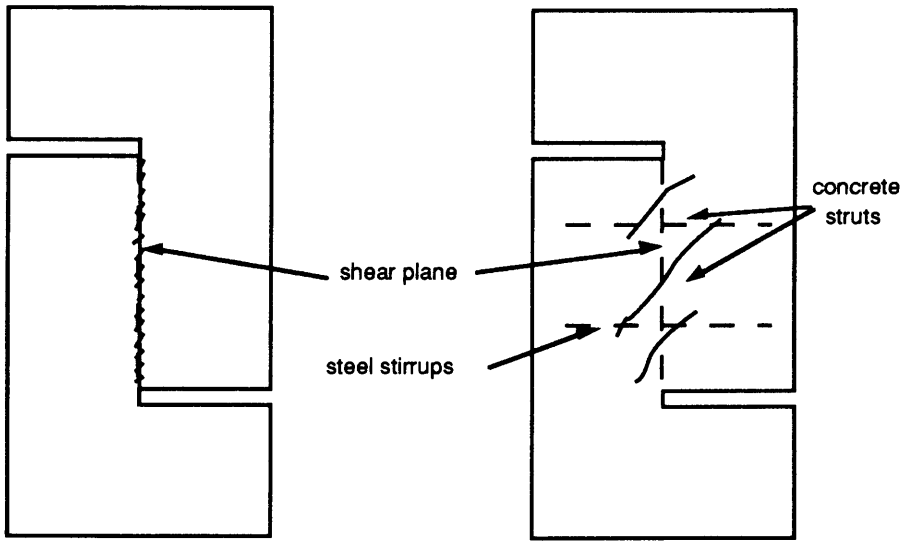

Fig. 5.9 Cracking patterns for push-off specimens: (a) with no steel stirrups crossing the shear plane; (b) with steel stirrups crossing the shear plane.

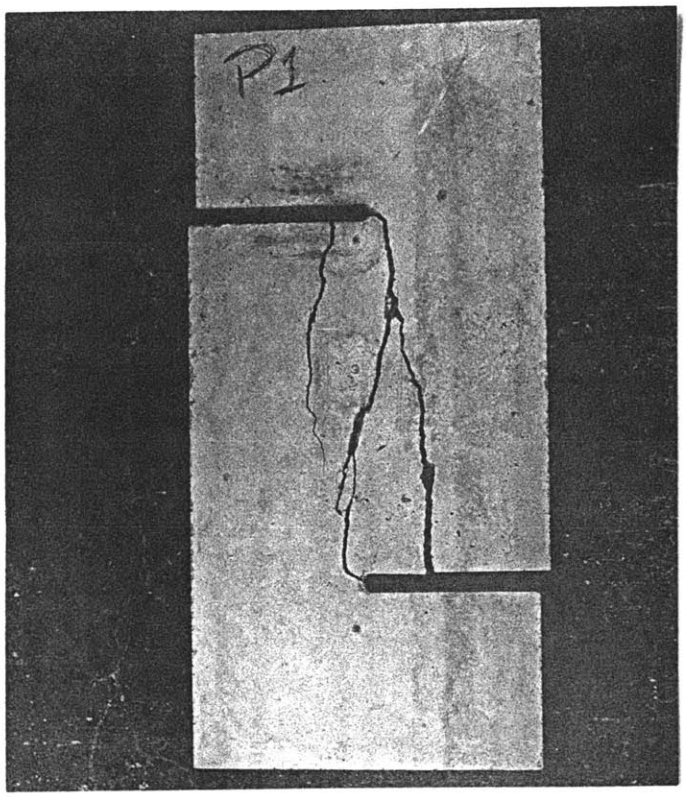

Fig. 5.10 NC specimen after failure.

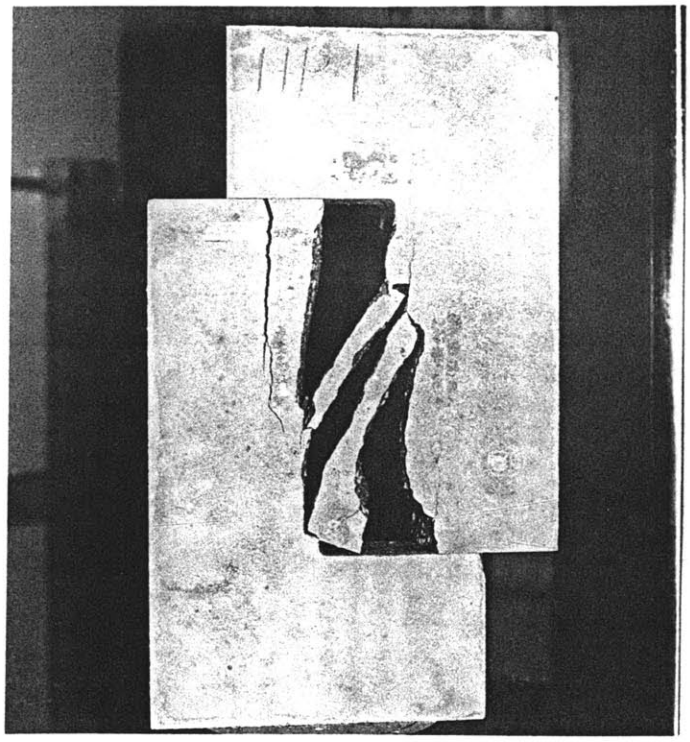

Fig. 5.11 HC specimen after failure.

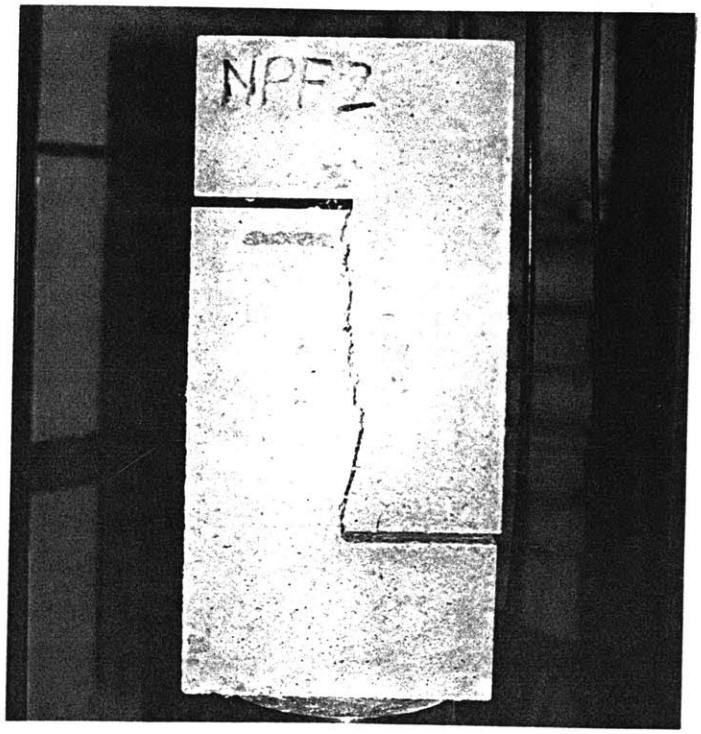

Fig. 5.12 PNC specimen after failure.

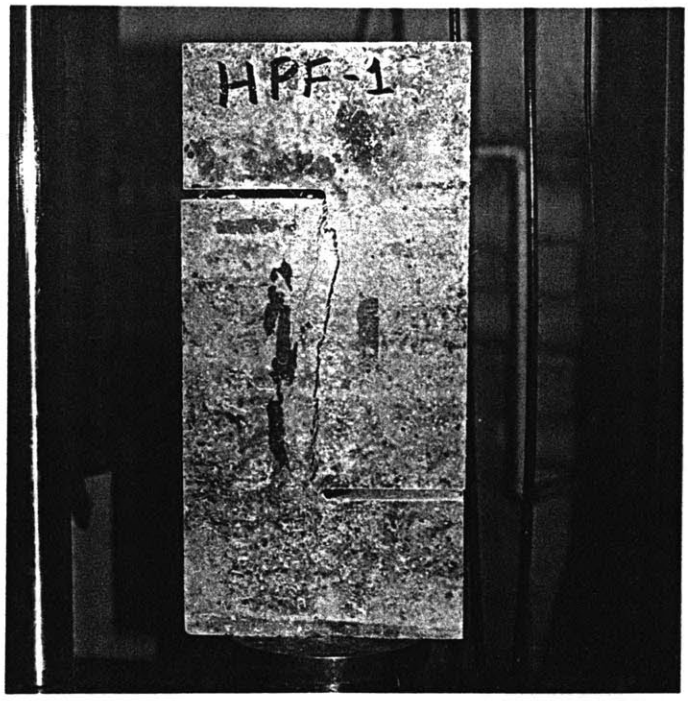

Fig. 5.13 PHC specimen after failure.

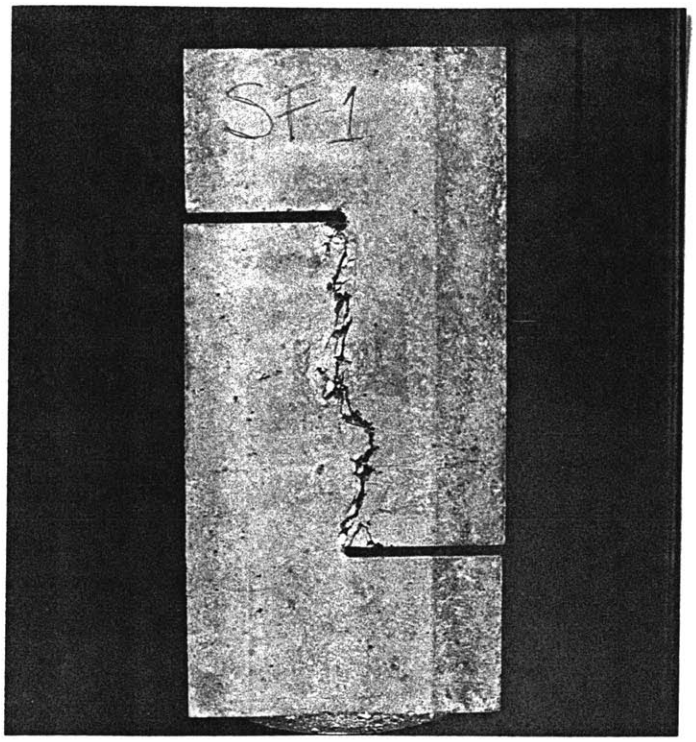

Fig. 5.14 SNC specimen after failure.

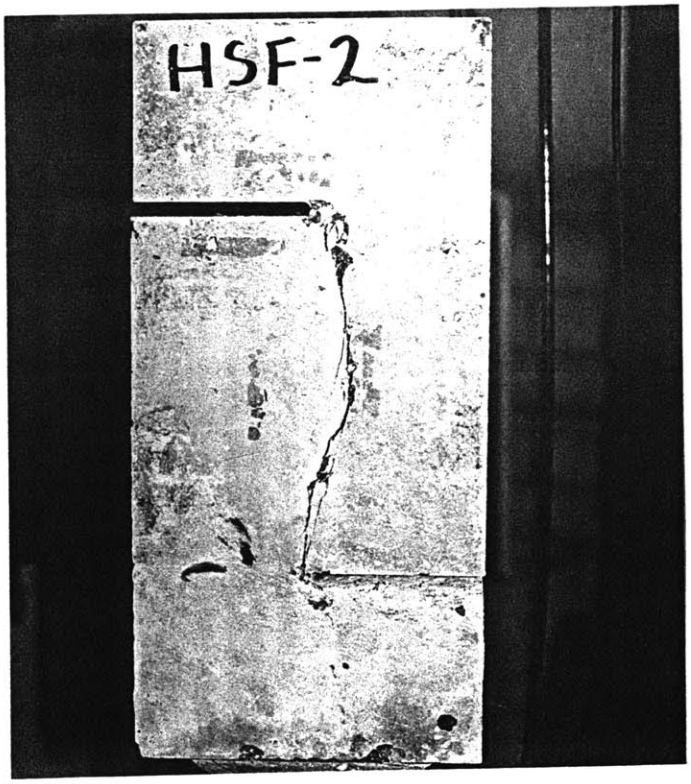

Fig. 5.15 SHC specimen after failure.

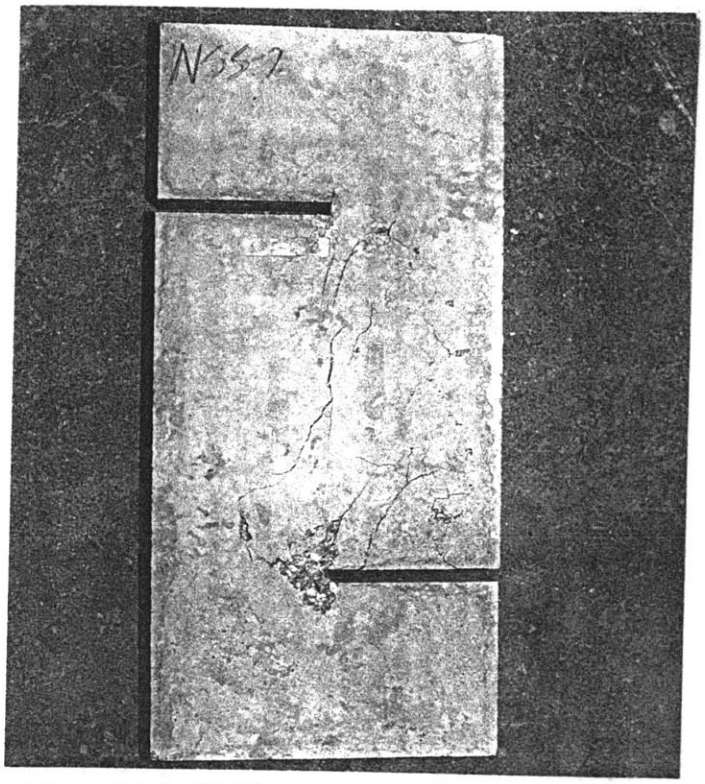

Fig. 5.16 NCS specimen after failure.

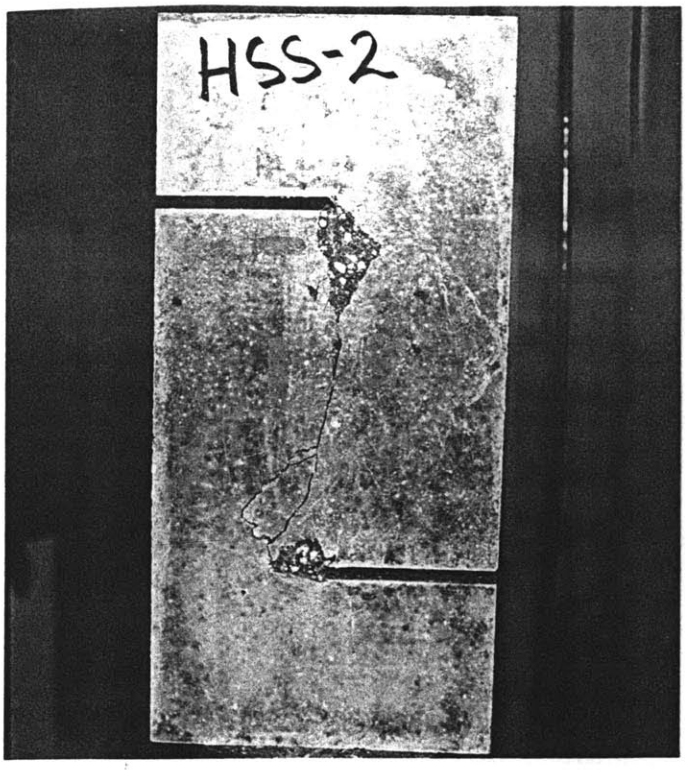

Fig. 5.17 HCS specimen after failure.

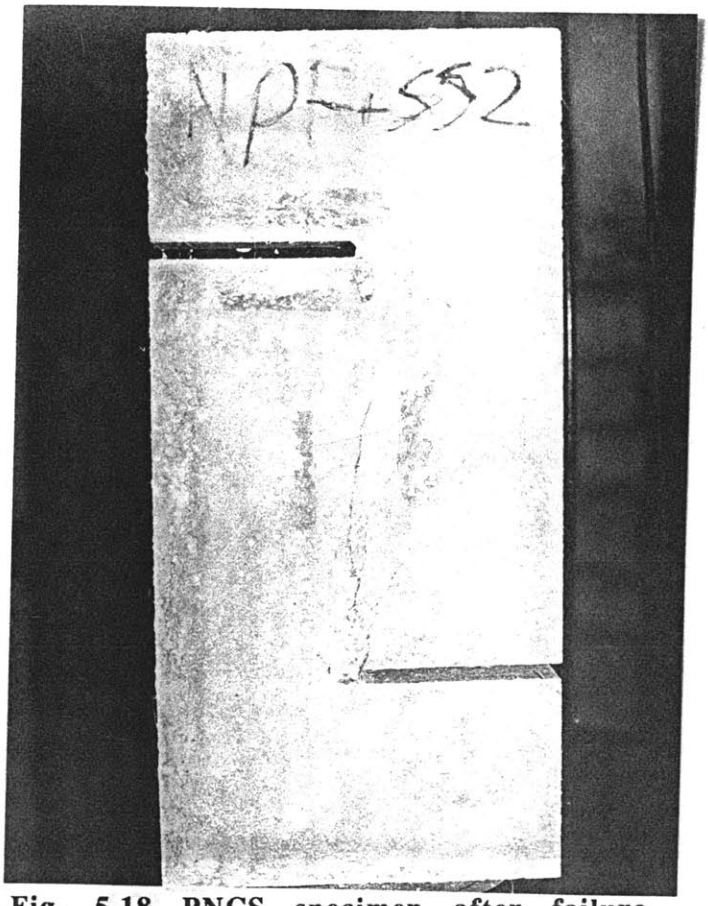

Fig. 5.18 PNCS specimen after failure.

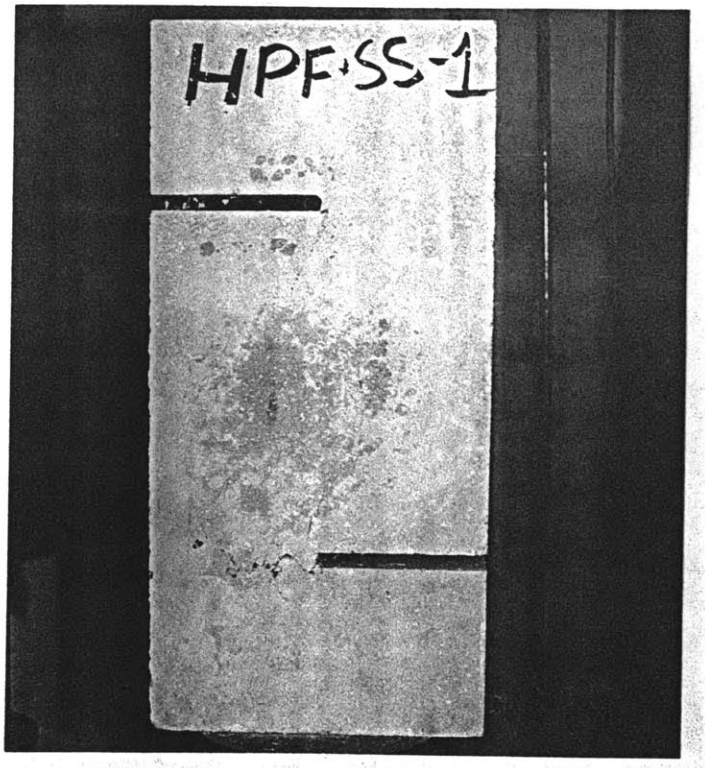

Fig. 5.19 PHCS specimen after failure.

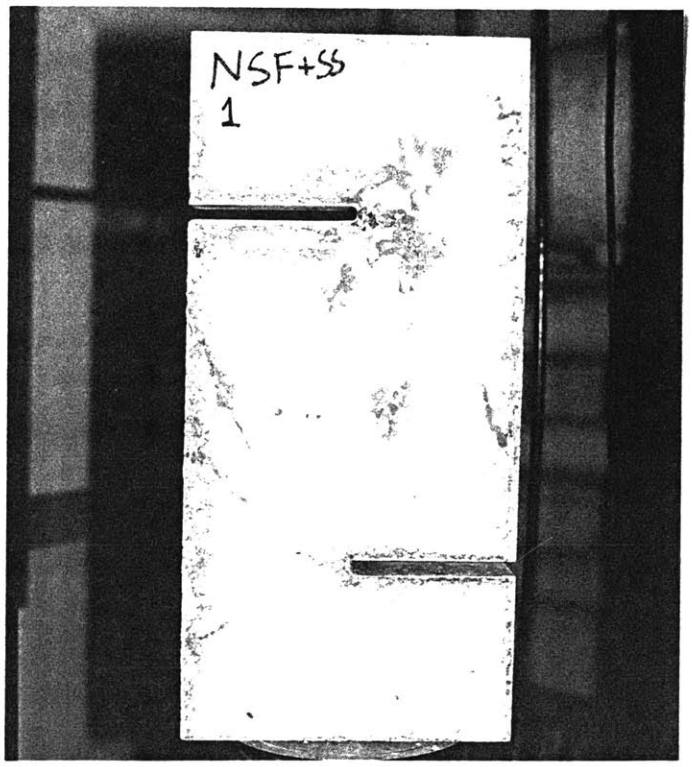

Fig. 5.20 SNCS specimen after failure.

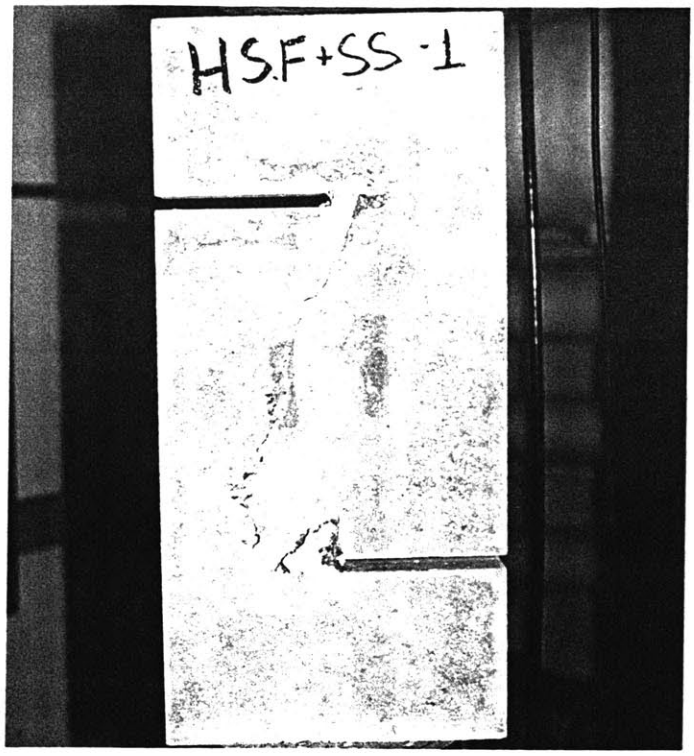

Fig. 5.21 SHCS specimen after failure.

After failure in the specimens reinforced with stirrups, even though the testing machine continued to strain the specimen, since the truss action was no longer present, the steel stirrups relaxed and caused the vertical displacement to decrease. In the specimens involving normal strength concrete(NCS, SNCS, and PNCS), the vertical displacement returned to its starting point (zero value)(see Fig. 5.3); while the specimens with high strength concrete HCS, SHCS, and PHCS, showed this unloading behavior but to a permanent deformation (see Fig. 5.7). In view of this, it was proposed that the steel stirrups in the specimens with NC did not reach their yielding strength, since the vertical displacement returned to its original value; while in the case of the specimens involving HC, the steel stirrups did develop their yield strength, causing a permanent deformation. This behavior was later confirmed by performing an additional test on an HCS specimen, where the strain in the steel stirrups was monitored. The test showed that the steel stirrups did yield, leaving a permanent deformation, as shown in Fig. 5.22. This test also confirmed the assumption that the stirrups develop tensile stresses.

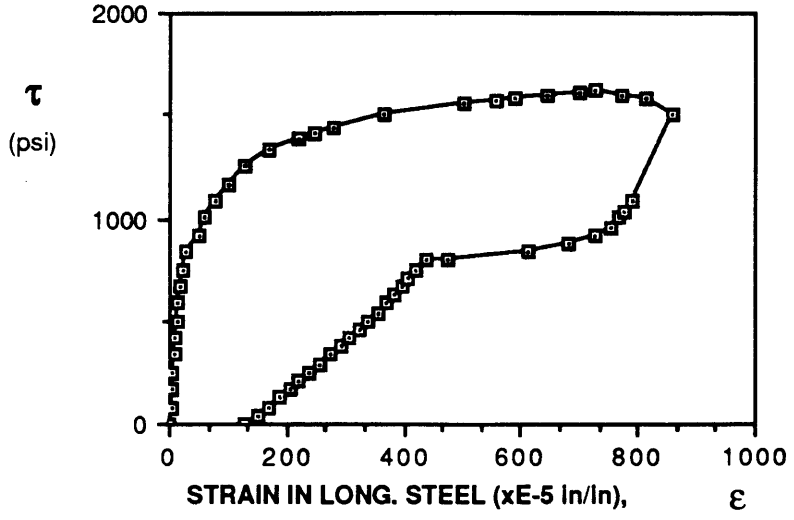

Fig. 5.22 Shear stress vs. strain in longitudinal steel bars for HCS specimen.

(c)Toughness

In order to calculate the relative toughness associated with each type of specimen under shear loading, the toughness indexes proposed by ACI committee 544[51], shown in Fig. 5.23, have been used. In Fig. 5.23, δ is defined as the deflection at first cracking. These toughness indexes were obtained from the shear stress vs. vertical displacement plots of each push-off specimen. The corresponding calculated values are contained in Tables 5.3 and 5.4, for NC and HC specimens respectively.

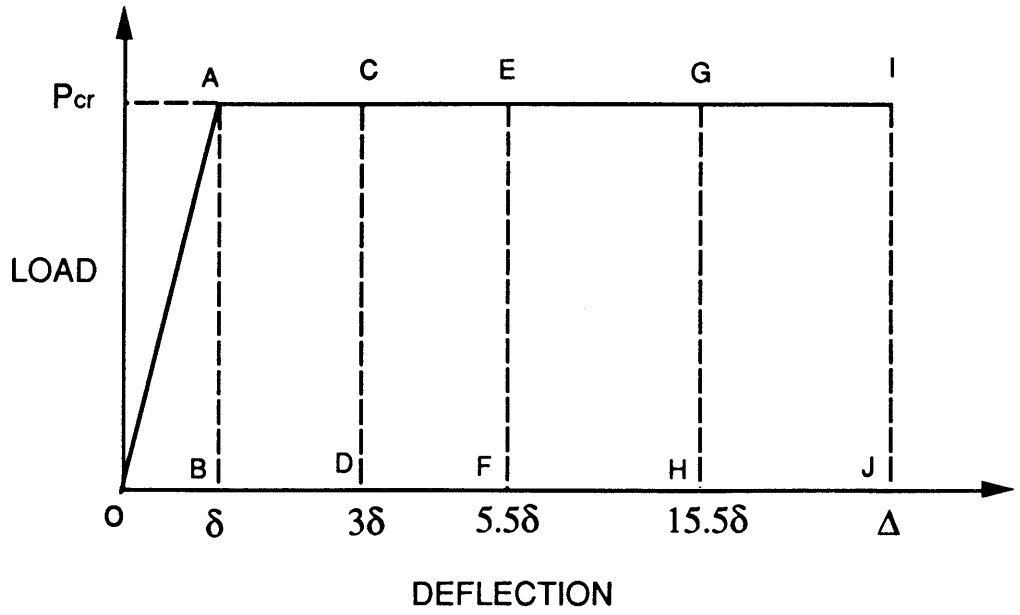

$$I_5 = \frac{\text{area(OACD)}}{\text{area(OAB)}} \qquad I_{10} = \frac{\text{area(OAEF)}}{\text{area(OAB)}}$$

$$I_{30} = \frac{\text{area(OAGH)}}{\text{area(OAB)}} \qquad I_\Delta = \frac{\text{area(OAIJ)}}{\text{area(OAB)}} \qquad \Delta = 1.9\text{mm}$$

Fig. 5.23 Definition of Toughness indices.

Table 5.3 Calculated toughness indices for normal strength specimens.

specimen	I_5	I_{10}	I_{30}	I_Δ
NC-1	1.00	-	-	1.00
NC-2	1.00	-	-	1.00
SNC-1	6.45	13.89	28.41	29.32
SNC-2	5.78	12.90	25.60	27.78
PNC-1	3.51	5.51	10.50	10.50
PNC-2	3.80	5.79	9.22	7.04
NCS-1	6.33	13.02	13.85	13.85
NCS-2	6.15	12.87	13.30	13.30
SNCS-1	6.32	14.19	21.90	21.90
SNCS-2	5.92	12.67	29.37	29.37
PNCS-1	6.58	16.58	16.94	16.94
PNCS-2	6.90	17.10	17.50	17.50

Table 5.4 Calculated Toughness indexes for high strength specimens.

specimen	I_5	I_{10}	I_{30}	I_Δ
HC-1	1	1	1	1
HC-2	1	1	1	1
SHC-1	4.48	-	-	4.48
SHC-2	5.76	-	-	5.76
PHC-1	4.88	9.26	14.32	13.9
PHC-2	5.51	8.73	11.49	9.97
HCS-1	6.82	-	-	-
HCS-2	6.26	-	-	-
SHCS-1	6.96	15.32	24.99	18.11
SHCS-2	6.79	14.93	22.83	15.9
PHCS-1	6.85	14.65	18.19	18.19
PHCS-2	6.56	14.07	17.8	17.8

In general, the addition of fibers shows an improvement of ductility for all cases. Also, the toughness indexes calculated were consistent within the same specimen types. For normal strength concrete specimens the average toughness indices I_5 are shown in Fig. 24. In the case of specimens NC, failure occurred at the time of first cracking, resulting in a toughness index of 1. For the PNC specimens, a higher average value of approximately 3.6 was calculated than for NC specimens; but not as high as for SNC, NCS, SNCS, and PNCS specimens, for which a value of approximately 6 was found. This relatively low toughness value of PNC is attributed to the rapid fiber pull-out after cracking occurred. For the toughness indices values I_{10} (Fig. 5.25), the specimens PNCS showed the highest average value, equal to 16.8; while for specimens SNC, NCS and PNCS almost the same average value equal to 13 was found. PNC specimens resulted in the lowest relative average toughness value of

5.65. Further, for the I_{30} indices (Fig. 5.26), specimens SNC and SNCS resulted in the highest values, with 27 and 25.6 respectively. PNCS specimens reached a value of 17.22, while PNC specimens only resulted in a I_{30} equal to 13.6. In normal strength concrete, the steel fibers alone, SNC specimens, resulted in highest relative toughness values (I_{30}=27), followed by the combination of steel fibers and stirrups (I_{30}=25.6). Furthermore, the combination of polypropylene fibers and stirrups (I_{30}=17.22) presented enhanced toughness characteristics over stirrups alone (I_{30}=13.6).

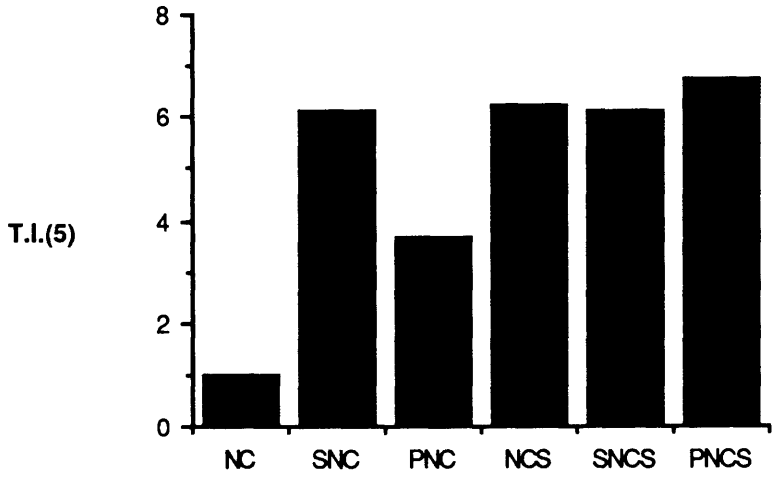

Fig. 5.24 I_5 toughness index values for normal strength concrete specimens.

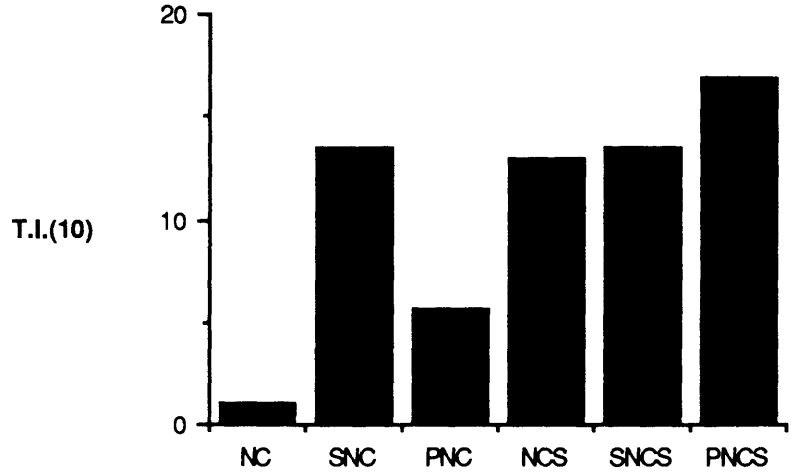

Fig. 5.25 I_{10} toughness index values for normal strength concrete specimens.

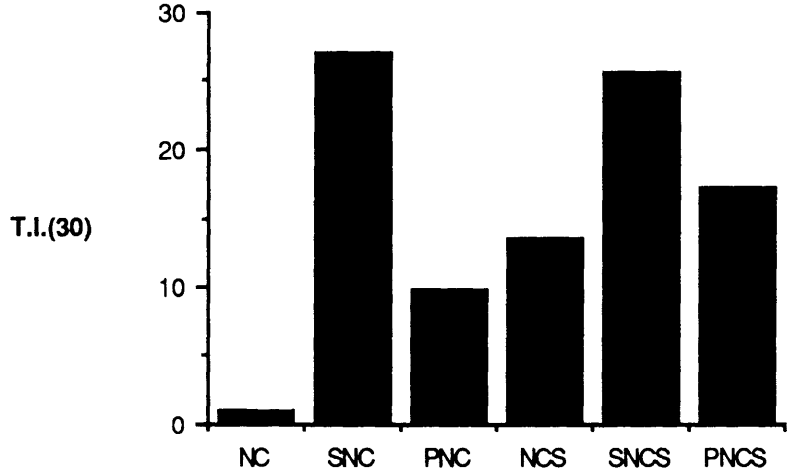

Fig. 5.26 I_{30} toughness index values for normal strength concrete specimens.

For the specimens involving high strength concrete, overall lower relative toughness values were obtained than for normal strength concrete. This implies that high strength concrete manifests a considerably more brittle behavior than normal strength concrete.

In this respect, the addition of fibers proved to be very beneficial when compared to the behavior of non-fiber reinforced high strength concrete. The average values of I_5 obtained for the high strength concrete specimens were similar for all specimens (Fig. 5.27). The only exception were the HC specimens, for which a toughness index value of 1 was found. For specimens reinforced with fiber only, SHC and PHC, I_5 was equal to approximately 5; while for specimens reinforced with stirrups alone or fiber plus stirrups, HCS, SHCS and PHCS, I_5 was found to have an average value of approximately 6.7. The values found for the toughness index I_{10} (Fig. 5.28) can be divided in to two groups. First, for the specimens with no stirrups, HC, SHC and PHC, the PHC specimens showed the largest I_{10} value equal to 9; while HC and SHC specimens showed the same values as for I_5. The higher toughness obtained in PHC specimens is attributed to the improved fiber-matrix bond that HC presents, which probably enabled the polypropylene fibers to develop plastic deformation before it pulled-out of the matrix. For the SHC specimens, relatively lower toughness values were observed, due to the yielding and braking of the steel fibers. In the case of specimens with steel stirrups, HCS, SHCS and PHCS, considerably higher I_{10} values were obtained for the specimens with fibers, SHCS and PHCS, than for the HCS specimens. For specimens SHCS and PHCS average values equal to 15.12 and 14.36 were found, respectively; while for HCS specimens the same values as for I_5 were obtained for I_{10}. Here, the interaction of stirrups and fibers resulted in a much more ductile behavior than the stirrups alone. For the values obtained for the index I_{30} (Fig. 5.29) specimens SHCS resulted in the highest average

value of 23.91, followed by PHCS specimens with an average value equal to 18. For PHC specimens a I_{30} value equal to 12.9 was calculated, while specimens HCS and SHC resulted in I_{30} values equal to the ones obtained for I_{10}. Overall, in high strength concrete, for the specimens with no steel stirrups, polypropylene fibers resulted in the most ductile behavior with an increase of almost 13 times of the toughness obtained with plain high strength concrete. Also, for specimens involving steel stirrups as well as fibers, the interaction of this two type of shear reinforcement resulted in a very ductile behavior, with improvements of 265% for SHCS specimens and 175% for PHCS specimens over the high strength concrete reinforced with steel stirrups alone (HCS).

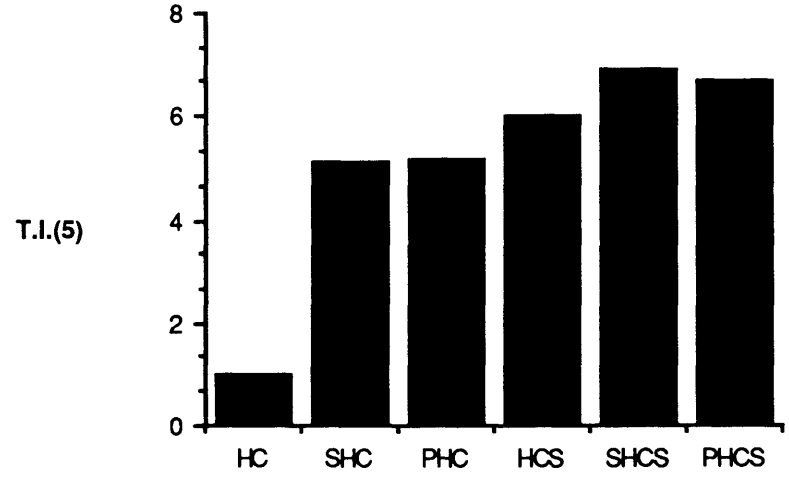

Fig. 5.27 I_5 toughness index values for high strength concrete specimens.

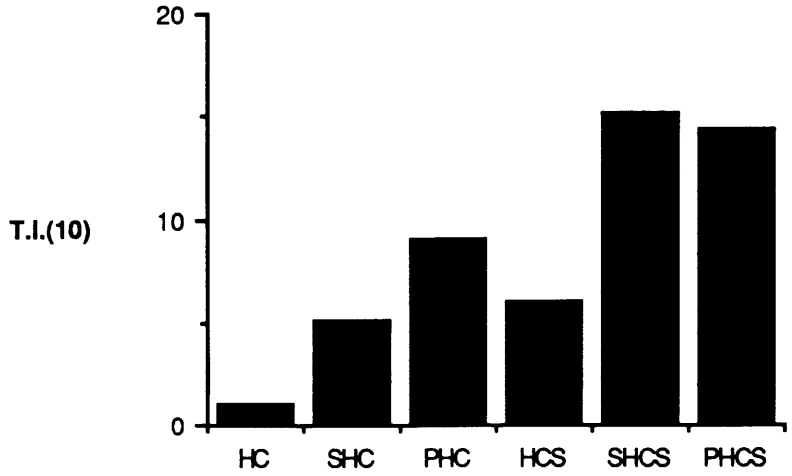

Fig. 5.28 I_{10} toughness index values for high strength concrete specimens.

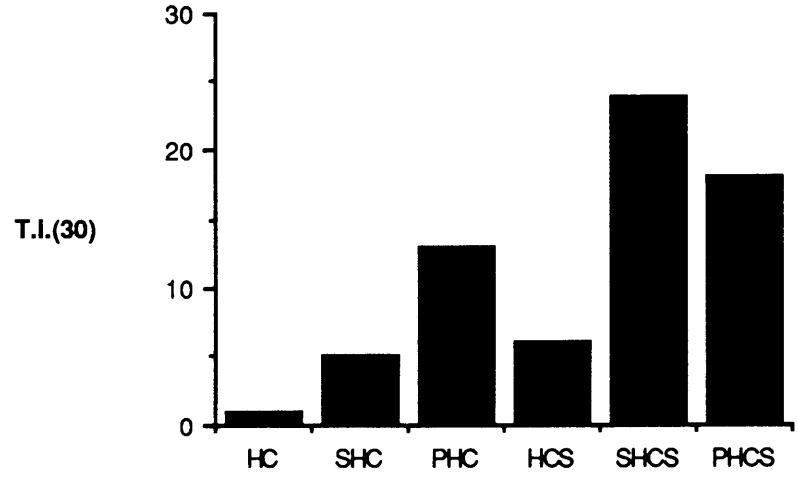

Fig. 5.29 I_{30} toughness index values for high strength concrete specimens.

(d) Distribution of shear strain along the shear plane

The distribution of the shear strain along the shear plane was investigated in the last test performed on a push-off specimen. The shear strain is obtained by dividing the vertical deflection measured by the vertical LVDT in the test by the gage length perpendicular to the shear plane. In this test two LVDTs were positioned with the same orientation along the shear plane, as explained in Chapter 4, section 4.5.2. Fig. 5.30 shows the deformation at these two locations of the shear plane, obtained from the test. It is clear from this figure that before cracking the vertical deformation at the two points are quite different, being almost zero at the center and increasing linearly with the applied stress for the edge. After cracking, the vertical deformation of the two points follow the same path, with an offset equal to the difference of displacements at the cracking stress. This leads to the conclusion that the strain distribution along the shear plane after cracking becomes almost uniform. Using this information, and the stress distribution along the shear plane proposed by Cholewicki[53], the shear strain and shear stress distributions shown Fig. 5.31a&b, were assumed.

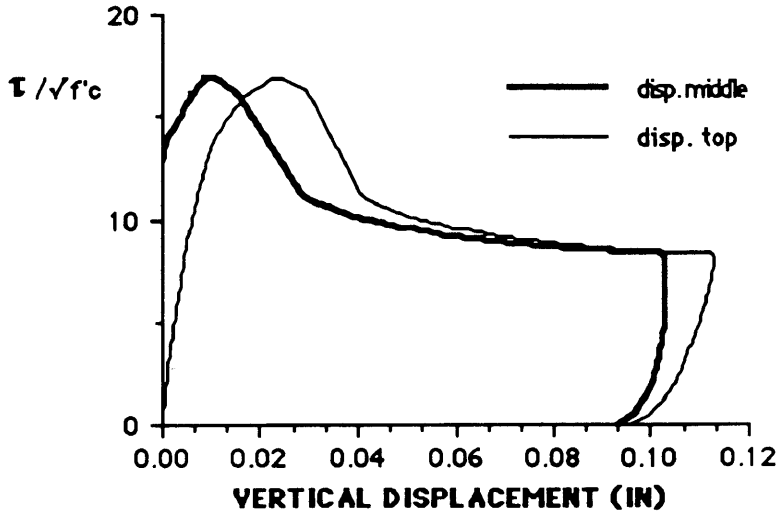

Fig. 5.30 Vertical displacement at the top and middle of the shear plane for HCS specimen.

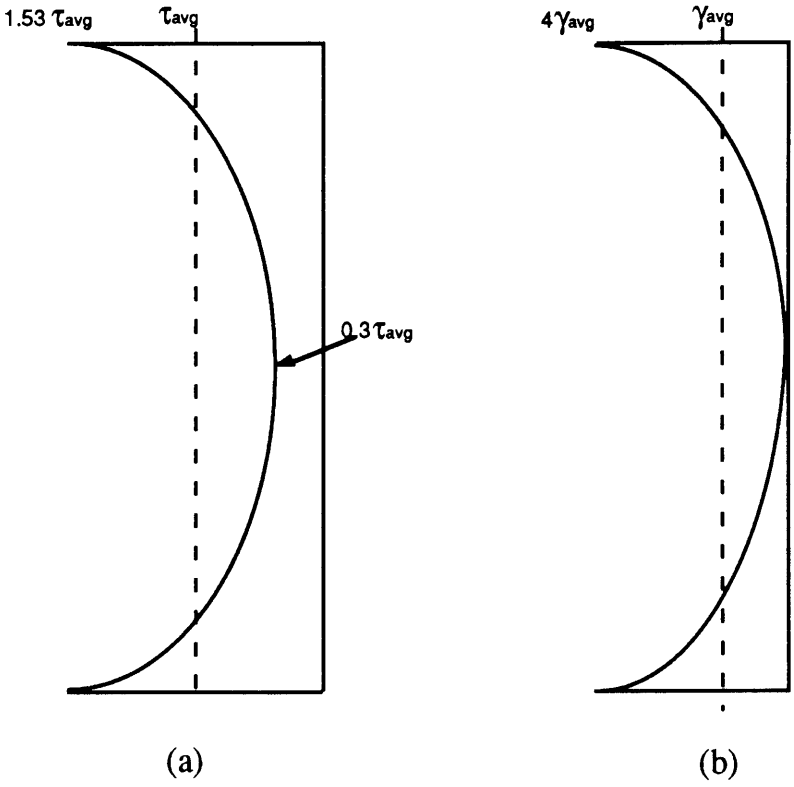

Fig. 5.31 Shear stress and shear strain distribution before cracking: (a) Shear stress distribution (b) assumed shear strain distribution.

5.1.4 Summary of Findings

(a) Material Properties

In the production of the fiber reinforced concrete mixes a reduction in workability was observed due to the presence of fibers. This reduction did not affect the placing of the concrete; except in the case of PNC, where very porous specimens were obtained leading to a decrease of the initial stiffness of these specimens. The compressive strength of the concrete remained unchanged with the addition of fibers, with the exception of SHC mixes, where a 20% increase in compressive strength was observed. Also, the addition of steel fibers increased the splitting tensile strength of concrete by 86% in normal strength concrete and 116% in high strength concrete. No increases in the compressive or splitting tensile strengths of either normal strength or high strength concrete were observed from the addition of polypropylene fibers.

(b) Shear Strength

Overall, the addition of fibers to concrete proved to be beneficial to the shear transfer behavior of this material. Higher increases in shear strength were obtained in high strength concrete specimens reinforced with fibers alone than in normal strength concrete specimens with fibers only. For the case of steel fibers, a 60% increase in shear strength was observed in SHC over plain HC; while only a 36% increase for SNC over NC was obtained. For polypropylene fibers no increase in shear strength was observed for PNC over NC, while a 17% increase was present for PHC over HC. The higher shear strengths obtained from high strength mixes reinforced with fibers than the ones obtained in normal strength concrete is

attributed to the improved fiber-matrix bond that high strength concrete with silica fume presents. For the specimens reinforced both with steel stirrups and fibers, generally, no significant increases in shear strengths were observed over the specimens reinforced with steel stirrups alone. However, for the case of SHCS specimens a 24% increase in shear strength over the HCS specimens was obtained. Also, when comparing the shear strengths of the two types of concrete used with the different forms of reinforcement, it is interesting to note that SHC specimens were able to develop up to 18% higher shear strengths than NCS specimens.

(c) Shear Ductility

For all cases where fibers were added, the deformation and ductility characteristics of the concrete were improved. In high strength concrete, the use of polypropylene fibers alone resulted in the highest toughness index values, almost 13 times the value obtained for plain high strength concrete, within the specimens with no stirrup reinforcement. High strength concrete specimens reinforced with steel fibers and stirrups resulted in approximately 265% higher shear ductility than high strength concrete specimens reinforced with steel stirrups alone. In normal strength concrete, steel fibers alone resulted in the most ductile behavior, with a toughness index value equal to twice the value obtained from normal strength concrete reinforced with stirrups only, for both specimens with and without stirrups.

(d) Failure Modes

From all the shear tests performed, two distinct failure modes were identified depending on the type of shear reinforcement used.

In the case where only fibers were used, first a series of small inclined cracks developed along the shear plane of the specimen (see Fig. 5.9a). Ultimate failure occurred when these small cracks joined and formed a single crack along the shear plane. When stirrups were present, with or without fibers, the failure mechanism changed. Only a few diagonal cracks developed along the shear plane; and as these cracks propagated they created well defined concrete struts(Fig. 5.9b). The concrete struts and the steel stirrups created a truss mechanism to transfer shear. In this case, ultimate failure occurred by crushing of the concrete struts in compression.

(e) Shear Strain Distribution Along the Shear Plane

Finally, the shear strain distribution along the shear plane was studied. From a test, the relation between the vertical deformation at the top and the center of the shear plane was obtained. Using this information, and a previously proposed shear stress distribution, a parabolic shear strain distribution along the plane for the precracking stage was assumed (Fig. 5.31). After cracking, the shear strain distribution was assumed to be uniform.

5.2 COMPARISON OF MODEL AND EXPERIMENTAL RESULTS

In order to compare the test results with the model predictions, the shear strain measured in the tests performed had to be calibrated to account for the non-uniformity of the shear strain and shear stress along the shear plane before cracking. Since the model predicts the average shear strain along the plane, and the measured

shear strain in the tests was located at the edge of the plane, this correction was needed. To obtain this correction factor, as mentioned before, an additional test was performed in which the shear deformations at two points, the center and the edge, in the shear plane were measured. By assuming a parabolic distribution of the shear strain along the shear plane, shown in Fig. 5.31a, it was found that the shear strain at the top was equal to 4 times the average shear strain.

Overall, good agreement between the test results and the model predictions were found for both before and after cracking. Table 5.5 summarizes the test and model predictions for all the specimen types studied; including cracking shear stress, τ_{cr}, cracking shear strain, γ_{cr}, maximum shear stress, τ_{max}, and shear strain at maximum shear stress, γ_{max}. Figs. 5.32 through 5.43 show both the calibrated test and model shear stress vs. shear strain curves for all the specimen types tested, that is specimens NC, SNC, PNC, NCS, SNCS, PNCS, HC, SHC, PHC, HCS, SHCS, and PHCS, respectively. From these figures it can be seen that the model has good agreement with the test results at all loading stages for both shear stress and shear strain. Only for specimens PNCS (Fig. 5.37) correlation between the model and the test results is not satisfactory. This is attributed to manufacturing problems,discussed before, that resulted in a lowering of the stiffness of these specimens. In Fig. 5.44, a comparison between the test results and model predictions for the cracking and maximum shear stresses for each of the specimens studied is shown. As it can be seen in the figure almost all shear stress predictions fall within 15% of the values obtained in the tests. Figs. 5.45 and 5.46

show a comparison of the cracking shear strain and shear strain at the maximum shear stress between test and model predictions. Here an improvement in the prediction of the shear strain was obtained when compared to results reported by Hsu et al.[7] These improvements are attributed to the correction factor introduced by the assumed shear strain distribution before cracking as well as to the lowering of the stiffness of the concrete in tension thru the empirical constant described in Chapter 3.

For the specimens involving steel stirrups and fibers as shear reinforcement, the model consistently over-estimated the maximum shear stress by 15 to 20%. This is probably due to an interaction of the fibers and the steel stirrups, which is not considered in the model. Other possibilities for this overestimation could be: 1) compaction problems in test specimens, since the presence of steel stirrups made the placing of the fiber reinforced concrete more difficult; or 2) in specimens involving stirrups and fibers, the tensile stress-strain relationship may be different than for the case of fiber reinforcement alone due to a different crack spacing and propagation, as shown in Fig. 5.9. Nevertheless, this model represents a good tool for further investigation, and could be used as a basis for a parametric study of the variables involved in the shear transfer of fiber reinforced concrete.

The overall understanding of the shear behavior concrete has been broaden through the model studies performed. One can say that the shear behavior of concrete can be accurately described as a biaxial stress state. This is true for both unreinforced and reinforced concrete, whether the reinforcement is in the form of steel bars,

randomly oriented fibers, or a combination of these two types of reinforcement.

Table 5.5 Model and experimental results.

specimen	τ_{cr} test (psi)	γ_{cr} test (x E-4)	τ_{cr} model (psi)	γ_{cr} model (x E-4)	τ_{max} test (psi)	γ_{max} test (x E-3)	τ_{max} model (psi)	γ_{max} model (x E-3)
NC	744.13	5.99	741.45	6.13	-	-	-	-
SNC	618.26	5.9	627.45	4.46	1010.1	6.75	1022.6	5.38
PNC	788.39	8.88	694.94	6.2	788.39	0.888	782.07	2.22
NCS	823.87	6.6	876.02	6.62	1308.6	4.5	1485.8	5.059
SNCS	669.46	4.26	559.58	5.78	1200.8	8.52	1439.7	6.98
PNCS	747.6	10.9	841.18	6.4	1284.5	14.8	1567.2	4.67
HC	869.63	3.93	853.11	4.2	-	-	-	-
SHC	1129.7	7.1	1091.9	4.86	1540.5	4.2	1664.5	3.35
PHC	884.3	3.53	865.86	4.48	992.1	3.19	950.85	2.6
HCS	1054.7	5.8	942.7	4.5	2005.2	5.3	2003.4	5.25
SHCS	1259.8	6.8	1124	5.03	2251.9	5.59	2566.6	4.35
PHCS	1009.6	5.78	945.93	4.77	1645.9	6.94	2054.6	4.29

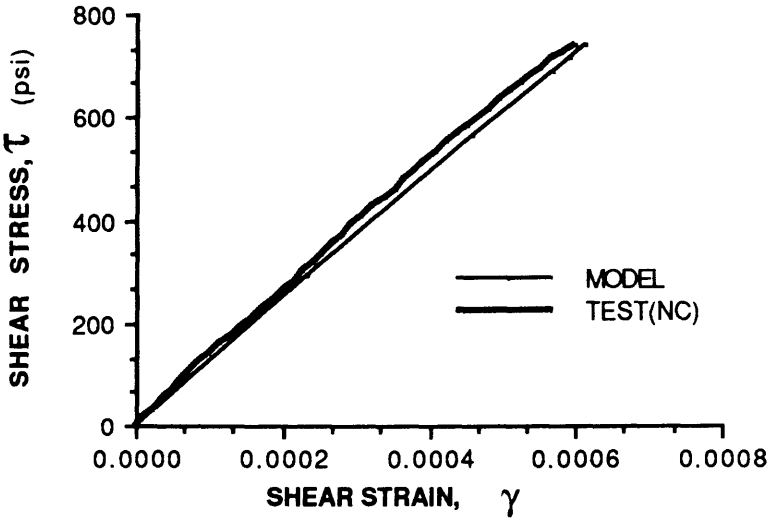

Fig. 5.32 Shear stress vs. shear strain curve for NC specimen.

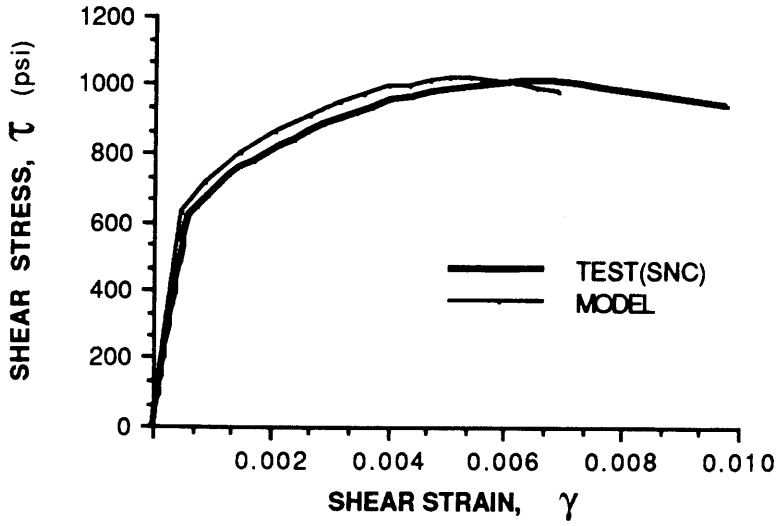

Fig. 5.33 Shear stress vs. shear strain curve for SNC specimen.

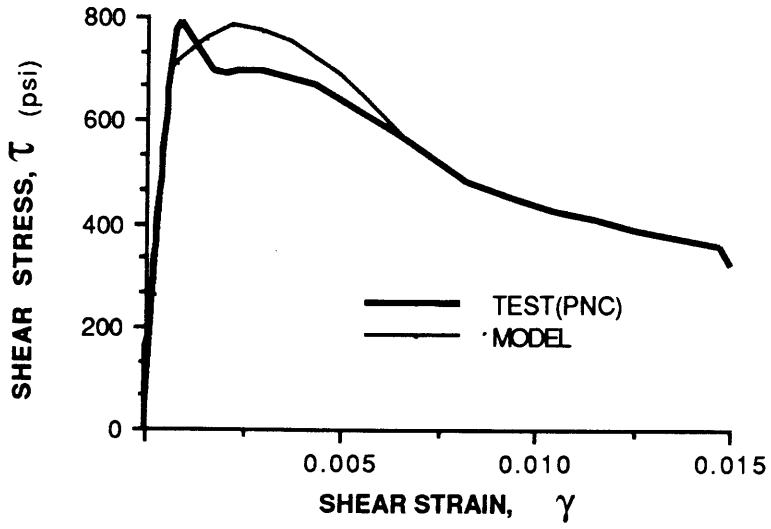

Fig. 5.34 Shear stress vs. shear strain curve for PNC specimen.

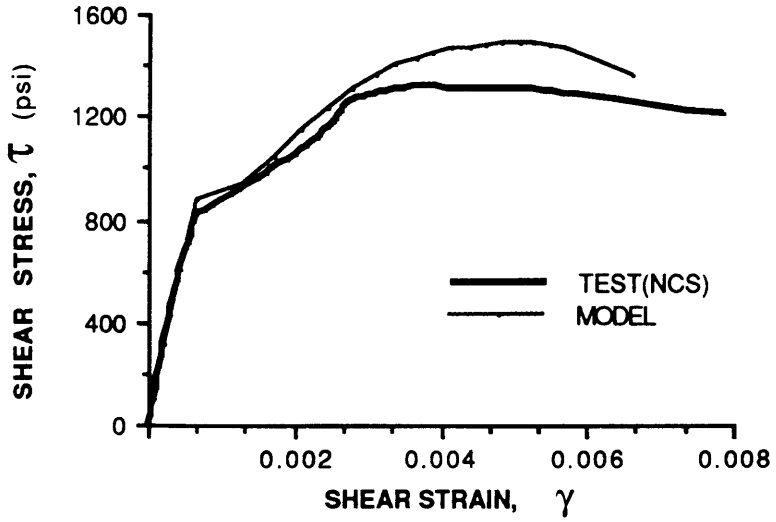

Fig. 5.35 Shear stress vs. shear strain curve for NCS specimen.

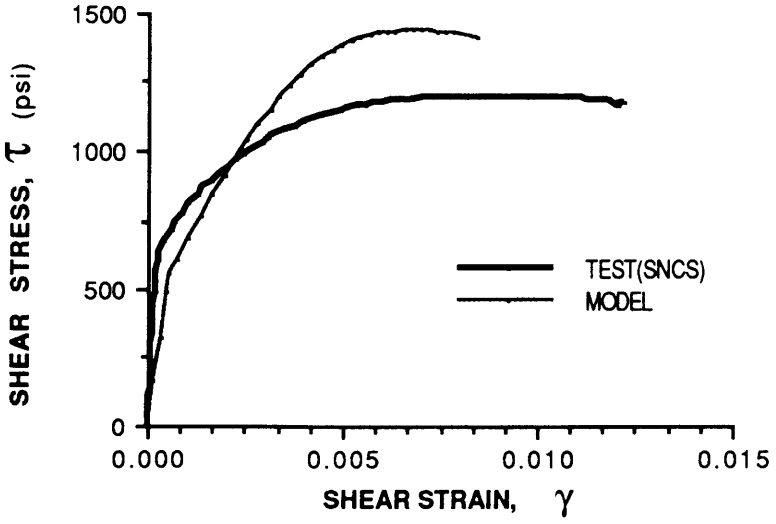

Fig. 5.36 Shear stress vs. shear strain curve for SNCS specimen.

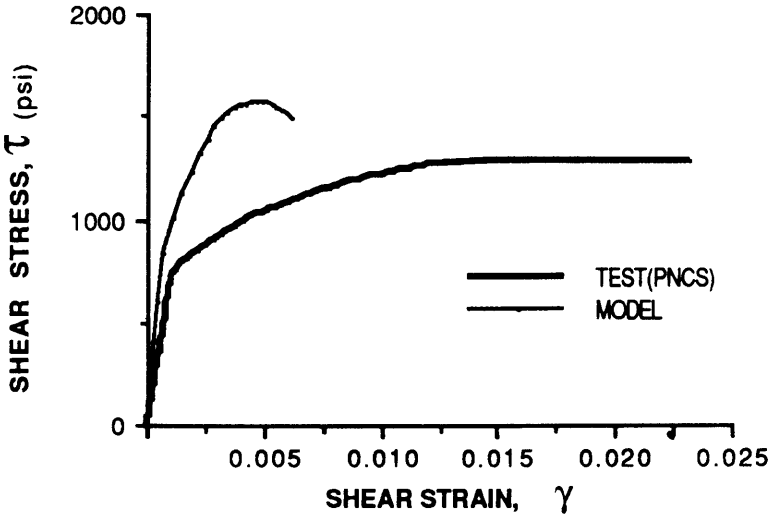

Fig. 5.37 Shear stress vs. shear strain curve for PNCS specimen.

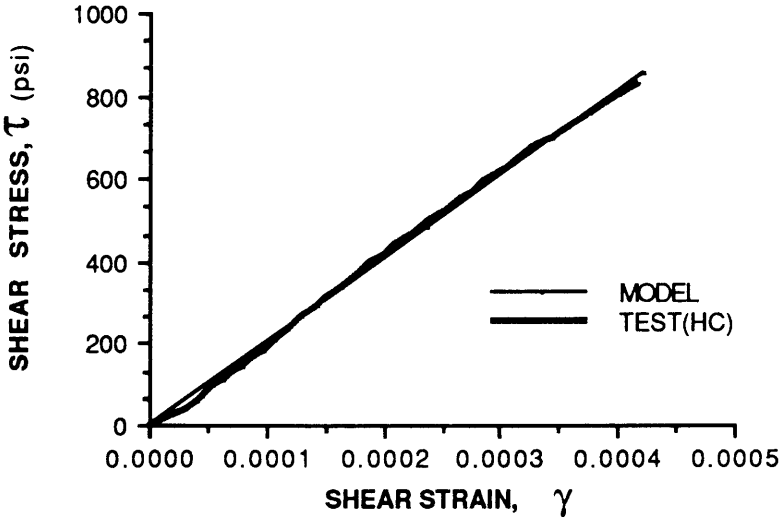

Fig. 5.38 Shear stress vs. shear strain curve for HC specimen.

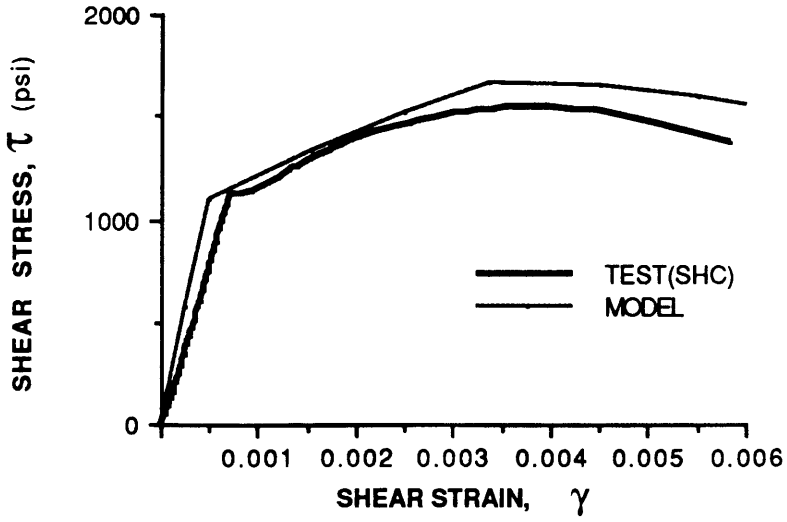

Fig. 5.39 Shear stress vs. shear strain curve for SHC specimen.

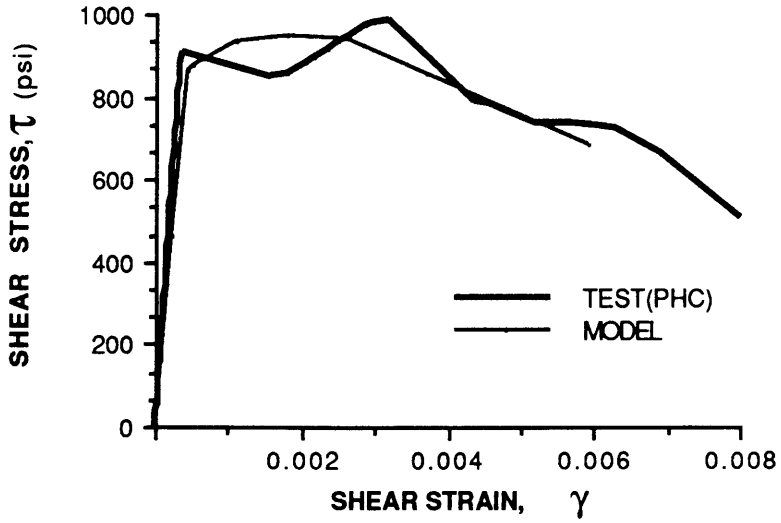

Fig. 5.40 Shear stress vs. shear strain curve for PHC specimen.

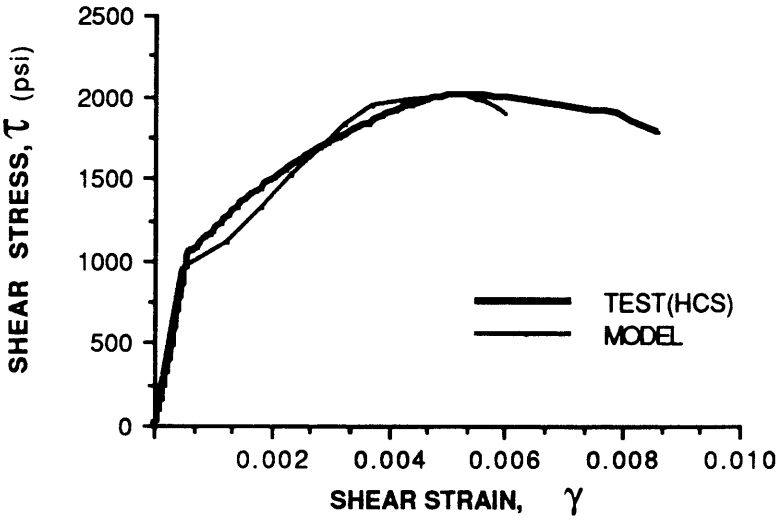

Fig. 5.41 Shear stress vs. shear strain curve for HCS specimen.

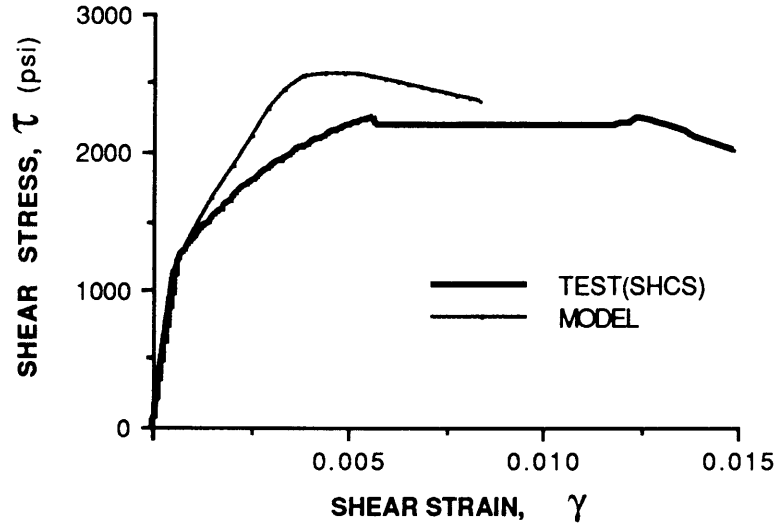

Fig. 5.42 Shear stress vs. shear strain curve for SHCS specimen.

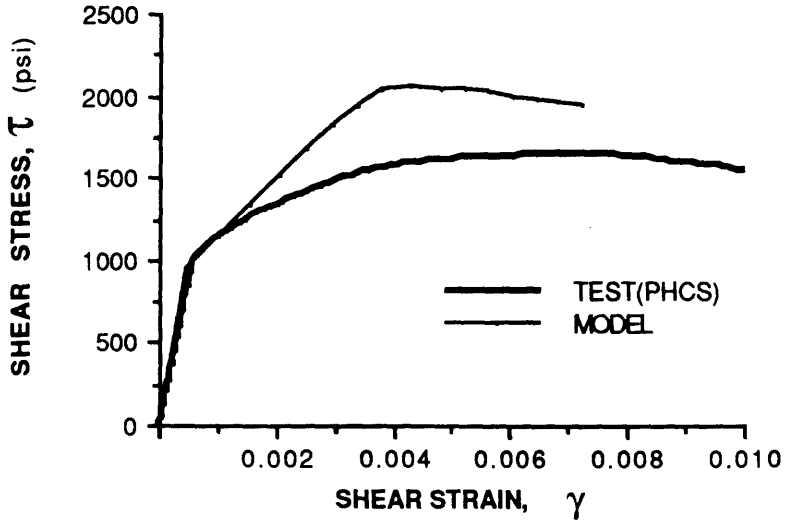

Fig. 5.43 Shear stress vs. shear strain curve for PHCS specimen

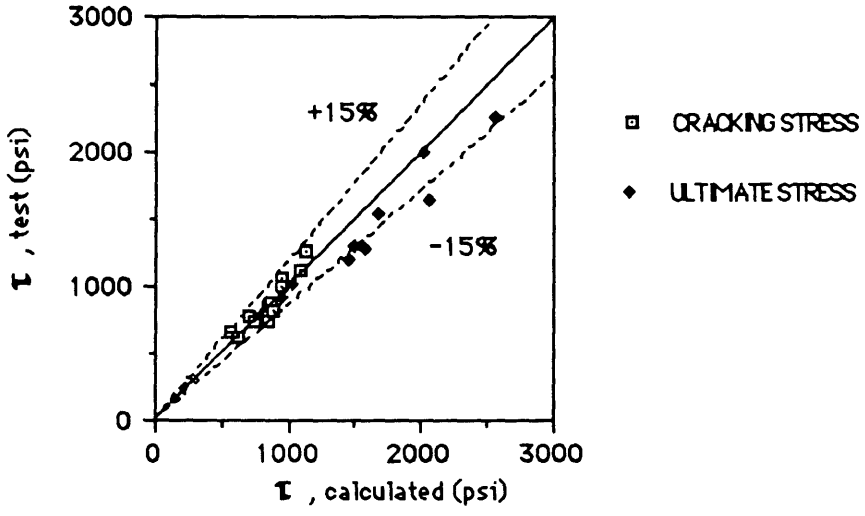

Fig. 5.44 Comparison of cracking and maximum shear stresses between model and tests.

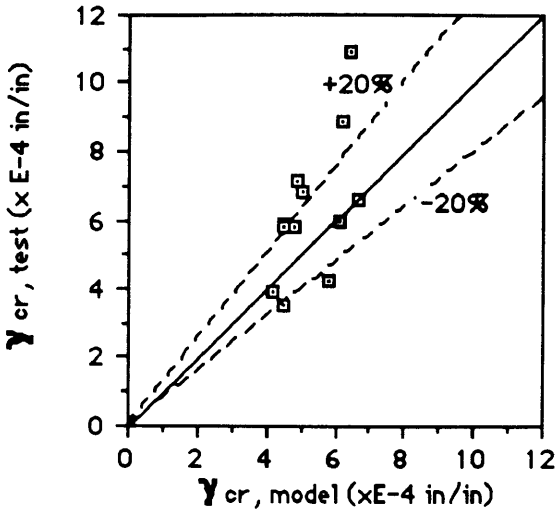

Fig. 5.45 Comparison of cracking shear strain between model and tests.

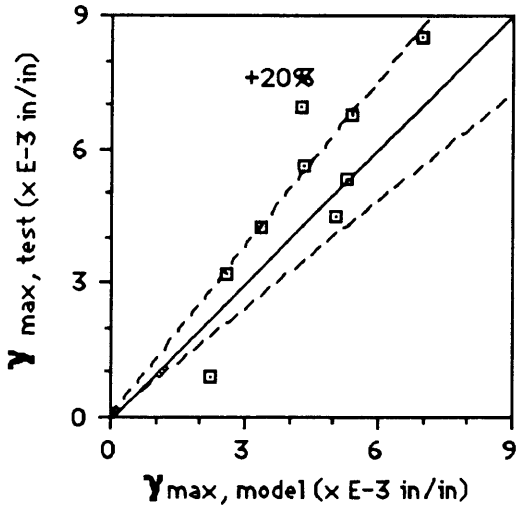

Fig. 5.46 Comparison of shear strain at maximum shear stress between model and tests.

CHAPTER 6

SUMMARY, CONCLUSIONS AND RECOMMENDATIONS FOR FUTURE WORK

6.1 SUMMARY

A study on the shear behavior of fiber reinforced normal strength concrete and fiber reinforced high strength concrete was performed. The investigation included the addition of steel and polypropylene fibers to both of these types of concrete mixture. It has been shown that the addition of fibers enhances the overall ductility of concrete as well as tensile strength of the material; two very important aspects related to the shear transfer behavior. Limited knowledge is available on the effect of fibers to the shear transfer behavior of concrete. This is especially true for the case of fiber reinforced high strength concrete, where no prior studies were found on the subject.

Both experimental and analytical programs were included in the investigation. In the experimental phase, 25 initially uncracked push-off specimens were tested. The parameters investigated included: concrete type (normal strength and high strength concrete), fiber type (steel vs. polypropylene fibers), and the presence of steel stirrups as shear reinforcement alone and in combination with one of

the fiber types. In the analytical program, an existing shear transfer theory based on the truss model was further developed. The model assumes a uniform shear stress and shear strain distribution along the shear plane of the push-off specimens and its formulation is based on: equilibrium, compatibility and material law. As used in the context of this investigation, the model takes into account the softening of concrete in compression as well as in tension due to the biaxial stress state (compression-tension). Overall, the goal of the program was to broaden the basic understanding of the shear behavior of concrete reinforced with fibers.

6.2 CONCLUSIONS

In general, the controlled addition of fibers in concrete enhanced the shear transfer behavior of both normal strength and high strength concrete. Further, addition of fibers showed to be more effective in providing improved strength and ductility properties in high strength concrete than in normal strength concrete. From the results obtained in Chapter 5, the following conclusions are drawn:

1-. Greater shear strength increases were found in fiber reinforced high strength concrete specimens than in fiber reinforced normal strength concrete specimens, compared to the respective unreinforced plain concrete specimens. Steel fibers increased the maximum shear strength of high strength concrete by almost 60%, while only a 38% increase was observed in normal strength concrete.

Addition of polypropylene fibers in high strength concrete produced a 17% increase in the shear strength, while resulted essentially no shear strength increase in normal strength concrete. It is interesting to note that high strength concrete specimens reinforced with steel fibers only showed a 18% higher shear strength than normal strength concrete specimens reinforced with stirrups only. The enhanced performance of fibers in high strength concrete is attributed to the improved bond characteristics between the fiber and the matrix associated with the high strength concrete with silica fume.

2-. In all instances, fibers improved the shear deformation and ductility characteristics of concrete. Addition of steel fibers in high strength concrete specimens produced a relative toughness which was approximately 5 times greater than for plain high strength concrete specimens. This improvement in shear deformation and ductility was even greater, up to 14 times, for specimens reinforced with polypropylene fibers compared to plain high strength concrete specimens. Comparable improvements in toughness were obtained in normal strength concrete reinforced with fibers alone.

3-. For the specimens reinforced with fibers alone, failure occurred by the formation of numerous small cracks diagonal to the shear plane, which ultimately joined and formed a single crack along the plane. Both steel and polypropylene fibers in normal strength concrete pulled-out of the matrix, producing a very ductile failure with softening. In high strength concrete specimens reinforced with polypropylene fibers, also a very ductile failure was observed, with

the fibers pulling-out of the matrix after some plastic deformation occurred in the polypropylene fibers. In high strength concrete with steel fibers, the cracking pattern to failure was similar, but because of the improved bond between the fiber and the matrix, some of the steel fibers bridging the cracks yielded and broke. The somewhat less ductilily observed in high strength concrete reinforced with steel fibers compared to that of high strength concrete with polypropylene fibers is attributed to this breaking behavior of the steel fibers.

4-. For normal strength concrete the measured shear strengths did not vary significantly for specimens containing both fibers and steel stirrups, when compared to the specimens with steel stirrups alone. However, for high strength concrete specimens containing both stirrups and steel fibers, a 24% increase in the shear strength was observed over the shear strength of high strength concrete reinforced with stirrups alone. This is attributed to the improved fiber-matrix bond in high strength concrete, and thus, the interactive behavior of fibers and stirrups.

5-. The combination of fibers and steel stirrups proved to increase the overall ductility when compared to concrete reinforced with steel stirrups alone; resulting in a 265% increase in toughness for high strength concrete specimens reinforced with both stirrups and fibers over high strength concrete specimens reinforced with stirrups alone, and approximately 100% increase for normal strength concrete specimens reinforced with fibers and stirrups over normal strength specimens reinforced with stirrups only.

6-. For the specimens reinforced with stirrups alone and for those with stirrups plus fibers, failure initiated by the formation of several discrete diagonal cracks, which extended and eventually formed well defined compression concrete struts. These concrete struts (in compression) in combination with the steel stirrups (in tension) form a truss action to transfer shear. Ultimately, final failure occurred by crushing of the compression concrete struts. After crushing of the concrete, an unloading behavior of the shear load vs. deformation was observed. This unloading appears to occur due to the vanishing of the truss action and the relaxing of the steel.

7-. The obtained model predictions for the shear behavior of the tested specimens correlate well with the experimental results. Both shear stresses and shear strains are predicted with good accuracy. With the proposed improvement of the model incorporating, 1) the tensile softening behavior of concrete before cracking (due to biaxiality effects), and 2) calibration of the measured shear strain due to non-uniformity of the shear strain along the shear plane before cracking, the model predictions for the precracking behavior are improved. Thus, the model represents a good basis for a parametric study of the variables involved in the shear transfer of fiber reinforced concrete.

6.3 RECOMMENDATIONS FOR FUTURE RESEARCH

In view of the results obtained in this investigation, the use of fibers alone or in combination with steel stirrups as shear

reinforcement in concrete appears to have a promising future. This is especially true for high strength concrete, where fiber reinforcement was observed to be more effective. Using the presented model, a parametric study can be performed on the shear transfer behavior of non-fiber as well as fiber reinforced concrete in not only direct shear transfer but also in structural beams. This study should include beam test results, as well as an optimization program for the combined use of fibers and stirrups as shear reinforcement for most effective and economical design solutions.

In addition, more pull-out and tension tests are needed for fibers in high strength concrete, in order to develop better models for the tensile behavior of this composite. While an extensive data base exists for pull-out strengths and tensile behavior of steel fiber reinforced normal strength concrete, this is not true for other type of fibers like polypropylene. Also, a study can be carried out to optimize the fiber shape. This could apply to polypropylene fibers, by introducing larger cross-sections at the ends of the fibers that would improve the fiber-matrix pull-out strength.

The interaction of fiber and stirrups reinforcement should be further investigated. The results obtained in this program are only preliminary, but show an important increase in ductility when these two types of reinforcement are used. Future work should include an optimization study of the combined use of stirrups and fibers as shear reinforcement, to obtain economic solutions with higher shear capacities and ductility. Also, the possibility of including two types of fibers like steel and polypropylene in the same high strength concrete mixture should be looked into. By including this two types

of fibers in the same high strength mixture, both significant increases in shear strength, from steel fibers, and increases in ductility, from polypropylene fibers, could be obtained.

REFERENCES

1. Green, E. C., " Behavior of High Strength Fiber Reinforced Concrete," M.S. Thesis, Department of Civil Engineering, Massachusetts Institute of Technology, 1989.

2. Kani, G.N.J., "Basics Facts Concerning Shear Failure", *ACI Journal*, Vol. 63, No. 6, June 1966, pp. 675-691.

3. Park, R. and Paulay, T., "Reinforced Concrete Structures", 1975, John Wiley & Sons, Inc.

4. Nawy, E.G., "Reinforced Concrete," 1985, Prentice-Hall, Inc., Englewood Cliffs, New Jersey.

5. ACI Committee 318, "Building Code Requirements for Reinforced Concrete," ACI, Detroit, 1983.

6. Mattock, A. H. and Hawkins, N. M., "Shear Transfer in Reinforced Concrete-Recent Research," *PCI Journal*, Vol. 17, No. 2, March-April 1972, pp. 55-75.

7. Hsu, T.T., Mau, S.T., and Chen B., "Theory of Shear Transfer Strength of Reinforced Concrete," *ACI Structural Journal*, Vol. 84, No. 2, 1987, pp. 149-160.

8. Naaman, A. E., "Fiber Reinforcement for Concrete," *Concrete International*, Vol. 7, No. 3, March 1985, pp. 21-25.

9. ACI Committee 544, "Design Considerations for Steel Fiber Reinforced Concrete," *ACI Structural Journal*, Vol. 85, No. 5, September-October 1988, pp. 563-580.

10. Craig, R. J., "Structural Applications of Reinforced Fibrous Concrete," *Concrete International*, Vol. 6, No. 12, December 1984, pp. 28-32.

11. Hannant, D. J. and Edgington, J., "Durability of Steel-Fiber Concrete," Fiber Reinforced Cement and Concrete, RILEM, Landcaster, 1975, pp. 159-170.

12. Naaman, A. E. and Shah, S. P., "Some Developments in Polypropylene Fibers for Concrete," Fiber Reinforced Concrete, ACI SP-81, ACI, Detroit, 1984, pp. 375-396.

13. Zollo, R.F., "Collated Fibrillated Polypropylene Fibers in FRC," Fiber Reinforced Concrete, ACI SP-81, ACI, Detroit, 1984, pp. 397-409.

14. Lyle, D. S., "Modern Textiles," John Wiley and Sons., pp. 454.

15. Majumdar, A. J. et al., "Properties of Glass Fibers in Cement Environment," *Journal of Materials Science*, Vol. 12, No. 5, May 1977, pp. 927-936.

16. Ali, M. A., Majumdar, A. J., and Rayment, D. L., "Carbon Fiber Reinforcement of Cement," *Cement and Concrete Research*, Vol. 2, No. 2, March 1972, pp. 201-212.

17. Walton, P. L. and Majumdar, A. J., "Cement Based Composites with Mixtures of Different Types of Fibers," *Composites*, Vol. 6, No. 5, Sept. 1975, pp. 209-216.

18. Wang, Y., Backer, S., and Li, V. C., "An Experimental Study of Synthetic Fiber Reinforced Cementitious Composites," *Journal of Materials Science*, Vol. 22, 1987, pp. 4281-4291.

19. Walton, P. L. and Majumdar, A. J., "Properties of Cement Composites Reinforced with Kevlar Fibers," *Journal of Materials Science*, Vol. 13, No. 5, May 1978, pp. 1075-1083.

20. Zahar, G.J., "Flexural Behavior of Mortar Reinforced with Carbon Fibers", S.M. Thesis, Department of Civil Engineering, Massachusetts Institute of Technology, 1987.

21. Ward, R., "Steel and Synthetic Fibers as Shear Reinforcement," M.S. Thesis, Department of Civil Engineering, Massachusetts Institute of Technology, 1989.

22. Kohno, K., Horii, K., Yukitomo, K., and Gotoh, Y., "Shearing Strength of Steel Fiber Reinforced Concrete,"*Transactions of the Japan Concrete Institute,* Vol. 5, No. 4, 1983, pp. 231-238.

23. Hara, T., "Effects of Steel Fibers on Shear Transfer," *Transactions of the Japan Concrete Institute,* Vol. 6, 1984, pp. 425-432.

24. Van de Loock, L., "Influence of Steel Fibers on the Shear Transfer in Cracks", *Proceedings of the International Symposium on Fiber Reinforced Concrete*, Madras, India, 1987, pp. 1.101-1.112.

25. Swamy, R.N., Jones, R., and Chiam, T., "Shear Transfer in Steel Fiber Reinforced Concrete," Fiber Reinforced Concrete Properties and Applications, ACI SP-105, 1987, pp. 565-592.

26. Barr, B., "The Fracture Characteristics of FRC Materials in Shear," Fiber Reinforced Concrete Properties and Applications, ACI SP-105, 1987, pp. 27-53.

27. Tan, K.H., and Mansur, M.A., "Shear Transfer in Reinforced Fiber Concrete," *Journal of Materials in Civil Engineering*, Vol. 2, No. 4, Nov. 1990, pp. 202-214.

28. Fattuhi, H.I.,"SFRC Corbel Tests," *ACI Structural Journal*, Vol. 84, No. 2, 1987, pp. 119-123.

29. Hara, T., and Kitada, Y., "Shear Strength of Reinforced Concrete Corbels and Steel Fibers as Reinforcement," *Transactions of the Japan Concrete Institute,* Vol. 2, 1980, pp. 279-286.

30. Shanmugam, N.E., and Swaddiwndhipong, S., "The Ultimate Load Behavior of Fiber Reinforced Concrete Deep Beams," *Indian Concrete Journal*, Vol. 58, No. 8, 1988, pp. 211-218.

31. Swamy, R.N., and Bahia, M. H., "The Effectiveness of Steel Fibers as Shear Reinforcement," *Concrete International*, Vol. 7, No. 3, March 1985, pp. 35-40.

32. Swamy, R.N. and Bahia, M. H., "Influence of Fiber Reinforcement on the Dowel Resistance to Shear," *ACI Journal*, Vol. 76, No. 2, February 1979, pp. 327-355.

33. Narayan, R., and Darwish, I.Y.S., "Use of Steel Fibers as Shear Reinforcement," *ACI Structural Journal*, Vol. 39, No. 138, March 1987, pp. 42-50.

34. Sharma, G. N. J., "Shear Strength of Steel Fiber Reinforced Concrete Beams," *ACI Journal*, Vol. 83, No. 4, July-August 1986, pp. 624-628.

35. Ward, R. J. and Li, V. C., "Dependance of Flexural Behavior of Fiber Reinforced Mortar on Material Fracture Resistance and Beam Size," *ACI Materials Journal*, Vol. 87, No. 6, Nov.-Dec. 1990, pp. 627-637.

36. Batson, G. B., Jenkins, E., and Spatney, R., "Steel Fibers as Shear Reinforcement in Beams", *ACI Journal*, Vol. 69, No. 10, 1972, pp. 640-644.

37. Lim, T.Y., Paramassiram, and Lee, S.L., "Shear and Moment Capacity of Reinforced Steel-Fiber-Concrete Beams", *Magazine of Concrete Research*, Vol. 39, No. 140, 1987, pp. 148-160.

38. Mansur, M.A., Ong, C.G., and Paramasivam, P., "Shear Strength of Fibrous Concrete Beams without Stirrups," *Journal of Structural Engineering*, Vol. 112, No. 9, 1986, pp. 2066-2079.

39. Batson, G. B., "Use of Steel Fibers for Shear Reinforcement and Ductility," Steel Fiber Concrete US-Sweden joint seminar (NSF-STU), Stockholm, 1985, pp. 377-419.

40. Task Committee on Finite Element Analysis of Reinforced Concrete, "State-of-the-Art Report on Finite Element Analysis of Reinforced Concrete", Structural Division, ASCE, 1982.

41. Fardis, M.N. and Buyukozturk, O., "Shear Transfer Model for Reinforced Concrete," *Journal of the Engineering Mechanics Division*, ASCE, Vol. 105, No. EM2, April 1979.

42. Bazant, Z. P. and Gambarova, P., "Rough Crack in Reinforced Concrete," *Journal of the Structural Division*, ASCE, Vol. 106, No. ST4, Proc. Paper 15330, April 1980, pp. 819-842.

43. Walraven, J. C., "Fundamental Analysis of Aggregate Interlock," Preprint 80-011, ASCE Convention, Portland, April 1980.

44. Tasuji, M. E., Slate, F. O., and Nilson, A. H., "Stress-Strain Response and Fracture of Concrete in Biaxial Loading," ACI Journal, Vol. 75, No. 7, July 1978, pp. 306-312.

45. Fanella, D. A. and Naaman, A. E., "Stress-Strain Properties of Fiber Reinforced Mortar in Compression," *ACI Journal*, Vol. 82, No. 4, July-August 1985, pp. 475-483.

46. Vecchio, F. and Collins, M.P.,"Stress-Strain Characteristics of Reinforced Concrete in Pure Shear," Final Report, IABSE Colloquium on Advanced Mechanics of Reinforced Concrete (Delft, 1981), International Association for Bridge and Structural Engineering, Zurich, pp. 211-225.

47. Lim,T.Y., Paramasivam, P., and Lee, S.L., "Analytical Model for Tensile Behavior of Steel-Fiber Concrete," *ACI Material Journal*, Vol. 84, No. 2, 1987, pp. 286-298.

48. ACI Committee 363, "State-of-the-art-Report on High Strength Concrete," *ACI Journal*, Vol. 81, No. 4, July-August 1984, pp. 364-406.

49. Beattie, S. M., Buyukozturk, O., and Bakhoum, M. M., "Behavioral Improvements in Precast Concrete Segmental Bridge Joints Through the Use of Steel Fibers", Research Report R89-03, Department of Civil Engineering, Massachusetts Institute of Technology, February 1989.

50. Buyukozturk, O. Bakhoum, M. M., and Beattie, S. M. , "Shear Behavior of Joints in Precast Concrete Segmental Bridges," *Journal of Structural Engineering,* ASCE, Vol. 116, No. 12, December 1990, pp. 3380-3401.

51. ACI Committee 544, "Measurement of Properties of Fiber Reinforced Concrete," *ACI Materials Journal*, Vol. 85, No. 6, November-December 1988, pp. 583-593.

52. Narayanan, R. and Kareem-Palanjian, A. S., "Effect of Fibre Addition on Concrete Strengths", *Indian Concrete Journal*, Vol. 58, No. 4, April 1984, pp. 100-103.

53. Cholewicki, A., "Loadbearing Capacity and Deformability of Vertical Joints in Structural Walls of Large Panels," *Building Science*, Vol. 6, Pergamon Press, 1971, pp. 163-184.

APPENDIX

COMPUTER PROGRAM

An example listing of the computer programs used to implement the shear transfer model described in Chapter 4 is included. Six programs were used for each of the six different concretes used in the experimental work. All of the programs were identical except for the material laws included for each type of concrete. This particular listing corresponds to the program used to analyze steel fiber reinforced high strength concrete. The programs were written in Microsoft Quick Basic, in a Apple Macintosh SE/30 computer.

```
5  INPUT "ENTER FILE NAME FOR RESULTS=",filename$
10 OPEN filename$ FOR OUTPUT AS #1
20 INPUT "f'c (psi) =",fc
30  INPUT  "e0 (negative)=",e0
40 INPUT "eU (negative)=",eU
50 INPUT "fy (psi) =",fy
60  Es=29000000&
70 INPUT "pl=",pl
80 INPUT  "pt=",pt
90 INPUT "K=",K
100 PRINT "INPUT DATA FOR FRC TENSILE BEHAVIOR"
110  INPUT  "fcr=",fcr
120  INPUT  "fu=",fu
130 INPUT "Ec=",Ec
140  INPUT  "volume fraction (%)=",vf
150  ecr=fcr/Ec:PRINT  "ecr=",ecr
160   ecr2=ecr+(fu-fcr)/(.14*vf*Es)
170   ecr3=1.2*ecr2
180  ey=fy/Es: PRINT  "ely=ety=",ey
190  WRITE #1,fc,e0,fcr,Ec,ecr
200  WRITE #1,fy,Es,ey,pl,pt
210  ed=0:sigr=0:er=0:el=0:et=0:flag=0:lsy$="n"
220 INPUT "NEW VALUE FOR ed=",ed
230  INPUT  "new value for sigr=",sigr
240  INPUT  "passed ecr (y/n)?",pecr$
       INPUT "passed ecr2 (y/n)?",pecr2$
250 IF lsy$<>"y" THEN INPUT "has long. steel yielded (y/n)?",lsy$
260 PRINT "ed=",ed
270 IF pecr$="n"  THEN
280    er=sigr/Ec
290 ELSE
300   IF pecr2$<>"y" THEN
310     PRINT "******passed ecr********"
320       er=(sigr-fcr)/(.14*vf*Es) + ecr
      ELSE
          PRINT "*******passed ecr2*******"
            er= ecr2+(fu-sigr)/(.14*vf*Es)
       END IF
330 END IF
340 PRINT "er=",er
350  lam=SQR(.7  -er/ed)
```

```
360 PRINT "lam=",lam
370  ep=  e0/lam
380 PRINT "ep=",ep
390 IF ABS(ed) <= ABS(ep)  THEN
400      sigd=-fc*(2*(ed/e0)  -  lam*(ed/e0)^(2))
410 ELSE
420      sigd=-(fc/lam)  +  .15*fc*(ed-ep)/(eU-e0)
430 END IF
440 PRINT "sigd=",sigd
450 IF lsy$="y" THEN
460      c2=  (-sigr-pl*fy)/(sigd-sigr)
470 ELSE
480       c2=(-sigr-pl*Es*er)/(sigd-sigr+pl*Es*(ed-er))
490 END IF
500  s2=1-c2:c1=SQR(c2):s1=SQR(s2)
510  t1=s1/c1:ALPHA=ATN(t1)
520  a=K*s1*c1-s2:  b=K*s1*c1+c2
530 IF et >= ey  THEN
540      sigr1=  (sigd*a-pt*fy)/b
550 ELSE
560     d=ed*s2+er*c2
570       sigr1=(sigd*a-pt*Es*d)/b
580 END IF
590  PRINT "sigr1=",sigr1:PRINT "sigr=",sigr
600 IF sigr1 >= .98*sigr THEN
610     IF sigr1 <= 1.02*sigr THEN 650 ELSE 230
620 ELSE
630    GOTO 230
640 END IF
650  Tlt=(sigd-sigr1)*s1*c1
660 PRINT "found T=",Tlt
670  el=ed*c2+er*s2
680 IF el>=ey AND lsy$<>"y" THEN 690 ELSE 700
690  PRINT "**long. steel has yielded, recalculate with this condition":
       GOTO 230
700  et=ed*s2+er*c2
710 IF et>=ey THEN 720 ELSE 740
720  PRINT "**trans. steel has yielded, recalculate with this
       condition": GOTO 230
740  jlt=2*(ed-er)*s1*c1
750 REM IF pl=0 AND ((sigr+sigr1)/2) > fcr THEN PRINT "passed
       fcr,recalc.(smaller ed)": GOTO 220
760 IF el <= ey THEN
```

```
770   fl=Es*el
780 ELSE
790   fl=fy:flag=1:PRINT "****long. steel yielded*****"
800 END IF
810 IF et <= ey THEN ft=Es*et ELSE ft=fy
820 WRITE #1,Tlt, jlt, fl, el, ft, et,sigr,er,sigd,ed
830 IF ABS(Tlt) > Tmax THEN
840     Tmax=ABS(Tlt):jmax=jlt:alphamax=ALPHA:edmax=ed
850 END IF
860 IF ABS(ed) > ABS(eU/lam) THEN
870   GOTO 910
880 ELSE
890   GOTO 220
900 END IF
910 PRINT "Tmax=",Tmax
920 PRINT "at",jmax
930 PRINT "ed=",edmax
940 PRINT "angle=",alphamax*57.295
950 IF flag=1 THEN PRINT "long. steel yielded"
960 END
```